

Copyright Warning & Restrictions

The copyright law of the United States (Title 17, United States Code) governs the making of photocopies or other reproductions of copyrighted material.

Under certain conditions specified in the law, libraries and archives are authorized to furnish a photocopy or other reproduction. One of these specified conditions is that the photocopy or reproduction is not to be “used for any purpose other than private study, scholarship, or research.” If a user makes a request for, or later uses, a photocopy or reproduction for purposes in excess of “fair use” that user may be liable for copyright infringement,

This institution reserves the right to refuse to accept a copying order if, in its judgment, fulfillment of the order would involve violation of copyright law.

Please Note: The author retains the copyright while the New Jersey Institute of Technology reserves the right to distribute this thesis or dissertation

Printing note: If you do not wish to print this page, then select “Pages from: first page # to: last page #” on the print dialog screen

The Van Houten library has removed some of the personal information and all signatures from the approval page and biographical sketches of theses and dissertations in order to protect the identity of NJIT graduates and faculty.

ABSTRACT

INVESTIGATING THE NEUROVASCULAR CORRELATES OF COGNITIVE FUNCTION IN INDIVIDUALS WITH SPINAL CORD INJURY USING FUNCTIONAL NEAR-INFRARED SPECTROSCOPY

by

Donna Yali Chen

Individuals with spinal cord injury (SCI) have a 13 times greater risk of cognitive impairment than able-bodied individuals and commonly report symptoms of depression and anxiety. The reports of cognitive impairment in individuals with SCI are independent of concomitant brain injury. Although the direct cause of cognitive impairment in individuals with SCI is unknown, key contributors may include comorbid depression, chronic pain, anxiety, fatigue, brain injury, or cardiovascular dysfunction. Previous studies have focused on SCI at the level of the spinal cord but have under-investigated the supraspinal levels. Due to the lack of neuroimaging studies on SCI rehabilitation, it is unclear how neurovascular activation and functional brain connectivity are altered in cognitive processing areas due to the injury.

The high costs of routine functional magnetic resonance imaging (fMRI) coupled with highly rigid supine-positioning make fMRI infeasible for longitudinal monitoring during SCI rehabilitation. Therefore, it is critical to use a more accessible neuroimaging method such as functional near-infrared spectroscopy (fNIRS) to study the neurovascular correlates of cognition in individuals with SCI. The long-term goal of this project is to facilitate the development of effective rehabilitation treatments for individuals with SCI and to accurately monitor injury recovery. Decreased functional brain connectivity in the

sensorimotor and prefrontal areas have been observed in individuals with SCI. Thus, it is hypothesized that corticospinal tract disruption after SCI will decrease neurovascular activation and functional brain connectivity in regions associated with cognitive processing. The central hypothesis is tested with three specific aims: Aim 1) to determine the task-induced neurovascular correlates of cognitive function in individuals with SCI, Aim 2) to investigate differences in the resting-state functional connectivity patterns of cognitive processing areas between individuals with SCI and able-bodied (AB) controls using fNIRS, and Aim 3) to investigate the differences in cerebrovascular reactivity between individuals with SCI and AB controls. This dissertation is one of the first to comprehensively investigate cognitive function in individuals with SCI using fNIRS and aids in the understanding of the neuropsychological consequences after SCI, which will progress the development of effective rehabilitation treatments.

**INVESTIGATING THE NEUROVASCULAR CORRELATES OF COGNITIVE
FUNCTION IN INDIVIDUALS WITH SPINAL CORD INJURY USING
FUNCTIONAL NEAR-INFRARED SPECTROSCOPY**

**by
Donna Yali Chen**

**A Dissertation
Submitted to the Faculty of
New Jersey Institute of Technology
and Rutgers University Biomedical and Health Sciences – Newark
in Partial Fulfillment of the Requirements for the Degree of
Doctor of Philosophy in Biomedical Engineering**

Department of Biomedical Engineering

August 2024

Copyright © 2024 by Donna Yali Chen

ALL RIGHTS RESERVED

APPROVAL PAGE

**INVESTIGATING THE NEUROVASCULAR CORRELATES OF COGNITIVE
FUNCTION IN INDIVIDUALS WITH SPINAL CORD INJURY USING
FUNCTIONAL NEAR-INFRARED SPECTROSCOPY**

Donna Yali Chen

Dr. Bharat B. Biswal, Dissertation Co-Advisor Date
Distinguished Professor of Biomedical Engineering, NJIT

Dr. Hai Sun, Dissertation Co-Advisor Date
Associate Professor of Neurosurgery,
Rutgers Robert Wood Johnson Medical School, New Brunswick, NJ

Dr. Tara L. Alvarez, Committee Member Date
Distinguished Professor of Biomedical Engineering, NJIT

Dr. Xiaobo Li, Committee Member Date
Associate Professor of Biomedical Engineering, NJIT

Dr. Saikat Pal, Committee Member Date
Associate Professor of Biomedical Engineering, NJIT

Dr. Xin Di, Committee Member Date
Research Professor of Biomedical Engineering, NJIT

Dr. Nancy Chiaravalloti, Committee Member Date
Director of Neuropsychology and Neuroscience Lab,
Kessler Foundation, West Orange, NJ

BIOGRAPHICAL SKETCH

Author: Donna Yali Chen
Degree: Doctor of Philosophy
Date: August 2024

Undergraduate and Graduate Education:

- Doctor of Philosophy in Biomedical Engineering, New Jersey Institute of Technology and Rutgers School of Graduate Studies, Newark, NJ, 2024
- Bachelor of Engineering in Biomedical Engineering, The City College of New York, New York, NY, 2019

Major: Biomedical Engineering

Presentations and Publications:

Chen, D. Y., Di, X., & Biswal, B. (2024). Cerebrovascular reactivity increases across development in multiple networks as revealed by a breath-holding task: A longitudinal fMRI study. *Human Brain Mapping*. 45(1), e26515. <https://doi.org/10.1002/hbm.26515>

Chen, D. Y., Di, X., Yu, X., & Biswal, B. B. (2024). The significance and limited influence of cerebrovascular reactivity on age and sex effects in task- and resting-state brain activity. *Cerebral Cortex*. 34(2), bhad448. <https://doi.org/10.1093/cercor/bhad448>

Chen, D. Y., & Biswal, B. B. (2023). 1—Introduction to resting-state fMRI. In J. Chen & C. Chang (Eds.), *Advances in Resting-State Functional MRI* (pp. 1–20). Academic Press. <https://doi.org/10.1016/B978-0-323-91688-2.00011-4>

Chen, D. Y., Ji, K. C., Varshney, S., Hafiz, R., & Biswal, B. B. (2021). Chapter 4—Resting state functional connectivity in pediatric populations. In H. Huang & T. P. L. Roberts (Eds.), *Advances in Magnetic Resonance Technology and Applications* (Vol. 2, pp. 65–87). Academic Press. <https://doi.org/10.1016/B978-0-12-816633-8.00005-3>

- Chen, D. Y., Di, X., Karunakaran, K. D., Sun, H., Pal, S., & Biswal, B. B. (2024). Delayed cerebrovascular reactivity in individuals with spinal cord injury in the right inferior parietal lobe: A breath-hold functional near-infrared spectroscopy study (p. 2024.06.03.24307819). medRxiv. <https://doi.org/10.1101/2024.06.03.24307819>
- Chen, D. Y., Di, X., Amaya, N., Sun, H., Pal, S., & Biswal, B. B. (2024). Brain activation during the N-back working memory task in individuals with spinal cord injury: A functional near-infrared spectroscopy study (p. 2024.02.09.579655). bioRxiv. <https://doi.org/10.1101/2024.02.09.579655>
- Chen, D. Y., Di, X., Sun, H., Pal, S., & Biswal, B. B. (2024). Increased fractional amplitude of low frequency fluctuations in individuals with spinal cord injury: a resting-state fNIRS study (Manuscript in preparation).
- Chen, D.Y., Niu, H., Hong, T., Shu, H., Biswal, B.B. (2024). Development of functional topological organization throughout childhood revealed by functional near-infrared spectroscopy imaging. (Manuscript in preparation)
- Ji, K., Chen, D. Y., Karunakaran, K.D, Biswal, B. B. (2023). Altered brain hemodynamic response and cognitive function after sleep deprivation: a functional near-infrared spectroscopy study. *Brain-Apparatus Communication: A Journal of Bacomics*, 2:1, 2169589. <https://doi.org/10.1080/27706710.2023.2169589>
- Guan, S., Jiang, R., Chen, D. Y., Michael, A., Meng, C., & Biswal, B. (2023). Multifractal long-range dependence pattern of functional magnetic resonance imaging in the human brain at rest. *Cerebral Cortex*, bhad393. <https://doi.org/10.1093/cercor/bhad393>
- Karunakaran, K. D., Chen, D. Y., Ji, K., Chiaravalotti, N., & Biswal, B. B. (2022). Task-based and Resting-state Cortical Functional Differences after Spinal Cord Injury: A Pilot Functional Near-Infrared Spectroscopy Study. *Journal of Neurotrauma*. <https://doi.org/10.1089/neu.2022.0131>.
- Canario, E., Chen, D., Han, Y., Niu, H., & Biswal, B. (2022). Global Network Analysis of Alzheimer's Disease with Minimum Spanning Trees. *Journal of Alzheimer's Disease*, 89(2), 571–581. <https://doi.org/10.3233/JAD-215573>
- Algarin, C., Peirano, P., Chen, D., Hafiz, R., Reyes, S., Lozoff, B., & Biswal, B. (2022). Cognitive control inhibition networks in adulthood are impaired by early iron deficiency in infancy. *NeuroImage: Clinical*, 35, 103089. <https://doi.org/10.1016/j.nicl.2022.103089>

- Hu, P., Niu, B., Yang, H., Xia, Y., Chen, D., Meng, C., Chen, K., & Biswal, B. (2022). Analysis and visualization methods for detecting functional activation using laser speckle contrast imaging. *Microcirculation*, *29*(6–7), e12783. <https://doi.org/10.1111/micc.12783>
- Canario, E., Chen, D., & Biswal, B. (2021). A review of resting-state fMRI and its use to examine psychiatric disorders. *Psychoradiology*, *1*(1), 42–53. <https://doi.org/10.1093/psyrad/kkab003>
- Karunakaran, K. D., Ji, K., Chen, D. Y., Chiaravalloti, N. D., Niu, H., Alvarez, T. L., & Biswal, B. B. (2021). Relationship Between Age and Cerebral Hemodynamic Response to Breath Holding: A Functional Near-Infrared Spectroscopy Study. *Brain Topography*, *34*(2), 154–166. <https://doi.org/10.1007/s10548-021-00818-4>
- Chen, K., Azeez, A., Chen, D. Y., & Biswal, B. B. (2020). Resting-State Functional Connectivity: Signal Origins and Analytic Methods. *Neuroimaging Clinics*, *30*(1), 15–23. <https://doi.org/10.1016/j.nic.2019.09.012>

To my dear mother and father, Mu Lan Wang and Zhi Xiang Chen, who are the most hardworking and resilient people I know. They came to the US without knowing a word of English and had nothing in their pockets. They have sacrificed so much for me and my siblings to pursue higher education and have a better quality of life.

It is through them that a fire burns within me. I am forever grateful for them.

To my sister and brother, Nina and Jeremy, who have unconditionally supported me throughout this journey and always manage to put a smile on my face.

To my friends, who keep me sane and remind me of the powerful small joys of life.

“You never fail until you stop trying”
- Albert Einstein

ACKNOWLEDGMENTS

I would like to express my sincerest gratitude to my advisor, Dr. Bharat B. Biswal, who helped guide me on this journey and offered continuous support and expertise throughout the years. Through you, I have had the opportunity to explore such exciting research in the world of brain imaging. Thank you for always believing in me, even when I was consumed with doubts. I would also like to thank my co-advisor, Dr. Hai Sun, for the continued guidance and support throughout this scientific endeavor.

To my committee members, Dr. Xin Di, Dr. Saikat Pal, Dr. Tara Alvarez, Dr. Xiaobo Li, and Dr. Nancy Chiaravalloti, I sincerely thank all of you for your dedication to seeing this dissertation through, providing constructive feedback, and always lending a helping hand.

Many thanks go to the Department of Biomedical Engineering and staff members for making things run as smoothly as possible. I would also like to thank all the wonderful BME undergraduate students I've had the pleasure of mentoring and learning from.

I would like to acknowledge support from the New Jersey Alliance for Clinical and Translational Science (NJACTS) for the TL1TR003019 pre-doctoral fellowship award. I am truly grateful for Dr. Kathy Scotto and Anda Cytroen for their endless efforts in helping fellows like me succeed in research and learn more about translational sciences.

Tremendous thanks to Dr. Christopher Cirnigliaro, Ms. Annie Kutlik, and Mr. Steven Knezevic from the Spinal Cord Damage Research Center, James J. Peters Veterans Affairs Medical Center, Bronx, NY for helping with patient recruitment. You gave me hope when I thought I'd never complete recruitment and provided the fuel to

complete this dissertation. And to all the individuals who participated in this study, especially those with spinal cord injuries who travelled far for this research study, thank you! This dissertation would not be possible without your participation. I have learned so much from our conversations in between experiments and hope to be as resilient as you.

I would also like to sincerely thank Dr. James Mandala for all his help in keeping my sanity in check. Thank you for your wise words and compassion during tough times. I am very grateful to have met you and I stand a little taller because of you.

Many thanks for excellent career advice and support from Dr. Elisa Kallioniemi and her wonderful students, Kutluhan Mahmat and Negar Namdar, who have both accompanied me on incredible NYC adventures. Thank you for making my last couple of months filled with so much fun and friendship.

I would like to thank Ayushi Sangoi and the United Council of Academics at NJIT (UCAN) for continuously supporting the PhD students at NJIT and fighting for us. We are stronger together.

To all my colleagues and good friends at the Brain Connectivity Lab: Dr. Xin Di, Dr. Rakibul Hafiz, Berk Can Yilmaz, Katherine Ji, Alexandros Tzalavras, Edgar Canario, Wonbum Sohn, Le Gao, Pratik Jain, and Dr. Sukesh Das, thank you so much for making this experience filled with so much fun and joy, especially with our endless intellectual discussions. We've shared so many great memories together and you've made this PhD journey such a positive one. I have learned so much about the brain from your incredible brains and am sure you will all do amazing things.

And to all the PhD students in the BME department, thank you! Thank you for your comradery. I would like to thank all my friends, especially Jessica Kydd and Iman Nassef, who have continued to bear with me since high school and never once doubted me.

Last but definitely not least, I would like to thank my parents, Mu Lan Wang and Zhi Xiang Chen, and my siblings, Jeremy Chen and Nina Chen, for always sticking by my side through ups and downs and providing me with so much love and support. You truly warm and nourish my soul. I could not have done this without you all.

TABLE OF CONTENTS

Chapter	Page
1 OBJECTIVE.....	1
2 SPINAL CORD INJURY.....	4
2.1 Background.....	4
2.2 Neuroplasticity.....	5
2.3 Cognitive Function.....	6
3 FUNCTIONAL NEAR-INFRARED SPECTROSCOPY.....	8
3.1 Overview of fNIRS.....	8
3.2 Clinical Applications.....	10
4 BRAIN ACTIVATION DURING THE N-BACK WORKING MEMORY TASK IN INDIVIDUALS WITH SPINAL CORD INJURY (AIM 1).....	11
4.1 Introduction.....	11
4.2 Materials and Methods.....	15
4.2.1 Participants.....	15
4.2.2 Cognitive testing.....	16
4.2.3 N-back task.....	17
4.2.4 fNIRS data acquisition.....	19
4.2.5 Preprocessing.....	21
4.2.6 Behavioral scores.....	21
4.2.7 fNIRS task activation metrics.....	22
4.2.8 Statistical analysis.....	23

TABLE OF CONTENTS
(Continued)

Chapter	Page
4.3 Results.....	24
4.3.1 NUCOG scores.....	24
4.3.2 N-back task performance.....	25
4.3.3 fNIRS task activation differences.....	28
4.3.4 Task activation and behavioral scores.....	30
4.4 Discussion.....	32
4.4.1 Lower executive function scores in individuals with SCI.....	32
4.4.2 Similar N-back scores between SCI and AB groups.....	34
4.4.3 Increased brain activation in individuals with SCI during the 2-Back task.....	35
4.4.4 fNIRS task activation and its association with behavioral scores.....	36
4.4.5 Limitations.....	36
4.5 Conclusion.....	37
5 INCREASED FRACTIONAL AMPLITUDE OF LOW FREQUENCY FLUCTUATIONS IN INDIVIDUALS WITH SPINAL CORD INJURY (AIM 2).....	38
5.1 Introduction.....	38
5.2 Materials and Methods.....	41
5.2.1 Participant data collection.....	41
5.2.2 fNIRS data acquisition.....	42
5.2.3 fNIRS data preprocessing.....	44

TABLE OF CONTENTS
(Continued)

Chapter	Page
5.2.4 fALFF calculation.....	45
5.2.5 Resting-state functional connectivity.....	47
5.3 Results.....	47
5.3.1 fALFF comparison between SCI and AB groups.....	48
5.3.2 fALFF in Slow-5, Slow-4, and Slow-3 frequency bands.....	51
5.3.3 RSFC comparison between SCI and AB groups.....	58
5.4 Discussion.....	60
5.4.1 fALFF is increased in individuals with SCI in the inferior parietal lobes.....	60
5.4.2 Distinct fALFF patterns in Slow-5, Slow-4, and Slow-3 frequency bands.....	61
5.4.3 Limitations.....	62
5.5 Conclusion.....	62
6 DELAYED CEREBROVASCULAR REACTIVITY IN INDIVIDUALS WITH SPINAL CORD INJURY IN THE RIGHT INFERIOR PARIETAL LOBE: A BREATH-HOLD FNIRS STUDY (AIM3).....	64
6.1 Introduction.....	64
6.2 Materials and Methods.....	67
6.2.1 Participants.....	67
6.2.2 Breath-hold task paradigm.....	69
6.2.3 fNIRS data acquisition.....	70
6.2.4 fNIRS data preprocessing.....	71

TABLE OF CONTENTS
(Continued)

Chapter	Page
6.2.5 Principal component analysis.....	74
6.2.6 Breath-hold CVR response delays.....	75
6.2.7 CVR and injury characteristics.....	76
6.2.8 Statistical analysis.....	76
6.3 Results.....	77
6.3.1 CVR amplitude in SCI vs. AB.....	78
6.3.2 CVR delays in SCI vs. AB.....	80
6.3.3 CVR association with duration since injury and injury level.....	83
6.3.4 Variability in CVR across the brain.....	84
6.4 Discussion.....	86
6.4.1 No differences in CVR amplitude between the SCI and AB groups.....	86
6.4.2 Individuals with SCI have significantly longer CVR delays than AB individuals.....	87
6.4.3 CVR delays in the right inferior parietal lobe is associated with the duration since injury.....	88
6.4.4 Variability in CVR across the brain.....	89
6.4.5 Limitations.....	89
6.5 Conclusion.....	90
7 SUMMARY AND FUTURE WORK.....	91
7.1 Summary.....	91

TABLE OF CONTENTS
(Continued)

Chapter	Page
7.2 Future Work.....	93
REFERENCES.....	94

LIST OF TABLES

Table	Page
4.1 Demographic Information and Clinical Characteristics from Participants with SCI Enrolled in the Study.....	16
4.2 Montreal Neurological Institute (MNI) Coordinates Displayed for each Region of Interest (ROI) used in the fNIRS Setup. PFC: Prefrontal Cortex; DLPFC: Dorsolateral Prefrontal Cortex.....	20
4.3 Pearson’s Correlations Between fNIRS Metrics and Performance Metrics that are Significant after Multiple Comparison Correction using the Benjamini-Hochberg’s False Discovery Rate (BH-FDR) Method.....	31
5.1 For Participants with SCI, Clinical Characteristics such as the Level of Injury and Duration Since Injury are Summarized.....	42
5.2 Short Channels that were used in the Short Channel Regression Model for each Respective Long Channel are Listed.....	44
5.3 Mixed-effects Modeling Results for fALFF Scores Comparing Between the SCI and AB Groups across all ROI. The LDLPFC Region is not Shown Here for the Mixed-effects Modeling Results due to being Held Out as the Reference Level for Comparisons.....	51
5.4 Mixed-effects Modeling Results for fALFF-Slow-5 Scores Comparing Between the SCI and AB Groups across all ROI. The LDLPFC Region is not Shown Here for the Mixed-effects Modeling Results due to being Held Out as the Reference Level for Comparisons.....	54
5.5 Mixed-effects Modeling Results for fALFF-Slow-4 Scores Comparing Between the SCI and AB Groups across all ROI. The LDLPFC Region is not Shown Here for the Mixed-effects Modeling Results due to being Held Out as the Reference Level for Comparisons.....	56

LIST OF TABLES
(Continued)

Table	Page
5.6 Mixed-effects Modeling Results for fALFF-Slow-3 Scores Comparing Between the SCI and AB Groups across all ROI. The LDLPFC Region is not Shown Here for the Mixed-effects Modeling Results due to being Held Out as the Reference Level for Comparisons.....	58
6.1 Demographic Information and Clinical Characteristics from Participants with SCI Enrolled in the Current Study.....	68
6.2 Mixed Effects Model Results for CVR Amplitude Comparisons between SCI and AB groups, across each ROI. One ROI is left out in the Reports (the LDLPFC region) due to being the Reference Level for all Comparisons.....	80
6.3 Mixed Effects Model Results for CVR Delay Comparisons between SCI and AB groups, across each ROI. One ROI is left out in the Reports (the LDLPFC region) due to being the Reference Level for all Comparisons.....	83

LIST OF FIGURES

Figure		Page
3.1	Schematic of light propagation through the cortex using fNIRS optode source and detectors. Short channels are defined by an optode source to detector position of approximately 0.86 cm whereas long channels are defined by an optode source to detector position of approximately 3 cm. fNIRS light passes through the scalp, skull, and gray matter regions before being reflected back to the detectors.....	9
4.1	N-back task design showing each block and each task level, with examples of letters shown on a computer screen. ITI = inter-trial interval. For each N-back task level, a total of three blocks were implemented. Participants were asked to press a ‘right’ computer key on all target letters and press a ‘left’ computer key for all non-target letters.....	18
4.2	Optode layout design used for the fNIRS study. The channel #, source, and detectors are displayed, along with the following regions of interest: medial prefrontal cortex, right & left dorsolateral prefrontal cortex, right & left motor cortex, and right & left inferior parietal lobe. There are a total of 26 channels and 4 short source-detector separation channels (S1-S4), containing 10 sources and 24 detectors.....	20
4.3	A) Neuropsychiatric Unit Cognitive Assessment Tool (NUCOG) scores for both able-bodied (AB) and spinal cord injury (SCI) groups are shown in green and orange bars, respectively. B) Sub-domains of the NUCOG test scores are also indicated, with significant differences shown between the AB and SCI group in executive function (independent-samples t-test, $t(42) = 2.98$, $p = .0047$, 95% confidence interval: [0.35, 1.81], Bonferroni adjusted $\alpha = .01$ (.05/5)). The total scores from the NUCOG subdomains: attention, visuoconstructional, memory, executive, and language, are added to obtain the composite NUCOG score. ** $p < .01$	25
4.4	A) Accuracy, B) response time, and C) d-prime scores are shown for both spinal cord injury (SCI) and able-bodied (AB) groups, for each N-back task (0-Back, 2-Back, and 3-Back) and each block (first, second, and third). *** $p < .001$	28

**LIST OF FIGURES
(Continued)**

Figure	Page	
4.5	<p>N-back working memory task fNIRS metrics between SCI and AB groups, across all 26 channels. The following fNIRS metrics (z-scored) are shown: area under the curve (AUC), time-to-peak (TTP), maximum HbO (maxHbO), standard deviation of HbO (stdHbO), and beta values from GLM analysis. Black ovals indicate significant differences between AB and SCI groups before correcting for multiple comparisons ($p < .05$). The green oval in maxHbO, Channel #14, during the 2-back task shows significant differences between the AB and SCI groups after FDR correction, $\alpha = 0.05$. FDR correction was performed for each N-back task and each fNIRS metric, across all channels.....</p>	30
5.1	<p>Optode layout map showing the number of sources and detectors used for the present study. Sources are indicated by blue squares whereas detectors are indicated by red squares. A total of 26 long channels (source-to-detector distance of 3 mm) were used in this study, with 4 short channels (source-to-detector distance of 8.4 mm) used to regress out physiological noise.....</p>	43
5.2	<p>A) Signal to noise ratio calculated for each channel, for both light intensity wavelengths: 690 nm and 830 nm, across all subjects in each group. A threshold of 10dB was applied so that channels with less than 10dB SNR were excluded from further analyses, as shown by the red line. B) Channels included or excluded for each subject, as indicated by 1's and 0's, respectively.....</p>	48
5.3	<p>fALFF scores shown between the AB and SCI group for each ROI. Significantly higher fALFF scores are observed for the left inferior parietal lobe (LIPL) and the right inferior parietal lobe (RIPL) region.....</p>	50
5.4	<p>fALFF-Slow-5 scores between the AB and SCI group for each ROI. Significant differences found between the AB and SCI groups in the LIPL region.....</p>	53

**LIST OF FIGURES
(Continued)**

Figure	Page
5.5	fALFF-Slow-4 scores between the AB and SCI group for each ROI. Significant differences found between the AB and SCI groups in the LIPL and RIPL regions..... 55
5.6	fALFF-Slow-3 scores between the AB and SCI group for each ROI. Significant differences found between the AB and SCI groups in the LIPL and RIPL regions..... 57
5.7	Resting-state functional connectivity (RSFC) maps for SCI and AB groups (right and left columns, respectively). The RSFC maps are generated for HbO, HbR, and HbT concentrations using Pearson’s correlation. A total of 26 channels were utilized for the calculation of RSFC..... 59
6.1	A) fNIRS Breath-hold (BH) task paradigm consisting of 6 breath-hold sessions, 15s each, interleaved with 30s of rest. B) fNIRS Optode layout with 10 optode sources and 24 detectors configured across the medial prefrontal cortex, dorsolateral prefrontal cortex, motor cortex, and inferior parietal lobe. A total of 26 channels are used with a source-detector distance of 30mm and 4 short separation channels are used with a source-detector distance of 8.4mm, as denoted by S1, S2, S3, and S4..... 70
6.2	fNIRS preprocessing pipeline applied to both SCI and AB groups. The preprocessing steps were carried out in the following order: 1) convert raw intensity data to optical density data, 2) perform wavelet-based head motion correction with 1.5 times the interquartile range threshold, 3) band-pass filter from 0.01 to 0.15 Hz, 4) convert the filtered optical density data to oxy-hemoglobin (HbO), deoxy-hemoglobin (HbR), and total-hemoglobin (HbT) data, 5) regress the short source-detector channel from the long channels, and 6) perform channel exclusion using the relative power in the breath-hold frequency range. The short source-detector channel regression and channel exclusion steps were applied to all hemoglobin species..... 74

**LIST OF FIGURES
(Continued)**

Figure	Page
6.3	Relative power in the breath-hold frequency range shown for each subject across all channels, shown for A) oxygenated hemoglobin (HbO), B) deoxygenated hemoglobin (HbR), and C) total hemoglobin (HbT). Subjects 1-25 are individuals in the AB group whereas subjects 26-45 are individuals in the SCI group. After applying a threshold of 50% relative power, channels that were included are indicated by 1's and channels that were excluded are indicated by 0's, for D) HbO, E) HbR, and F) HbT..... 78
6.4	PC1 Loadings shown for both AB and SCI groups, for all hemoglobin species: A) oxy-hemoglobin (HbO), B) deoxy-hemoglobin (HbR), and C) total hemoglobin (HbT), across all brain regions of interest: left dorsolateral prefrontal cortex (LDLPFC), left inferior parietal lobe (LIPL), left motor cortex (LMOTOR), medial prefrontal cortex (MPFC), right dorsolateral prefrontal cortex (RDLPFC), right inferior parietal lobe (RIPL), and right motor cortex (RMOTOR). The means of the PC1 Loadings are indicated by black circles and the distribution of the AB and SCI groups are shown, denoted by green and orange, respectively..... 79
6.5	Breath-hold CVR delay values between AB and SCI groups for A) oxy-hemoglobin (HbO), B) deoxy-hemoglobin (HbR), and C) total hemoglobin (HbT), across the left dorsolateral prefrontal cortex (LDLPFC), left inferior parietal lobe (LIPL), left motor cortex (LMOTOR), medial prefrontal cortex (MPFC), right dorsolateral prefrontal cortex (RDLPFC), right inferior parietal lobe (RIPL), and right motor cortex (RMOTOR). The black circles indicate the mean of the CVR delays and the distributions of the delays are shown for the AB and SCI groups, denoted by green and orange, respectively..... 82
6.6	Association between the mean CVR delays in the right inferior parietal lobe and the A) duration since injury (years) and B) spinal injury level score in the SCI group, for oxygenated hemoglobin (HbO), deoxygenated hemoglobin (HbR), and total hemoglobin (HbT) concentrations. Pearson's correlation was performed and a least-squares line is shown in orange with the standard error of the mean in gray..... 84

**LIST OF FIGURES
(Continued)**

Figure		Page
6.7	Variability in breath-hold CVR A) amplitude (PC1 Loading) and B) delays across the brain between the AB and SCI groups, shown in green and orange, respectively. For HbO data, we found significant differences between the AB and SCI groups in the variability of delays across the brain (across channels) (two-sample t-test, $p = 0.0168$). Error bars indicate ± 1 standard error of the mean.....	85

LIST OF ABBREVIATIONS

AB	Able-Bodied
ALFF	Amplitude of Low-Frequency Fluctuations
AUC	Area Under the Curve
BH	Breath Hold
BH-FDR	Benjamini-Hochberg's False Discovery Rate
BOLD	Blood Oxygen Level Dependent
CBF	Cerebral Blood Flow
CBV	Cerebral Blood Volume
CCA	Canonical Correlation Analysis
CMRO ₂	Cerebral Oxygen Metabolic Rate
CVR	Cerebrovascular Reactivity
DTI	Diffusion Tensor Imaging
fALFF	Fractional Amplitude of Low Frequency Fluctuations
fMRI	Functional Magnetic Resonance Imaging
fNIRS	Functional Near-Infrared Spectroscopy
GLM	General Linear Model
HbO	Oxygenated Hemoglobin
HbR	Deoxygenated Hemoglobin
HbT	Total Hemoglobin
HRF	Hemodynamic Response Function
IRB	Institutional Review Board

LDLPFC	Left Dorsolateral Prefrontal Cortex
LIPL	Left Inferior Parietal Lobe
LMOTOR	Left Motor Cortex
M1	Primary Motor Cortex
maxHbO	Maximum Oxygenated Hemoglobin
MMSE	Mini-Mental State Examination
MNI	Montreal Neurological Institute
MPFC	Medial Prefrontal Cortex
NUCOG	Neuropsychiatric Unit Cognitive Assessment Tool
PCA	Principal Component Analysis
RDLPFC	Right Dorsolateral Prefrontal Cortex
RIPL	Right Inferior Parietal Lobe
RMOTOR	Right Motor Cortex
ROI	Regions of Interest
RSFC	Resting-State Functional Connectivity
SCI	Spinal Cord Injury
SNR	Signal to Noise Ratio
stdHbO	Standard Deviation of Oxygenated Hemoglobin
TBI	Traumatic Brain Injury
TTP	Time to Peak

CHAPTER 1

OBJECTIVE

Individuals with spinal cord injury (SCI) have a 13 times greater risk of cognitive impairment than able-bodied individuals and commonly report symptoms of depression and anxiety (Craig et al., 2017). SCI is caused by compression or contusion to the spinal cord, which leads to neurological changes in both the spinal and supraspinal levels of the central nervous system. Major reorganization occurs in the corticospinal tract after SCI, which contributes to the control of voluntary motor movement (Oudega & Perez, 2012). Rehabilitation programs often focus on the spinal cord itself and neglect direct observation of neural activity, partly due to the high costs of routine functional magnetic resonance imaging (fMRI) procedures. Due to the lack of neuroimaging studies on SCI rehabilitation, the role that cognition and functional brain reorganization play in motor recovery after SCI is not well understood. Therefore, it is critical to understand functional brain alterations after SCI, to develop effective rehabilitation treatments for individuals with SCI and to identify biomarkers of adaptive motor recovery.

Previous studies have utilized structural and functional MRI to study individuals who had sustained an SCI, which revealed gray matter atrophy and decreased functional connectivity in regions associated with cognitive and affective processing (Karunakaran et al., 2019, 2020). However, fMRI is not feasible for longitudinal monitoring in rehabilitation, as it is costly and may cause discomfort to patients with SCI. In contrast, functional near-infrared spectroscopy (fNIRS) is relatively low-cost, portable, and comfortable. It uses near-infrared light instead of magnetic pulses to quantify the brain's

hemodynamic changes; these changes are detected due to neurovascular coupling, in which neural activity is followed by cerebral blood flow to the region. Using fNIRS, decreased functional connectivity has been observed in the sensorimotor and prefrontal cortex of SCI patients performing adjusted motor tasks (Karunakaran et al., 2022). Furthermore, a recent study has shown that individuals with SCI perform worse than age-matched healthy controls on cognitive tasks evaluating information processing speed, learning and memory, and verbal fluency (Chiaravalloti et al., 2018). Thus, we hypothesized that corticospinal tract disruption after SCI will decrease neurovascular activation and functional brain connectivity in regions associated with cognitive processing. Accordingly, the specific aims of the dissertation are:

Aim 1. Determine the task-induced neurovascular correlates of cognitive function in individuals with SCI using fNIRS. Few studies have directly observed neural activity in individuals with SCI under the performance of cognitive tasks. We measured activation in the dorsolateral prefrontal cortex, medial frontal cortex, and inferior parietal lobes during N-back tasks to investigate working memory. The control group consisted of age-matched able-bodied individuals (AB) with no history of SCI or cognitive impairments.

Aim 2. Investigate differences in the resting-state connectivity patterns of cognitive processing areas between individuals with SCI and HC using fNIRS. Resting-state dynamics can reveal intrinsic baseline alterations of the brain after SCI. A resting-state scan of 10 minutes was collected from all participants, in the same regions of interest from Aim 1.

Aim 3. Investigate cerebrovascular health in individuals with SCI using a breath holding task. We proposed to quantify cerebrovascular reactivity (CVR) in individuals with SCI using a controlled 15 second breath hold task. The breath-hold task consisted of 6 blocks of breath-holding for 15 s each and a 30 s resting period between the breath-hold periods.

CHAPTER 2

SPINAL CORD INJURY

2.1 Background

Spinal cord injury (SCI) is characterized by damage to the spinal cord that can either temporarily or permanently alter its function. SCI is further divided into traumatic vs. non-traumatic SCI, in which traumatic SCI is caused by an external physical impact whereas non-traumatic SCI is caused by an acute or chronic disease process, i.e., infection or degenerative disc disease (Roth et al., 1989). During a traumatic SCI event, the primary injury to the vertebral column causes damage to neurons and oligodendrocytes, and disruption of vasculature at the blood-spinal cord barrier (Ahuja et al., 2017). During the primary traumatic injury, there is an immediate neuroinflammatory response in which astrocytes and microglia activate and infiltrate the site of injury, which persists into the secondary injury phase (Lee et al., 2022). After the primary injury event, secondary injury mechanisms in the sub-acute and chronic phases occur, leading to further damage to the spinal cord such as cell death, glial scar formation, tissue degeneration, and axonal degeneration (Alizadeh et al., 2019). These primary and secondary injury mechanisms lead to a series of changes to the spinal cord which typically result in permanent deficits in motor and/or sensory function below the level of injury.

There are life-long consequences after an individual sustains an SCI, leading to deficits in mobility and decreased quality of life. Every year in the United States, there are approximately 17,700 new cases of SCI and currently over 250,000 people live with SCI, with costs of managing the care of SCI patients estimated at approximately \$4 billion each

year (National Spinal Cord Injury Statistical Center, Birmingham, AL, 2022). Recovery after SCI is often limited and dependent on various factors such as physical therapy, pharmacological treatment, and psychosocial factors. It is rare for patients with SCI to achieve complete neurological recovery (less than 1%), while 30-80% of patients develop sensory abnormalities such as neuropathic pain (Rekand et al., 2012). Furthermore, individuals with SCI are at a higher risk for cognitive impairment and mood disorders than able-bodied individuals (Craig et al., 2017), which may negatively interfere with outcomes from motor rehabilitation (Yang et al., 2020).

2.2 Neuroplasticity

Functional brain reorganization occurs after SCI due to neuroplasticity, or the brain's ability to change its structure and function to adapt to demands (Fuchs & Flügge, 2014). As motor recovery improves after SCI, brain activation in the primary motor cortex has been shown to increase, while activation in the association sensorimotor regions decrease (Jurkiewicz et al., 2007). Functional brain reorganization after SCI results partly from changes in cortical anatomy, such as axonal sprouting (Henderson et al., 2011). Functional brain connectivity changes are also observed in the thalamus and its subnuclei in individuals with complete paraplegic SCI (Karunakaran et al., 2020). Furthermore, magnetic resonance imaging (MRI) studies have shown that the brain's gray matter volume is significantly atrophied in individuals with SCI as compared to able-bodied controls (Karunakaran et al., 2019). Wrigley and colleagues used MRI and diffusion tensor imaging (DTI) to investigate changes in the anatomical connected in the motor cortices and report significantly lower gray matter volume in the primary motor cortex in individuals with SCI

as compared to able-bodied controls (Wrigley et al., 2009). These studies reveal both structural and functional brain changes that occur after SCI.

2.3. Cognitive Function

One mechanism to increase neuroplasticity after SCI is through rehabilitative exercise, which is important for regaining motor control by promoting the growth of injured axons and strengthening any remaining neural circuits (Yang et al., 2020). However, some individuals with SCI have reported difficulties in attention span and limited learning ability, which are factors that could interfere with motor rehabilitation programs (Roth et al., 1989). Adults with SCI were found to be at a 13 times greater risk for cognitive impairment than adults without SCI and levels of depressive mood and anxiety were significantly greater in individuals with SCI (Craig et al., 2017). Cognitive impairment in individuals with SCI is also a strong predictor for psychological disorders (Craig et al., 2015). Furthermore, individuals with SCI typically score lower on information processing speed, verbal learning and memory, and verbal fluency tests than age-matched able-bodied controls (Chiaravalloti et al., 2018). A possible mechanism of cognitive impairment in individuals with SCI is cardiovascular dysfunction, since a majority of individuals with SCI experience orthostatic hypotension (Sachdeva et al., 2019). Another possible mechanism of cognitive decline is the induction of primary motor cortex (M1) type microglia and related cell cycle activation after SCI (Faden et al., 2016; J. Wu et al., 2014). Despite evidence of cognitive impairment in individuals with SCI, the extent to which cognitive decline alters function brain reorganization is not clear.

Although there is evidence of changes in neuroplasticity after SCI, rehabilitation programs often focus on the spinal cord itself and neglect direct observation of neural activity, partly due to the high costs and discomfort associated with routine functional MRI (fMRI) procedures. Due to the lack of neuroimaging studies on SCI rehabilitation, the role that cognition and functional brain reorganization play in motor recovery after SCI is not well understood. Therefore, it is important to understand functional brain alterations after SCI using a more accessible neuroimaging modality, such as functional near-infrared spectroscopy (fNIRS), to develop effective rehabilitation treatments and identify biomarkers of cognitive impairment.

CHAPTER 3

FUNCTIONAL NEAR-INFRARED SPECTROSCOPY

3.1 Overview of fNIRS

Functional near-infrared spectroscopy is a non-invasive neuroimaging modality which utilizes near-infrared light to image the brain and quantify levels of hemodynamic oxygenation (Ferrari & Quaresima, 2012). Near-infrared light is emitted through an optode source and collected by detectors, arranged across the brain in a user-specific configuration. As the source-to-detector distance increases, the propagation of light through the brain also increases (Figure 3.1). However, there is also greater scattering of light with increased source-to-detector distance, which could introduce noise to the collected signal. Therefore, the optimum source-to-detector distance has been calculated to be approximately 2-3 cm (Strangman et al., 2013).

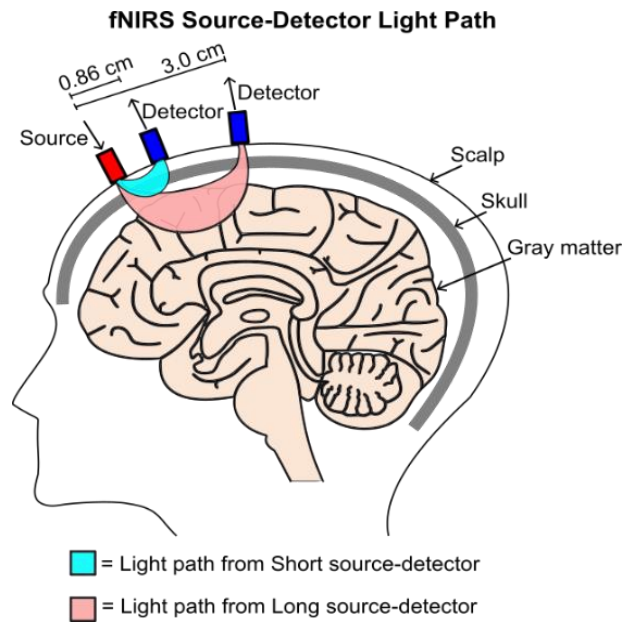


Figure 3.1 Schematic of light propagation through the cortex using fNIRS optode source and detectors. Short channels are defined by an optode source to detector position of approximately 0.86 cm whereas long channels are defined by an optode source to detector position of approximately 3 cm. fNIRS light passes through the scalp, skull, and gray matter regions before being reflected back to the detectors.

fNIRS measures neurovascular activation, based on the theory of neurovascular coupling, in which increased neural activity is followed by increased regional cerebral blood flow. Increased neuronal activation during an active task increases the demand of cerebral metabolites in specific task-associated regions, causing a cascade of changes in the cerebral blood flow (CBF), cerebral blood volume (CBV), oxygen metabolic rate (CMRO₂) and consequently the oxygenated hemoglobin (HbO) levels, and deoxygenated hemoglobin levels (HbR) (Attwell & Iadecola, 2002; Buxton, 2012). These changes in quantities can be measured using optical intensity levels at the near-infrared range (650-950 nm) of the electromagnetic spectrum. Near-infrared light passes through the skull and cortex painlessly and scatters in all paths achieving a maximum depth of ~20 mm from the scalp.

3.2 Clinical Applications

The use of fNIRS has become increasingly used in rehabilitation research due to its portability, comfort, high temporal resolution, robustness against motion artifacts, and ease-of-use (Yücel et al., 2017). fNIRS can also be used to measure functional brain connectivity, which is the synchronization of brain activity in spatially distinct areas of the brain (Friston, 1994). Using fNIRS to investigate functional connectivity between individuals with mild cognitive impairment vs. healthy controls, Nguyen et al. observed decreased left and inter-hemispheric connectivity in individuals with mild cognitive impairment during a verbal fluency test (Nguyen et al., 2019). The application of fNIRS in neurocognitive studies involving both neurological and psychiatric disorders such as Alzheimer's disease, Parkinson's disease, schizophrenia, etc., is well described in the literature. Vassena and colleagues have validated the use of fNIRS to show significant differences in the dorsolateral prefrontal cortex during effortful anticipation in a healthy population (Vassena et al., 2019). Similarly, fNIRS studies of clinical populations show group-level differences in the prefrontal cortex during working memory and visuospatial working memory tasks in individuals with ADHD and those with schizophrenia (Gu et al., 2017; Quaresima et al., 2009; Schecklmann et al., 2010). These studies show the different applications of fNIRS in studying patient populations.

CHAPTER 4

BRAIN ACTIVATION DURING THE N-BACK WORKING MEMORY TASK IN INDIVIDUALS WITH SPINAL CORD INJURY (AIM 1)

4.1 Introduction

Every year in the U.S., there are approximately 18,000 new cases of traumatic spinal cord injury (SCI), as of 2022 (National Spinal Cord Injury Statistical Center, Birmingham, AL, 2022). Cases of traumatic SCI are caused primarily by events such as vehicle accidents, falls, acts of violence, and sports/recreational activities. After injury, individuals with SCI are at a 13 times greater risk of cognitive impairment than able-bodied individuals, in addition to being at a high risk for developing pervasive mental disorders such as depression and anxiety (Craig et al., 2017; Lim et al., 2017; Pasipanodya et al., 2021; Pozzato et al., 2023). Furthermore, individuals with SCI typically score lower on cognitive tests evaluating information processing speed, verbal learning and memory, and verbal fluency than age-matched able-bodied individuals (Chiaravalloti et al., 2018). The mechanism of cognitive decline after SCI is not well understood, with studies suggesting cardiovascular dysfunction (Nightingale et al., 2020; Wecht & Bauman, 2013), concomitant traumatic brain injury (TBI) (Bradbury et al., 2008; Macciocchi et al., 2013; Nott et al., 2014), hypoxia (Hernandez-Gerez et al., 2019), sleep disorders such as obstructive sleep apnea (Carlozzi et al., 2022; Pasipanodya et al., 2021; Shafazand et al., 2019), and body temperature dysregulation (Wecht et al., 2015) as possible causes of cognitive impairment in individuals with SCI (Alcántar-Garibay et al., 2022). Despite evidence of cognitive decline in individuals with SCI, the extent to which cognitive decline

alters functional brain reorganization is unclear. This is partially attributed to the lack of neuroimaging studies focused on understanding cognitive function after SCI.

Structural and functional brain changes have been observed in individuals with SCI compared to able-bodied control groups using magnetic resonance imaging (MRI) (Henderson et al., 2011; Jurkiewicz et al., 2007; Karunakaran et al., 2019). Jurkiewicz and colleagues reported increased brain activation in the primary motor cortex as motor recovery improved after SCI, while activation in the associated sensorimotor regions was found to decrease (Jurkiewicz et al., 2007). Functional brain connectivity changes have also been observed in the thalamus and its subnuclei in individuals with complete paraplegic SCI (Karunakaran et al., 2020). Furthermore, MRI studies have shown that the brain's gray matter volume is significantly atrophied in individuals with SCI compared to able-bodied controls (Karunakaran et al., 2019). These structural and functional brain changes may be associated with cognitive decline in individuals with SCI. Although both structural and functional MRI (fMRI) have been used to study brain reorganization after SCI, the rigid supine-positioning inside the scanner bore and magnetic contraindications pose limitations for investigating supraspinal changes after SCI, particularly in rehabilitative settings. In order to study brain reorganization after SCI more systematically or longitudinally, a more portable neuroimaging device such as functional near-infrared spectroscopy (fNIRS) may be used.

fNIRS is a non-invasive neuroimaging modality which utilizes near-infrared light to image the brain and quantify levels of hemoglobin concentration (Delpy et al., 1988; Jöbsis, 1977; Villringer et al., 1993). Near-infrared light is emitted through an optode source and collected by photodiode detectors, arranged across the brain depending on the

regions of interest. Similar to fMRI, fNIRS measures neurovascular activity, based on the theory of neurovascular coupling, in which increased neural activity is followed by increased regional cerebral blood flow to a particular brain region (Girouard & Iadecola, 2006). Increased neuronal activation during an active task increases the demand for cerebral metabolites in specific task-associated regions, causing a cascade of changes in the cerebral blood flow, cerebral blood volume, oxygen metabolic rate, and consequently the oxygenated and deoxygenated hemoglobin concentration levels (HbO and HbR, respectively) (Buxton, 2010; Paulson et al., 2010). The use of fNIRS has become widespread in rehabilitation research due to its portability, high temporal resolution, robustness against motion artifacts, and ease-of-use (Yücel et al., 2017).

Despite the increasing use of fNIRS, it has not been widely used to study brain changes in individuals with SCI. We have previously used fNIRS to investigate functional brain changes in individuals with SCI compared to healthy controls and observed an overall decrease in functional brain hemodynamic response during finger tapping and ankle tapping tasks (Karunakaran et al., 2022). fNIRS has also been used in conjunction with robot-assisted gait training in individuals with SCI to measure functional brain activity changes in the primary motor cortex (Simis et al., 2018), in addition to being combined with repetitive transcranial magnetic stimulation to investigate the amelioration of neuropathic pain after SCI (Sun et al., 2019). These studies suggest that fNIRS can be a useful neuroimaging tool for investigating functional brain changes which occur in individuals with SCI. Not only can fNIRS be useful for investigating functional brain changes in the motor cortex regions, but it can also be used to investigate the cognitive deficits that have been reported in individuals with SCI (Alcántar-Garibay et al., 2022;

Sachdeva et al., 2018). There is currently a lack of fNIRS studies investigating cognitive function in individuals with SCI. This is a much-needed area, particularly since studies investigating cognitive function in individuals with SCI have reported both significant cognitive impairments (Chiaravalloti et al., 2018; Craig et al., 2017; Davidoff et al., 1992; Dowler et al., 1997; Hall et al., 1999; Macciocchi et al., 2013; Molina et al., 2018; Wilmot et al., 1985) and no significant impairments (Bradbury et al., 2008; Masedo et al., 2005; Nott et al., 2014; Sachdeva et al., 2018). The conflicting reports of cognitive impairment in individuals with SCI could be partly attributable to the heterogeneity of the sample population, differences in the cognitive tests utilized, differences in study design, or sample size (Sachdeva et al., 2018; Sandalic, Tran, et al., 2022). Therefore, due to our currently limited understanding of cognitive impairment in individuals with SCI, fNIRS may be a useful tool to better understand cognitive impairment by quantifying concrete functional brain activity changes in individuals with SCI.

In the present study, we investigated the neurovascular correlates of working memory in individuals with SCI in comparison to able-bodied (AB) individuals using fNIRS and an N-back task. The N-back task is a frequently used task paradigm in fMRI and fNIRS studies to investigate working memory function and has been shown to activate frontoparietal regions of the brain (Braver et al., 1997; Owen et al., 2005). We also evaluated cognitive function in individuals with SCI and AB controls by using a brief cognitive screening tool established by Walterfang and colleagues, known as the Neuropsychiatric Unit Cognitive Assessment Tool (NUCOG) (Walterfang et al., 2006). Measures of brain hemodynamic activity were collected using fNIRS and correlated with accuracy, response time, and d-prime scores on the N-back task, in addition to NUCOG

scores. The fNIRS-derived brain activity metrics, N-back performance scores, NUCOG scores, and brain-behavior associations were compared between the SCI and AB group.

4.2 Materials and Methods

4.2.1 Participants

Nineteen individuals with SCI (14M, 5F; mean age \pm standard deviation: 46.32 ± 10.18 years) and 25 age- and sex-matched able-bodied (AB) individuals (19M, 6F; mean age \pm standard deviation: 43.2 ± 12.28 years) enrolled in the current study. All participants were recruited from the New Jersey/New York metropolitan area and provided written informed consent. Institutional Review Board (IRB) approval was obtained from New Jersey Institute of Technology. The exclusion criteria for the SCI group were as follows: (1) within one-year post-spinal cord injury or in the acute phase of injury, (2) presence of tetraplegia or inability to perform upper limb motor movements, (3) history of or concurrent traumatic brain injury (TBI), (4) history of or concurrently has psychiatric disorders such as post-traumatic stress disorder, addiction, bipolar disorder, or schizophrenia, (5) presence of acute illness or infection, (6) history of chronic hypertension, diabetes mellitus, stroke, epilepsy or seizure disorders, multiple sclerosis, Parkinson's disease, (7) illicit drug abuse within the past 6 months, (8) has Alzheimer's disease or dementia, (9) not able to speak English, and (10) younger than 18 years of age or older than 65 years of age. For the AB group, the same exclusion criteria were applied; however, individuals in this group did not have any presence or history of SCI. The inclusion criteria were as follows: (1) have spinal cord injury with more than one-year post-injury duration (SCI group only), (2) voluntary movement of the arms, (3) within 18-65

years of age, and (4) able to speak English. Injury characteristics such as the spinal level of injury, duration since injury, and completeness of injury were obtained from all individuals with SCI (Table 4.1).

Table 4.1 Demographic Information and Clinical Characteristics from Participants with SCI Enrolled in the Study

ID	Age (years)	Sex	Spinal Level of injury	Duration since injury (years)	Complete (C) /Incomplete (I)	Presence of Neuropathic Pain	Handedness
SCI-01	46	M	T11	12	C	Yes	Right
SCI-02	46	M	T2	16	C	No	Left
SCI-03	57	M	T10/11	6	C	Yes	Right
SCI-04	34	M	T12	9	C	No	Right
SCI-05	35	M	T11	14	C	No	Right
SCI-06	60	M	T4	10	C	No	Right
SCI-07	29	F	T4	8	I	Yes	Right
SCI-08	37	F	L1	12	I	Yes	Left
SCI-09	49	M	T6	24	C	Yes	Right
SCI-10	43	F	T11	26	C	No	Left
SCI-11	46	M	T11/T12	26	C	Yes	Right
SCI-12	54	M	T1	27	I	No	Right
SCI-13	60	M	C5	30	I	Yes	Right
SCI-14	28	M	T6	2	I	Yes	Right
SCI-15	48	F	L1	30	I	Yes	Right
SCI-16	45	M	T7	30	I	Yes	Right
SCI-17	47	M	T7	10	C	No	Right
SCI-18	61	F	C4/C5	10	I	Yes	Left
SCI-19	55	M	T4	16	C	Yes	Right

4.2.2 Cognitive testing

All participants were administered the Neuropsychiatric Unit Cognitive Assessment Tool (NUCOG), which is a cognitive screening test that evaluates multiple cognitive domains such as attention, memory, visuoconstructional ability, executive function, and language skills (Walterfang et al., 2006). The duration of this test is approximately 20-30 minutes and scores for each of the sub-domains are calculated out of 20 points. The composite

NUCOG score is calculated as the sum of the scores from all five cognitive domains. The NUCOG test has been evaluated on patients with neuropsychiatric disorders, showing sensitivity in differentiating patients with dementia and psychiatric subgroups, and has shown to be highly correlated with Mini-Mental State Examination (MMSE) scores (Walterfang et al., 2006). This test has also been used in evaluating cognitive impairment in individuals with SCI, showing lower scores overall in adults with SCI compared to AB adults across all five domains of the NUCOG test (Craig et al., 2016, 2017). For the purpose of this study, the NUCOG test was administered to provide a simple and streamlined method to evaluate potential cognitive differences between SCI and AB groups.

4.2.3 N-back task

The N-back task was implemented with three separate levels of cognitive load: 0-back, 2-back, and 3-back, with stimuli presented via a computer screen, using E-Prime 2.0 software (Psychology Software Tools, Pittsburgh, PA) (Figure 4.1). The 1-back task was not used in this study due to its simplicity and similarity in cognitive load to the 0-back task. Participants were instructed to click either a left or right arrow key on a computer keyboard based on the letter stimulus displayed on the screen. With increasing N , the working memory load increased for participants, thus higher N is associated with greater task difficulty (Kane et al., 2007). Each N-back task consisted of three blocks, interleaved with 30 seconds of a resting period in which participants were instructed to not click any buttons. Within each block of the N-back task, participants were shown white letters on a black screen in succession, with an inter-trial interval of 2 seconds and 30 total letters, in pseudo-randomized order consistent across participants. Across all N-back tasks, the number of letters (or trials) were the same; however, different numbers of target and non-target letters

were used based on the N-back task level. For the 0-back task, there were 10 target letters and 20 non-target letters for each block; for the 2-back task, there were 8 target and 22 non-target letters per block; and lastly, for the 3-back task, there were 7 target and 23 non-target letters per block. In the 0-back task, participants were instructed to click the right arrow key only when the target letter 'X' appeared on the screen; otherwise, participants were instructed to click the left arrow key. For the 2-back task, participants were instructed to click the right arrow key only if they saw the same letter two letters ago; otherwise, they were instructed to click the left arrow key. Lastly, for the 3-back task, participants were instructed to click the right arrow key on the target letter, defined as the same letter that appeared three letters ago (Figure 4.1).

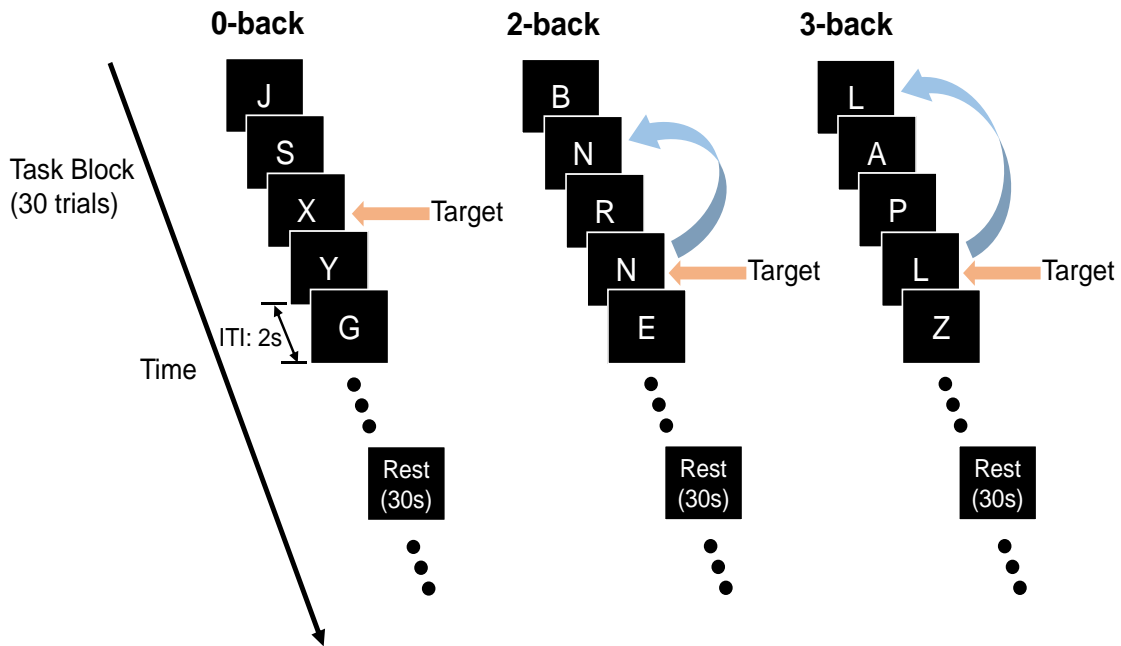


Figure 4.1 N-back task design showing each block and each task level, with examples of letters shown on a computer screen. ITI = inter-trial interval. For each N-back task level, a total of three blocks were implemented. Participants were asked to press a 'right' computer key on all target letters and press a 'left' computer key for all non-target letters.

4.2.4 fNIRS data acquisition

A continuous wave fNIRS system with 10 optode sources and 24 detectors was used, with 690 nm and 830 nm lasers (CW6 System, TechEn Inc., Milford, MA). A total of 30 channels were configured across the following regions of interest (ROI): right and left dorsolateral prefrontal cortex, medial prefrontal cortex, right and left inferior parietal lobe, and the right and left motor cortex (Figure 4.2). Four short source-detector separation (SDS) channels were configured at a distance of 0.84 cm between the source and detector, while 26 long SDS channels were placed at a distance of 3 cm between the source and detector. Short SDS channels are typically used to remove physiological signals from the extracerebral layers, recording information from the scalp and the cerebrospinal fluid (Brigadoi & Cooper, 2015). In the present study, data from the short SDS channels did not substantially improve the signal to noise ratio (SNR); thus, only data from the 26 long SDS channels were used and reported for subsequent analyses. Channel locations were determined and positioned with the aid of Brain Sight Neural Navigator (Rogue Research Inc. Neuronavigation System, Canada). For each participant, anatomical landmarks were collected, and the standard Montreal Neurological Institute (MNI) brain template was transformed into each individual's space. All channels were placed according to MNI coordinates pre-defined in the literature (Table 4.2).

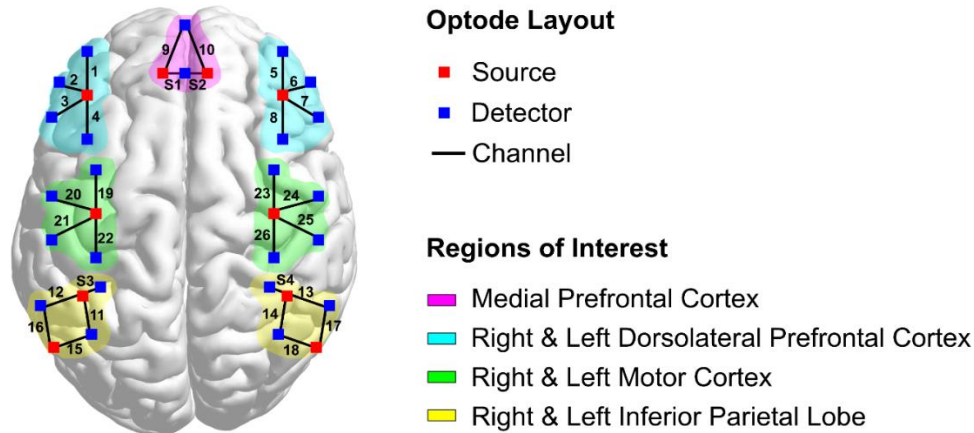


Figure 4.2 Optode layout design used for the fNIRS study. The channel #, source, and detectors are displayed, along with the following regions of interest: medial prefrontal cortex, right & left dorsolateral prefrontal cortex, right & left motor cortex, and right & left inferior parietal lobe. There are a total of 26 channels and 4 short source-detector separation channels (S1-S4), containing 10 sources and 24 detectors.

Table 4.2 Montreal Neurological Institute (MNI) Coordinates Displayed for each Region of Interest (ROI) used in the fNIRS Setup. PFC: Prefrontal Cortex; DLPFC: Dorsolateral Prefrontal Cortex

ROI	X	Y	Z	Reference	Channel #'s
Right DLPFC	48	21	38	(Watanabe et al., 2013)	5, 6, 7, 8
Left DLPFC	-48	21	38	(Watanabe et al., 2013)	1, 2, 3, 4
Medial PFC	0	61	22	(Brier et al., 2012; Greicius et al., 2004; Sestieri et al., 2011)	9, 10
Right Motor Cortex	40	-23	53	(Brier et al., 2012; Ellermann et al., 1998; Fox et al., 2009)	23, 24, 25, 26
Left Motor Cortex	-40	-23	53	(Brier et al., 2012; Ellermann et al., 1998; Fox et al., 2009)	19, 20, 21, 22
Right Inferior Parietal Lobe	52	-54	36	(Watanabe et al., 2013)	13, 14, 17, 18
Left Inferior Parietal Lobe	-52	-54	36	(Watanabe et al., 2013)	11, 12, 15, 16

4.2.5 Preprocessing

The raw fNIRS intensity data were first converted to optical density values, then wavelet-based head-motion correction was performed using 1.5 times the interquartile range as a threshold to remove outliers (Molavi & Dumont, 2012). Data were then bandpass filtered using a pass-band from 0.01 to 0.15 Hz to remove physiological noise sources such as cardiac rate and respiratory rate, while keeping the task frequency into consideration. The data were then converted from optical density values to oxygenated hemoglobin (HbO), deoxygenated hemoglobin (HbR), and total hemoglobin (HbT) values. Due to the highest signal to noise ratio observed in the HbO signal, subsequent analyses are shown for the HbO data. Data preprocessing was performed using custom scripts in MATLAB R2022b (The MathWorks Inc., Natick, Massachusetts) and HOMER2 functions (Huppert et al., 2009).

4.2.6 Behavioral scores

To evaluate performance, accuracy and response time were collected for each block and each N-back task across all participants. Accuracy was calculated for each block of the N-back task and is defined as the number of correct responses divided by the total number of responses. Accuracy was calculated for all three block periods of the N-back task separately, as well as averaged together to obtain a mean accuracy score across all blocks for each participant. Furthermore, the response time was collected from each participant during each N-back task trial and the mean response time was obtained by averaging across all trials in each block. Sensitivity was also calculated to evaluate performance on the N-back task, due to the imbalance in number of target and non-target trials. Sensitivity was quantified by calculating d-prime scores, which were obtained by subtracting the z-

transform of the false alarm rate from the z-transform of the hit rate (Stanislaw & Todorov, 1999). The hit rate was defined as the number of times the participant responded correctly to the target letters divided by the total # of targets, whereas the false alarm rate was defined as the number of times the participant responded incorrectly at non-target letters divided by the total number of non-target letters. In the case that the hit rate or false alarm rate values were equal to 1, the value was replaced by $1 - 1/(2*n)$, where n = total # of hits. Additionally, if the hit rate or false alarm rate values were equal to 0, then the value was replaced with $1/(2*n)$, according to Macmillan and Kaplan's rule for handling 1's and 0's (Macmillan & Kaplan, 1985).

4.2.7 fNIRS task activation metrics

For the N-back fNIRS data, block averaging and general linear model (GLM) analysis were performed. For block averaging, the time-series data were averaged for each block of the N-back task, as defined by 60 seconds of task followed by 30 seconds of rest. For each block, data collected during the 5 seconds prior to the start of each task stimulus were averaged and subtracted from the rest of the block's time-series data, to normalize the data. Subsequently, each of the three blocks were averaged to generate a block-averaged hemodynamic response curve for each channel. Characteristics from the block-averaged data were extracted as task activation metrics, as follows: the area under the curve (AUC) of the hemodynamic response, time-to-peak (TTP), maximum HbO (maxHbO), and standard deviation of the HbO (stdHbO) signal. The maxHbO and stdHbO signals were obtained using the concatenated time-series data from all three blocks. For GLM, the N-back task was represented as a box-car function convolved with the canonical hemodynamic response function (Ashburner et al., 2014). This convolved hemodynamic

response signal was input as the task regressor in the GLM model, with the preprocessed HbO time-series input as the outcome variable, and the beta coefficient was estimated for each channel to represent task activation. For each of the fNIRS metrics, the values were z-scored across all channels, for each participant. Each of the fNIRS task activation metrics were then correlated with performance metrics on the N-back task: accuracy, response time, and d-prime scores.

4.2.8 Statistical analysis

All statistical analyses were performed using R 4.2.3 (R Core Team, 2023). For the N-back behavioral scores, a mixed-design ANOVA was performed for accuracy and response time values separately, with the following independent variables: group (SCI vs. AB), block (first, second, vs. third), and task (0-back, 2-back, vs. 3-back). The “block” and “task” variables were treated as within-subjects factors while the “group” variable was treated as a between-subjects factor. Post-hoc analyses were subsequently performed using paired t-tests when comparing between N-back task levels or block periods, while independent-samples t-tests were performed when comparing between the AB vs. SCI group. To correct for multiple comparisons, Bonferroni corrections were performed accordingly. For the fNIRS metrics, similar mixed-design ANOVAs were performed with each fNIRS metric constituting a separate independent variable and independent-samples t-tests were performed for each metric, task, and channel, with Bonferroni corrections performed for post-hoc multiple comparison testing. For all correlation analyses, Pearson’s correlation method was used, with Benjamini-Hochberg’s false discovery rate corrections applied for multiple testing across brain regions.

4.3 Results

4.3.1 NUCOG scores

We observed no significant differences in the composite NUCOG scores between AB and SCI groups (independent-samples t-test, $t(42) = 0.93$, $p = .36$, 95% confidence interval: [-1.43, 3.87]), with the AB group showing a slightly higher mean NUCOG score than the SCI group (AB: 92.38 ± 4.50 , SCI: 91.16 ± 4.05) (Figure 4.3A). Since the composite NUCOG score is composed of 5 distinct cognitive domains, these sub-domains were further analyzed. Significant differences were observed in the executive function sub-domain of the NUCOG test, in which the SCI group scored significantly lower than the AB group (Figure 4.3B) (independent-samples t-test, $t(42) = 2.98$, $p = .0047$, 95% confidence interval: [0.35, 1.81], Bonferroni adjusted $\alpha = .01$ (.05/5). No significant differences between the two groups were observed across the other cognitive domains such as attention, visuoconstructional, memory, and language skills (Figure 4.3B).

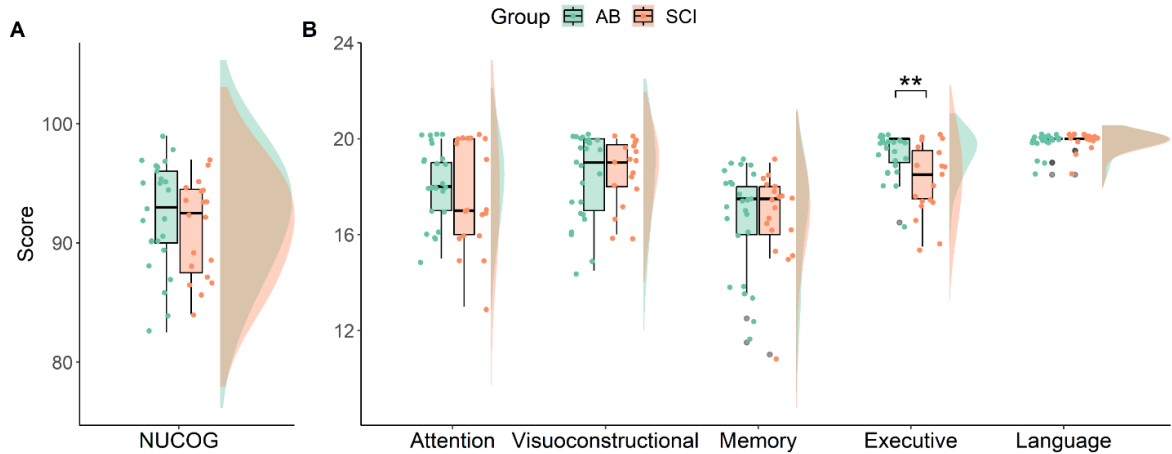


Figure 4.3 **A)** Neuropsychiatric Unit Cognitive Assessment Tool (NUCOG) scores for both able-bodied (AB) and spinal cord injury (SCI) groups are shown in green and orange bars, respectively. **B)** Sub-domains of the NUCOG test scores are also indicated, with significant differences shown between the AB and SCI group in executive function (independent-samples t-test, $t(42) = 2.98$, $p = .0047$, 95% confidence interval: [0.35, 1.81], Bonferroni adjusted $\alpha = .01$ (.05/5)). The total scores from the NUCOG subdomains: attention, visuoconstructional, memory, executive, and language, are added to obtain the composite NUCOG score. ** $p < .01$.

4.3.2 N-back task performance

For all three N-back task behavioral scores: accuracy, response time, and d-prime, significant differences were observed between the N-back tasks and between blocks of the 2-back task in particular (Figure 4.4A-C). We found no significant differences between the SCI and AB groups for accuracy (mixed-design ANOVA, $F(1,42) = 0.601$, $p = .44$), response time (mixed-design ANOVA, $F(1,42) = 0.188$, $p = .67$), and d-prime scores (mixed-design ANOVA, $F(1,42) = 1.76$, $p = .19$). Across all behavioral metrics, there were significant effects of the N-back task level (0-back, 2-back, and 3-back levels) (mixed-design ANOVA; accuracy: $F(2,84) = 72.43$, $p = 5.22e-19$; response time: $F(2,84) = 81.94$, $p = 1.83e-20$; d-prime: $F(2,84)$, $p = 2.82e-07$). This shows that the N-back task level contributes significantly to the behavioral scores. Within each task level, there were three

blocks, and significant block effects were found for all three behavioral metrics (mixed-design ANOVA; accuracy: $F(2,84) = 3.15$, $p = .048$; response time: $F(2,84) = 43.24$, $p = 1.23e-13$; d-prime: $F(2,84) = 6.78$, $p = .002$), in addition to an interaction effect between task level and block (mixed-design ANOVA; accuracy: $F(4,168) = 6.30$, $p = 9.57e-05$; response time: $F(4,168) = 24.70$, $p = 4.28e-16$; d-prime: $F(4,168) = 6.35$, $p = 8.81e-05$). Post-hoc paired t-tests revealed significant differences in accuracy scores between the 0-back and 3-back tasks, as well as the 2-back and 3-back tasks for both SCI and AB groups, across all blocks (Bonferroni corrected $\alpha = .0027$ (.05/18), all p-values $< .0027$) (Figure 4.4 A). For response time, across all blocks, significant differences were found between the 0-back and 2-back task, and between the 0-back and 3-back task (Bonferroni corrected $\alpha = .0027$ (.05/18), all p-values $< .0027$), but no significant differences were observed between the 2-back and 3-back tasks (Figure 4.4 B). Lastly, d-prime scores revealed significant differences between the 0-back and 2-back task only, across all blocks (Bonferroni corrected $\alpha = .0027$ (.05/18), all p-values $< .0027$) (Figure 4.4 C).

Between blocks, we found that performance was not constant and showed significant differences particularly during performance of the 2-back task (Figure 4.4 A-C). For accuracy on the 2-Back task, there were significant differences in the AB group, between the first block and second block (paired-samples t-test with Bonferroni adjusted $\alpha = .0027$ (.05/18), $p = 6.83e-04$) (Figure 4.4 A). For response time on the 2-Back task, there are significant differences in the SCI group, between the first block and second block (paired-samples t-test with Bonferroni adjusted $\alpha = 0.0027$ (.05/18), $p = 9.03e-05$), and between the first block and third block (paired-samples t-test with Bonferroni adjusted $\alpha = .0027$ (.05/18), $p = 1.09e-04$) (Figure 4.4 B). Similarly, significant differences for response

time on the 2-Back task were observed for the AB group as well, between the first block and second block (paired-samples t-test with Bonferroni adjusted $\alpha = .0027 (.05/18)$, $p = 1.28e-09$), and between the first block and third block (paired-samples t-test with Bonferroni adjusted $\alpha = .0027 (.05/18)$, $p = 1.93e-08$) (Figure 4.4 B). For d-prime scores, significant differences were observed between the second block and third block, only for the AB group (paired samples t-test with Bonferroni adjusted $\alpha = .0027 (.05/18)$, $p = .0015$) (Figure 4.4 C).

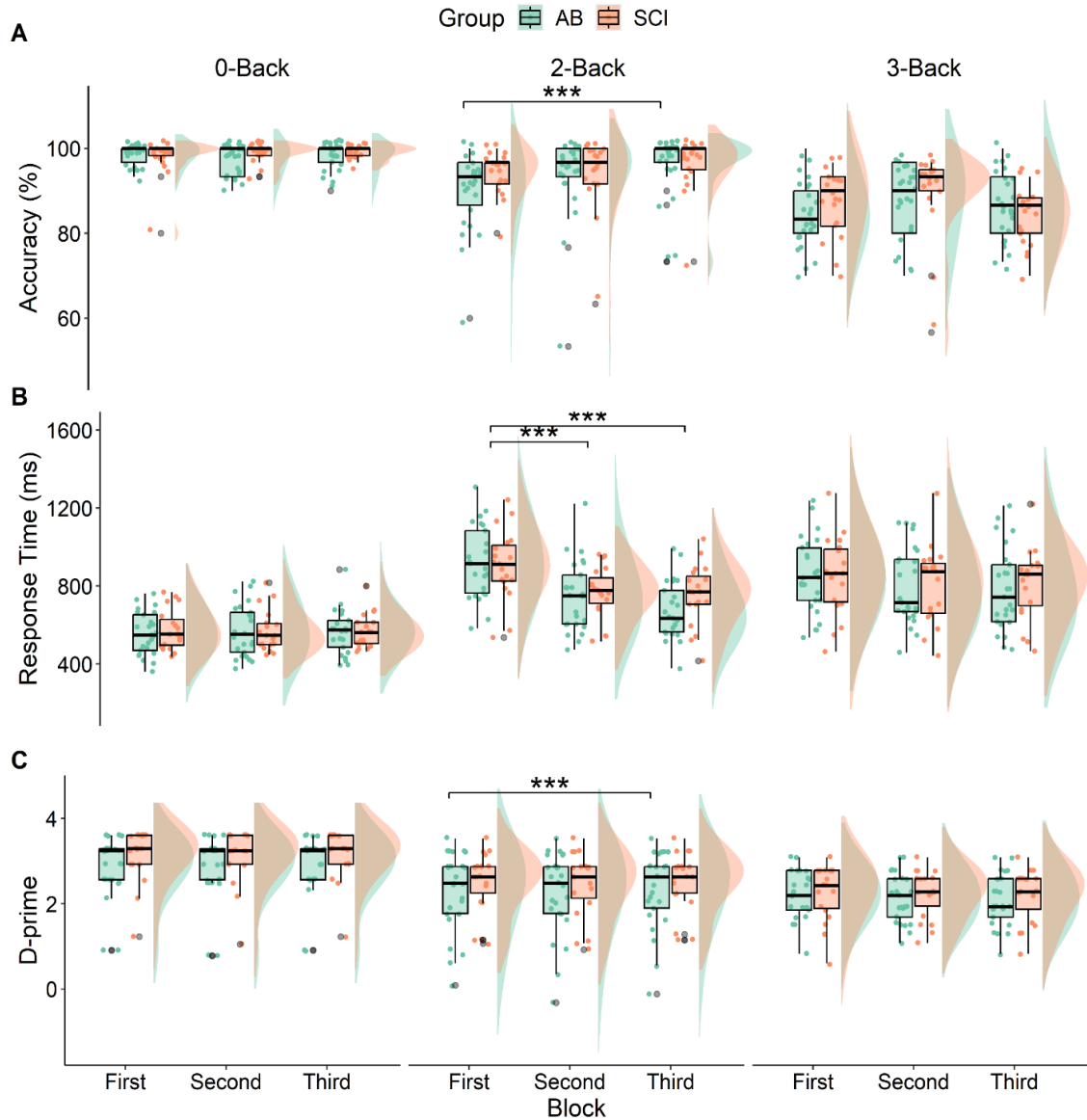


Figure 4.4 **A)** Accuracy, **B)** response time, and **C)** d-prime scores are shown for both spinal cord injury (SCI) and able-bodied (AB) groups, for each N-back task (0-Back, 2-Back, and 3-Back) and each block (first, second, and third). *** $p < .001$.

4.3.3 fNIRS task activation differences

The SCI group had a significantly higher maxHbO value than the AB group in channel #14, which corresponds to the right inferior parietal lobe, during the performance of the 2-back task (independent-samples t-test, $p = .0018$, FDR-correction at $\alpha=0.05$, adjusted $p =$

.0473) (Figure 4.5 B&E). In the same region, the AUC of the hemodynamic response curve was also higher in the SCI group compared to the AB control group; however, results were not significant after false discovery rate (FDR) correction (independent-samples t-test, $p = .044$, FDR-correction at $\alpha=0.05$, adjusted $p = .57$). Differences in task activation in channel #14 seem to be specific to the 2-back task and were not observed for the 0-back or 3-back tasks. During the performance of the 2-back task, there were some regions that showed higher task activation values in the AB group than SCI group, such as channels 19, 21, and 22 (Figure 4.5 B&E), which are located in the left motor cortex. In channels 19 and 21, beta values were higher in the AB group than the SCI group, and in channel 22, the AUC, TTP, and maxHbO values were all higher in the AB group than the SCI group; however, the results were not significant after FDR correction. Most differences in task activation metrics between the AB and SCI groups were found in the 2-back task, while the 0-back task showed the least number of differences, being of lower cognitive load (Figure 4.5 A&D). For the 3-back task, the SCI group showed higher beta values than that of the AB group, in channels 3 and 8 (left and right DLPFC, respectively); however, the results did not survive FDR correction (independent-samples t-test; channel 3: $p = .022$, adjusted $p = .47$; channel 8: $p = .036$, adjusted $p = .47$; FDR-correction at $\alpha=0.05$) (Figure 4.5 C&F).

The overall task activation patterns across channels were similar between the SCI and AB groups, such as overall increased activation in maxHbO and stdHbO from channels 11-15, which correspond to areas of the inferior parietal lobes, as compared to the other channels (Figure 4.5 A-F). This pattern was apparent across all levels of the N-back task. There were significant effects of the channel # on the following metrics: maxHbO, stdHbO,

and beta values (mixed-design ANOVA; maxHbO: $F(25, 1000) = 16.73, p = 1.00e-59$; stdHbO: $F(25, 1000) = 23.16, p = 6.08e-82$; beta: $F(25, 1000) = 1.76, p = .012$).

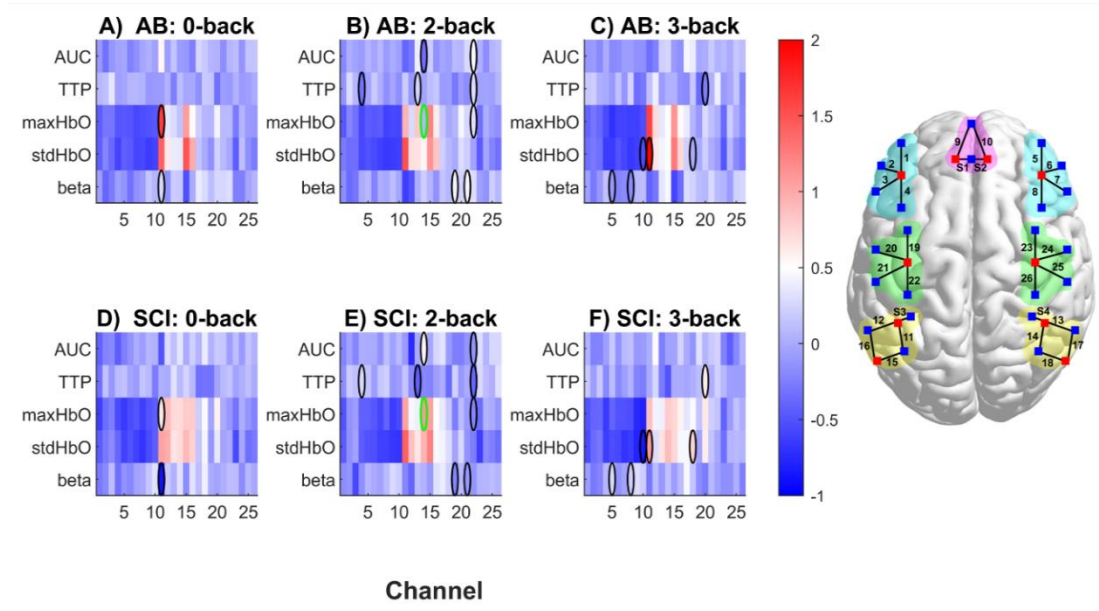


Figure 4.5 N-back working memory task fNIRS metrics between SCI and AB groups, across all 26 channels. The following fNIRS metrics (z-scored) are shown: area under the curve (AUC), time-to-peak (TTP), maximum HbO (maxHbO), standard deviation of HbO (stdHbO), and beta values from GLM analysis. Black ovals indicate significant differences between AB and SCI groups before correcting for multiple comparisons ($p < .05$). The green oval in maxHbO, Channel #14, during the 2-back task shows significant differences between the AB and SCI groups after FDR correction, $\alpha = 0.05$. FDR correction was performed for each N-back task and each fNIRS metric, across all channels.

4.3.4 Task activation and behavioral scores

Significant associations between fNIRS task activation metrics and performance on the N-back tasks were observed for both AB and SCI groups across all fNIRS metrics except for stdHbO, and across both accuracy and response time values, in different brain regions. These significant associations were only observed for the higher cognitive load N-back tasks such as the 2-back and 3-back tasks, with the majority found in the 3-back task. No significant relationship between fNIRS metrics and performance metrics were observed for

the 0-back task. All correlations were corrected for multiple comparisons using FDR correction at $\alpha = 0.05$. The following regions showed significant brain-behavior associations: left inferior parietal lobe (channel #12), right inferior parietal lobe (channel #18), and the right dorsolateral prefrontal cortex (channel #6 & #8) (Table 4.3). Furthermore, significant correlations between fNIRS task activation metrics and NUCOG scores were also observed, for the composite NUCOG scores, visuoconstructional, memory, and attention scores (Table 4.3).

Table 4.3 Pearson’s Correlations Between fNIRS Metrics and Performance Metrics that are Significant after Multiple Comparison Correction using the Benjamini-Hochberg’s False Discovery Rate (BH-FDR) Method

Group	Task	Channel #	Performance metric	fNIRS metric	r-value	p-value	FDR adjusted p-value
AB	2-Back	12	Accuracy	beta	-0.71	0.00091	0.024
AB	3-Back	6	Response Time	TTP	-0.65	0.00052	0.014
AB	3-Back	18	Accuracy	TTP	0.63	0.0010	0.027
SCI	3-Back	8	Response Time	AUC	0.71	0.00097	0.025
SCI	3-Back	8	Response Time	maxHbO	0.75	0.00047	0.012
AB	2-back	23	NUCOG	AUC	0.65	0.0013	0.035
AB	2-back	23	NUCOG	TTP	-0.60	0.0019	0.049
AB	3-back	22	NUCOG	TTP	0.61	0.0014	0.037
AB	2-back	8	Visuo-constructional	beta	0.65	0.0014	0.035
AB	2-back	23	Memory	AUC	0.66	0.0013	0.033
SCI	2-back	13	Attention	AUC	0.67	0.0016	0.042
SCI	3-back	3	Visuo-constructional	TTP	0.69	0.0011	0.028
SCI	3-back	26	Visuo-constructional	beta	0.70	0.0016	0.042

4.4 Discussion

In the present study, we investigated differences in cognitive function between individuals with SCI and AB controls using the NUCOG test and N-back task with three different cognitive loads of increasing difficulty. We also investigated differences in functional brain hemodynamic activity between the SCI and AB groups using fNIRS, and evaluated the relationship between the brain's hemodynamic characteristics and cognitive performance metrics. On the NUCOG test, we observed significant differences between the SCI and AB groups on measures of executive function, but no significant differences were observed in other sub-domains of the NUCOG test. For the N-back task, across the three levels of difficulty, no significant differences were observed between the SCI and AB group; however, both groups performed worse as the level of difficulty increased. Although there were no significant differences in N-back performance scores between the two groups, functional brain hemodynamic activity differences were observed between the SCI and AB groups, particularly in the right inferior parietal lobe.

4.4.1 Lower executive function scores in individuals with SCI

We found no significant differences in performance on the composite NUCOG scores between individuals with SCI and AB controls; however, significant differences were observed in the executive function sub-domain of the NUCOG test. The executive function test contains questions involving motor sequencing, categorical fluency, abstract thinking, and managing interference (Walterfang et al., 2006). Lower scores in executive function could potentially be due to the motor impairment observed in individuals with SCI, since the executive function test contains a motor sequencing task, which relies on the participants following a 3-step sequence of hand movements, repeated 5 times with each

hand. Although all participants had retained upper-body movement, some may have struggled with fine motor control of the hands, such as an SCI subject with C4-5 injuries, thus impacting the executive function score. Craig and colleagues observed reduced executive function in individuals with SCI compared to AB controls as well; however, they also reported reduced cognitive functions in the other NUCOG sub-domains as well, which were not apparent in our cohort (Craig et al., 2017). Furthermore, when administered the Delis-Kaplan Executive Function test for verbal fluency, individuals with SCI were shown to score significantly lower than age-matched healthy controls (Chiaravalloti et al., 2018). Cohen and colleagues evaluated executive function using flanker and card sorting tests, and also found that individuals with SCI performed significantly worse than controls, suggesting that cognitive screening tests for individuals with SCI may want to focus on targeting executive function (Cohen et al., 2017). In a meta-analysis conducted by Sandalic and colleagues, adults with SCI were found to experience deficits in cognitive functioning when compared to AB individuals, mostly in attention and executive functioning domains (Sandalic, Craig, et al., 2022). These studies are consistent with our findings of lower executive function scores in individuals with SCI as compared to AB controls. It is important to note that in evaluating the structural validity of the NUCOG test using congeneric confirmatory factor analyses, Sandalic and colleagues found that the total composite NUCOG score was sensitive to differences in neurocognitive capacity; however, subdomains such as executive function had poor fit, while attention and visuoconstruction had adequate model fit (Sandalic, Tran, et al., 2022).

4.4.2 Similar N-back scores between SCI and AB groups

To our knowledge, this is the first study which has implemented the N-back task to study working memory function in individuals with SCI. The SCI and AB groups performed similarly on the N-back tasks throughout all three levels of difficulty. This finding is consistent with results from the NUCOG test, particularly in the memory subdomain, which also revealed no significant differences between the SCI and AB groups. We observed decreased performance in both groups with increasing N-back task level, which was expected, since increasing working memory load increases the difficulty of the task, resulting in decreased accuracy, longer response times, and decreased d-prime values (Lamichhane et al., 2020). Both groups performed the worst in the 3-back task and we expect that increasing the working memory load further would display a similar downwards trajectory in performance.

Within the 2-back task, we observed significant differences between blocks. Both SCI and AB groups had a significantly longer response time in the first block compared to the second and third blocks. This may be due to learning effects which took place, since the 2-back task is much more difficult than the 0-back task; therefore, there is more room for improvement in scores throughout the blocks. Improvements in N-back task performance have been observed both within and between-sessions (Yeung & Han, 2023), and has been used in paradigms to train working memory (Miró-Padilla et al., 2019; Soveri et al., 2017). It is important to note that improvements in N-back task performance may not necessarily transfer to other domains or other measures of cognitive abilities in healthy adults (Thompson et al., 2013); however, it may be useful for cognitive training for individuals with SCI with working memory impairments. Therefore, future studies may

want to investigate the efficacy of the N-back task in training individuals with SCI with cognitive impairments.

4.4.3 Increased brain activation in individuals with SCI during the 2-Back task

Although we did not observe significant differences in N-back task performance metrics between individuals with SCI and AB controls, we found significant fNIRS task activation differences between the two groups. Significant differences in maximum hemoglobin concentration were observed in the right inferior parietal lobe during performance of the 2-back task. In this region, the SCI group had a higher maximum hemoglobin concentration value than the AB group, which may represent increased effort in performance of the 2-back task. The right inferior parietal lobe is consistently activated across subjects in n-back studies (Owen et al., 2005), and is involved in multiple functions, spanning from attention to action processing (Caspers et al., 2013). Brain activity has been found to be higher in more cognitively demanding tasks such as the 2-back task, as compared to lower cognitive load tasks such as the 0-back or 1-back task (Braver et al., 1997; Herff et al., 2014; Meidenbauer et al., 2021). We found greater similarity between the SCI and AB groups in the 0-back task, perhaps due to it being an easier task and involving fewer working memory faculties than the 2-back or 3-back tasks. Although the performance between the AB and SCI groups were not significantly different in the 2-back task, it is possible that the SCI group activated the right inferior parietal lobe more in order to focus and apply more cognitive effort to the task. Individuals who are trained with the N-back task over time typically show decreased activation in various brain regions including the inferior parietal cortex, particularly for higher load N-back tasks (Miró-Padilla et al., 2019; Vermeij et al., 2017; Yeung & Han, 2023). This likely resembles the lower amount of effort in task

activation needed as individuals improve on the N-back task. Therefore, further cognitive training in individuals with SCI may reduce task activation in the right inferior parietal lobe and warrants further investigation.

4.4.4 fNIRS task activation and its association with behavioral scores

We observed significant associations between fNIRS task activation metrics and performance scores on the N-back task, as well as on the NUCOG scores. The significant brain-behavior associations were observed for both SCI and AB groups; however, those in the SCI and AB groups showed significant associations in different regions of the brain. For the SCI group, increased response time in channel 8, corresponding to the right DLPFC, was associated with increased fNIRS task activation metrics, such as maxHbO and AUC values. Whereas for the AB group, significant associations were observed in channels 12, 6, and 18, in regions of the left IPL, right DLPFC, and right IPL regions, respectively. It is possible that brain-behavior interactions between the AB and SCI groups are differently expressed. No significant brain-behavior associations were observed for the 0-back task, which is consistent with Lamichhane and colleagues' study on cognitive load in the N-back task, as they revealed that brain-behavior relationships are stronger in high load conditions (up to the 6-back task), as compared to low-load conditions, such as the 0-back and 1-back task (Lamichhane et al., 2020).

4.4.5 Limitations

It is important to note limitations of the current study, such as the limited number of fNIRS channels covering the brain. Having more channels covering would allow for greater spatial resolution and analyses on the interactions between distinct brain regions. Additionally, having a larger sample size would allow for further analysis of high-

performers vs. low-performers, which may be investigated in future studies, particularly since there may be heterogeneity within the SCI group. The lower sample sizes may underpower some of these comparisons. In the current study, we only used the N-back task to evaluate working memory during fNIRS acquisition; however, it may be beneficial to also include other cognitive tasks such as the Stroop task and Flanker task to confirm if the differences observed in the N-back task are similar to that of other cognitive tasks.

4.5. Conclusion

Using fNIRS coupled with an N-back working memory task, the current study investigated differences in cognitive function between individuals with SCI and AB controls. We found increased activity in the right inferior parietal lobe in individuals with SCI during the 2-back task as compared to the AB group. However, no differences in N-back task performance were observed between the SCI and AB groups, despite differences in executive function scores on the NUCOG subdomain test.

CHAPTER 5

INCREASED FRACTIONAL AMPLITUDE OF LOW FREQUENCY FLUCTUATIONS IN INDIVIDUALS WITH SPINAL CORD INJURY (AIM 2)

5.1 Introduction

After spinal cord injury (SCI), major reorganization occurs in the corticospinal tract, leading to neurological changes in both the spinal and supraspinal levels of the central nervous system (Oudega & Perez, 2012). SCI results in the disruption of afferent and efferent pathways of the spinal cord and may lead to complications such as pressure sores, urinary sepsis, pneumonia, and deep vein thrombosis (Alizadeh et al., 2019; Sekhon & Fehlings, 2001). Rehabilitation programs often focus on the spinal cord itself but neglect direct observation of neural activity, partly due to the high costs of routine functional magnetic resonance imaging (fMRI) procedures. Due to the limited number of neuroimaging studies investigating SCI, it is not yet clear how functional brain activity is altered after SCI.

Previous studies using structural and functional magnetic resonance imaging (fMRI) have revealed gray matter atrophy and decreased functional connectivity in regions associated with cognitive and affective processing (Karunakaran et al., 2019, 2020). Choe and colleagues reported significantly increased resting-state functional connectivity (RSFC) in the sensorimotor and visual regions of an SCI patient experiencing progressive neurological recovery which persisted over 17 years (Choe et al., 2013). Another study by Hou and colleagues used resting-state fMRI and found that individuals with SCI had decreased inter-hemispheric connectivity between the bilateral primary sensorimotor network, while increased intra-hemispheric connectivity with the motor network (J.-M.

Hou et al., 2014). Furthermore, on a subcortical level, Karunakaran and colleagues used resting-state fMRI to study the thalamic structures of the brain in individuals with SCI and found decreased RSFC in the bilateral mediodorsal nucleus with the right superior temporal gyrus, and anterior cingulate cortex (Karunakaran et al., 2020). These resting-state fMRI studies provide evidence on brain reorganization after SCI (Athanasίου et al., 2017; Hawasli et al., 2018; Oni-Orisan et al., 2016) and may predict motor recovery outcomes after spinal cord injury (J. Hou et al., 2016). However, fMRI is not feasible for longitudinal monitoring in rehabilitation, as it is costly and may cause discomfort to individuals with SCI. In contrast to fMRI, functional near-infrared spectroscopy (fNIRS) is relatively low-cost, portable, and comfortable (Ferrari & Quaresima, 2012). It uses near-infrared light to quantify the brain's relative hemoglobin concentration changes at a high temporal resolution of up to 100 Hz (Jöbsis, 1977; Villringer et al., 1993); these changes are detected due to neurovascular coupling, in which increased neural activity is followed by cerebral blood flow to the active brain region (Phillips et al., 2016). Individuals with SCI can be in a seated position during fNIRS scanning and since fNIRS utilizes light waves, metallic implants are not an exclusion criterion.

During resting-state fNIRS scans, participants are typically asked to stay as still as possible and be in a rested wakeful state. This paradigm may be preferred for older populations and individuals with SCI, particularly if the subject is unable to perform motor tasks involving the upper limbs. Similar to that of resting-state fMRI, connectivity metrics such as RSFC can be obtained from resting-state fNIRS. Using resting-state fNIRS, Karunakaran and colleagues reported lower levels of RSFC in individuals with SCI in the sensorimotor regions as compared to that of able-bodied controls (Karunakaran et al.,

2022). In addition to pair-wise resting-state connectivity metrics such as RSFC, one can obtain regional resting-state metrics such as the amplitude of low-frequency fluctuations (ALFF) to characterize intrinsic resting-state activity in each brain region individually. Vallesi and colleagues observed increased ALFF scores in individuals with subacute SCI in the thalamus compared to that of the control group, suggesting brain reorganization during the subacute phase (mean time since injury of 12.2 weeks) (Vallesi et al., 2022). Altered ALFF scores derived from resting-state fMRI have also been reported in individuals with SCI in the sensorimotor cortex (J.-M. Hou et al., 2014), as well as in regions other than the sensorimotor cortex such as the lingual gyrus and cerebellum (Zheng et al., 2021). However, there are currently no fNIRS studies investigating changes in ALFF scores in individuals with SCI.

The goal of the present study was to characterize differences in regional resting-state activity between individuals with SCI and able-bodied (AB) individuals using fNIRS. We hypothesized that corticospinal tract disruption in individuals with SCI will decrease neurovascular activation and thus decrease resting-state intrinsic brain activity. Region-wise resting-state analyses were performed by quantifying the fractional ALFF (fALFF) scores and comparing these metrics between the SCI and AB groups across all brain regions in a mixed-effects model. Additionally, the fALFF scores were calculated for different frequency bands: Slow-5 (0.01 to 0.027 Hz), Slow-4 (0.027 to 0.073 Hz), and Slow-3 (0.073 to 0.198 Hz) (Buzsáki & Draguhn, 2004) to better characterize frequency-specific differences between the SCI and AB groups. It is critical to better understand functional brain alterations after SCI, to develop effective rehabilitation treatments for individuals with SCI.

5.2 Materials and Methods

5.2.1 Participant data collection

Data were collected from 20 participants with SCI (14M, 6F, mean age = 46.3 ± 10.2 years) and 25 age- and sex-matched able-bodied (AB) controls (19M, 6F, mean age = 43.2 ± 12.28 years) (Table 5.1). Institutional Review Board (IRB) approval was obtained, and participants were recruited from the New Jersey/New York metropolitan area. Prior to the start of the experiment, all participants provided written informed consent. The following exclusion criteria were applied to the spinal cord injury group: (1) being in the acute phase of injury or within 1-year post-spinal cord injury, (2) having tetraplegia or is unable to perform upper limb motor movements, (3) having a history of or concurrent traumatic brain injury (TBI), (4) history of or concurrently has psychiatric disorders such as post-traumatic stress disorder, addiction, bipolar disorder, or schizophrenia, (5) presence of acute illness or infection, (6) history of chronic hypertension, diabetes mellitus, stroke, epilepsy or seizure disorders, multiple sclerosis, Parkinson's disease, (7) illicit drug abuse within the past 6 months, (8) Alzheimer's disease or dementia, (9) not able to speak English, and (10) older than 65 years of age or younger than 18 years of age (D. Y. Chen, Di, Amaya, et al., 2024). The same exclusion criteria were applied to the AB group, except points (1) and (2), which were not relevant to the AB group, since they did not have any injury to the spinal cord.

Table 5.1 For Participants with SCI, Clinical Characteristics such as the Level of Injury and Duration Since Injury are Summarized

Subject #	Age (years)	Sex	Spinal Level of Injury	# Spinal Segments Affected	Complete (C) /Incomplete (I)	Duration since Injury (years)	Handedness
01	46	M	T11	11	C	12	Right
02	46	M	T2	20	C	16	Left
03	57	M	T10/11	12	C	6	Right
04	34	M	T12	10	C	9	Right
05	35	M	T11	11	C	14	Right
06	60	M	T4	18	C	10	Right
07	29	F	T4	18	I	8	Right
08	37	F	L1	9	I	12	Left
09	49	M	T6	16	C	24	Right
10	43	F	T11	11	C	26	Left
11	46	M	T11/T12	11	C	26	Right
12	54	M	T1	21	I	27	Right
13	60	M	C5	24	I	30	Right
14	28	M	T6	16	I	2	Right
15	48	F	L1	9	I	30	Right
16	45	M	T7	15	I	30	Right
17	47	M	T7	15	C	10	Right
18	61	F	C4/C5	25	I	10	Left
19	55	M	T4	18	C	16	Right
20	35	F	C5/C6	24	I	11	Left

5.2.2 fNIRS data acquisition

All participants underwent a resting-state fNIRS scan for 10 minutes. During this scan, participants were asked to keep their eyes open and stare at a computer screen with the word “rest” displayed on the screen in white letters on a black background. This was displayed using E-Prime 2.0 software (Psychology Software Tools, Pittsburgh, PA). During the resting-state scan, the fNIRS device recorded hemodynamic activity from the following cortical areas of the brain: the right and left inferior parietal lobe (RIPL & LIPL), right and left motor cortex (RMOTOR & LMOTOR), right and left dorsolateral prefrontal cortex (RDLPFC & LDLPFC), and the medial prefrontal cortex (MPFC). A continuous

wave fNIRS device with a sampling rate of 25 Hz and lasers of 690 nm and 830 nm wavelengths was used for recording (CW6 System, TechEn Inc., Milford, MA). A total of 26 channels were placed at an optode source to detector distance of 30 mm, while 4 short channels were placed at an optode source to detector distance of 8.4 mm (Brigadoi & Cooper, 2015). The short channels were placed in the following regions: RIPL, LIPL, and MPFC, to reduce physiological noise. Altogether, 10 optode sources and 24 detectors were used for this study (Figure 5.1). Neural navigation was performed for each participant using the Montreal Neurological Institute’s (MNI-152) average structural brain template as a reference to place the optodes in the regions of interest (Brain Sight Neural Navigator, Rogue Research Inc., Canada).

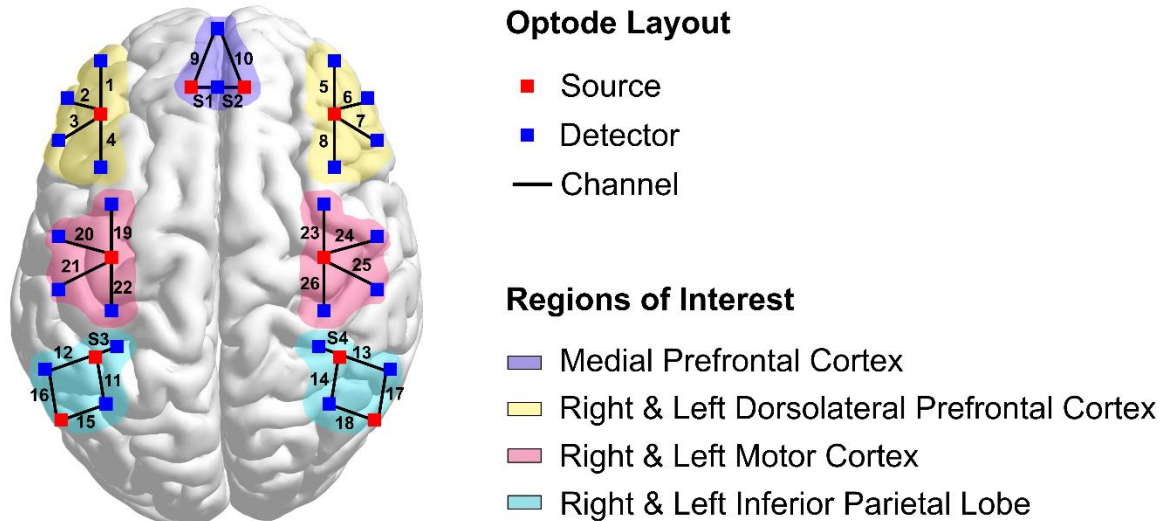


Figure 5.1 Optode layout map showing the number of sources and detectors used for the present study. Sources are indicated by blue squares whereas detectors are indicated by red squares. A total of 26 long channels (source-to-detector distance of 30 mm) were used in this study, with 4 short channels (source-to-detector distance of 8.4 mm) used to regress out physiological noise.

5.2.3 fNIRS data preprocessing

The raw fNIRS light intensity values were first converted to optical density values by taking the incident light intensity divided by the detected light intensity, and then taking the natural logarithm of that ratio (Huppert et al., 2009). Then, wavelet-based head-motion correction was applied to remove motion artifacts by using 1.5 times the interquartile range as a threshold (Molavi & Dumont, 2012). The data were not band-pass filtered since fALFF analysis was applied, which divides the power in the frequency band of interest to that of the entire frequency range. Subsequently, using the modified Beer-Lambert law and a partial pathlength factor of 6.0 for each wavelength (Delpy et al., 1988; Kocsis et al., 2006), the optical density data were converted to oxygenated hemoglobin (HbO), deoxygenated hemoglobin (HbR), and total hemoglobin (HbT). Short channel regression was then performed on the hemoglobin concentration data by taking the short channel that was most proximal to the long channel of interest (channels with a source to detector distance of 30 mm) and then regressing the short channel's signal from the long channel (Gagnon et al., 2012) (Table 5.2). The ordinary least squares method was used in the short channel regression models and the residuals were obtained for further analyses.

Table 5.2 Short Channels that were used in the Short Channel Regression Model for each Respective Long Channel are Listed

Short channel #	Long channel #
S1	1, 2, 3, 4, 9
S2	5, 6, 7, 8, 11
S3	11, 12, 15, 16, 19, 20, 21, 22
S4	13, 14, 17, 18, 23, 24, 25, 26

Channel pruning was performed by taking the signal to noise ratio (SNR) of each wavelength's raw light intensity data (690 nm and 830 nm). The SNR was calculated as

$$SNR = 20 \times \log_{10} \frac{mean(d)}{stdev(d)} \quad (5.1)$$

in which d represents the raw light intensity data from either the 690 nm or 830 nm lasers, and the mean and standard deviation of the raw intensity data during the full 10 minutes of resting-state were considered for SNR calculation (Yücel et al., 2021). An SNR threshold of 10 was used as the cut-off, and if data from either wavelength did not pass the threshold, the data were excluded for that particular channel in HbO, HbR, and HbT concentrations. Data preprocessing was performed in MATLAB R2024a (The MathWorks Inc., Natick, Massachusetts) and used HOMER3 functions (Huppert et al., 2009).

5.2.4 fALFF calculation

The fractional amplitude of low-frequency fluctuations (fALFF) was calculated for all channels by taking the ratio of the power in the low frequency range from 0.01 to 0.1 Hz to that of the total frequency range from 0 to 12.5 Hz (up to the Nyquist frequency) (Zou et al., 2008). For fALFF calculation, the data were not band-pass filtered during the preprocessing stage since we were interested in the power in the total frequency range as well as in that of the low-frequency resting-state activity range. The time-series data were first transformed to the frequency domain using the fast Fourier transform and then the power was calculated for the specified frequency range. fALFF calculation was performed for all subjects and each channel. The fALFF score is reflective of the regional spontaneous resting-state activity and allows us to characterize activity within each specific region of interest (Di, Kim, et al., 2013; Zang et al., 2007; Zou et al., 2008). Furthermore, fALFF calculation was performed by using the Slow-5, Slow-4, and Slow-3 frequency ranges,

from 0.01 to 0.027 Hz (fALFF-Slow-5), 0.027 to 0.073 Hz (fALFF-Slow-4), and 0.073 to 0.198 Hz (fALFF-Slow-3), respectively, in addition to the full resting-state band from 0.01 to 0.1 Hz (Buzsáki & Draguhn, 2004). These distinct frequency bands have been defined by previous studies that investigated the slow oscillations of neural activity (Buzsáki et al., 2003; Gohel & Biswal, 2015; Penttonen & Buzsáki, 2003). By further separating the resting-state data into the Slow-5, Slow-4, and Slow-3 categories, we can reveal the specificity in resting-state activity and better understand the frequency-specific differences in resting-state activity between the SCI and AB groups (Gohel & Biswal, 2015; Karunakaran et al., 2022). In addition to these frequency bands of neuronal oscillation, previous electrophysiological studies have defined Slow-2 (0.198 to 0.5 Hz) and Slow-1 (0.5 to 1.5 Hz) frequency bands as well (Penttonen & Buzsáki, 2003); however, it is important to note that these frequency bands may be contaminated with respiratory rate (typically from 0.16 to 0.33 Hz for healthy adults) and cardiac rate signals (Gohel & Biswal, 2015). Although short channel regression from the extracerebral layers should help minimize the effect of respiratory rate, it is still a large confounding variable to take note of. Therefore, results from the Slow-2 and Slow-1 frequencies were not analyzed for the current study.

Linear mixed-effects modeling was performed for the fALFF scores from each hemoglobin concentration data separately, using the *lme4* package in R and the restricted maximum likelihood algorithm (Bates et al., 2015). The fALFF scores were inputted as the dependent variable whereas the group (AB vs. SCI) and the ROI (7 different regions) were inputted as the independent variables, with the interaction between the group and ROI being of interest. The fixed effects variables in the mixed-effects model were group and

age, while the random effects variable was the “subject” variable, accounting for the different channels within each ROI, for each subject, as follows: $fALFF \sim \text{Group} * \text{ROI} + (1|\text{Subject})$. By taking a linear mixed-effects modeling approach, we could account for the different number of channels per subject due to the different number of channels per region per subject from the channel pruning stage of preprocessing. For each separate ROI, Satterthwaite’s t-tests were performed comparing the AB group’s fALFF scores with that of the SCI group (Kuznetsova et al., 2017).

5.2.5 Resting-state functional connectivity

Resting-state functional connectivity (RSFC) was calculated for all subjects and each hemoglobin concentration separately by using Pearson’s r-correlation. The preprocessed time-series data (0.01 to 0.1 Hz) from each channel were correlated with all other channels, yielding a 26x26 matrix of r-values per subject. The RSFC values were transformed to z-scores using Fisher’s r-to-z transform, and then two-sample t-tests were conducted for each channel-pair, comparing the SCI and AB groups. Multiple comparison corrections were performed using the Benjamini-Hochberg’s false discovery rate (BH-FDR) method (Benjamini & Hochberg, 1995).

5.3 Results

The SNR was calculated for all subjects and all light intensity wavelengths across all channels. Based on the histogram distribution of SNR values across all subjects and channels, an SNR threshold was chosen at 10dB to exclude subjects with noisy data, yet try to retain as much data as possible at the same time (Figure 5.2A). After excluding

channels based on the SNR threshold, most of the noisy channels were observed in channel #'s 11 to 20 (Figure 5.2 B).

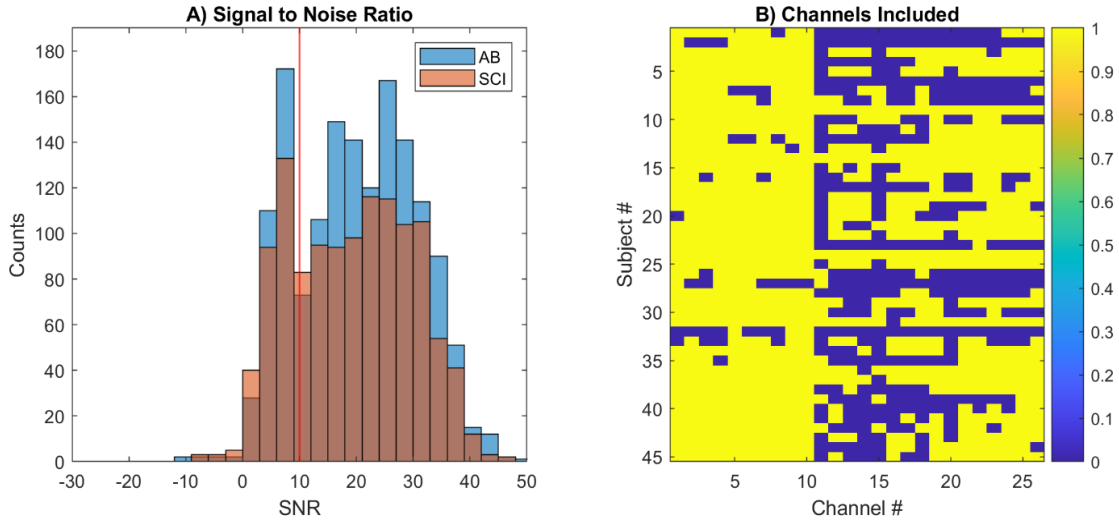


Figure 5.2 **A)** Signal to noise ratio calculated for each channel, for both light intensity wavelengths: 690 nm and 830 nm, across all subjects in each group. A threshold of 10dB was applied so that channels with less than 10dB SNR were excluded from further analyses, as shown by the red line. **B)** Channels included or excluded for each subject, as indicated by 1's and 0's, respectively.

5.3.1 fALFF comparison between SCI and AB groups

fALFF scores computed from resting-state data using the full frequency band were compared between the AB and SCI groups, for all three hemoglobin concentrations: HbO, HbR, and HbT. For HbO concentration data, we observed significantly higher fALFF scores in the SCI group compared to the AB group in the LIPL (linear mixed effects modeling, fixed-effects estimate = 7.991, $t = 3.650$, $p = 0.000281$) and RIPL regions (linear mixed effects modeling, fixed-effects estimate = 6.218, $t = 2.904$, $p = 0.0037$) (Table 5.3). Similarly, for HbT concentrations, higher fALFF scores were observed in the SCI group compared to that of the AB group (linear mixed-effects modeling, LIPL: fixed-effects

estimate = 9.188, $t = 3.957$, $p = 8.29E-05$; RIPL: fixed-effects estimate = 6.296, $t = 2.773$, $p = 0.0056$) in the same regions. For HbR concentrations, only the LIPL region showed significantly higher fALFF scores in the SCI group compared to that of the AB group (mixed-effects modeling, fixed-effects estimate = 9.535, $t = 4.219$, $p = 2.75E-05$) (Figure 5.3). For the rest of the ROI's, no significant differences between the AB and SCI groups were observed for any of the three hemoglobin concentrations (linear mixed effects modeling, Satterthwaite's t-tests, $p > 0.05$) (Table 5.3).

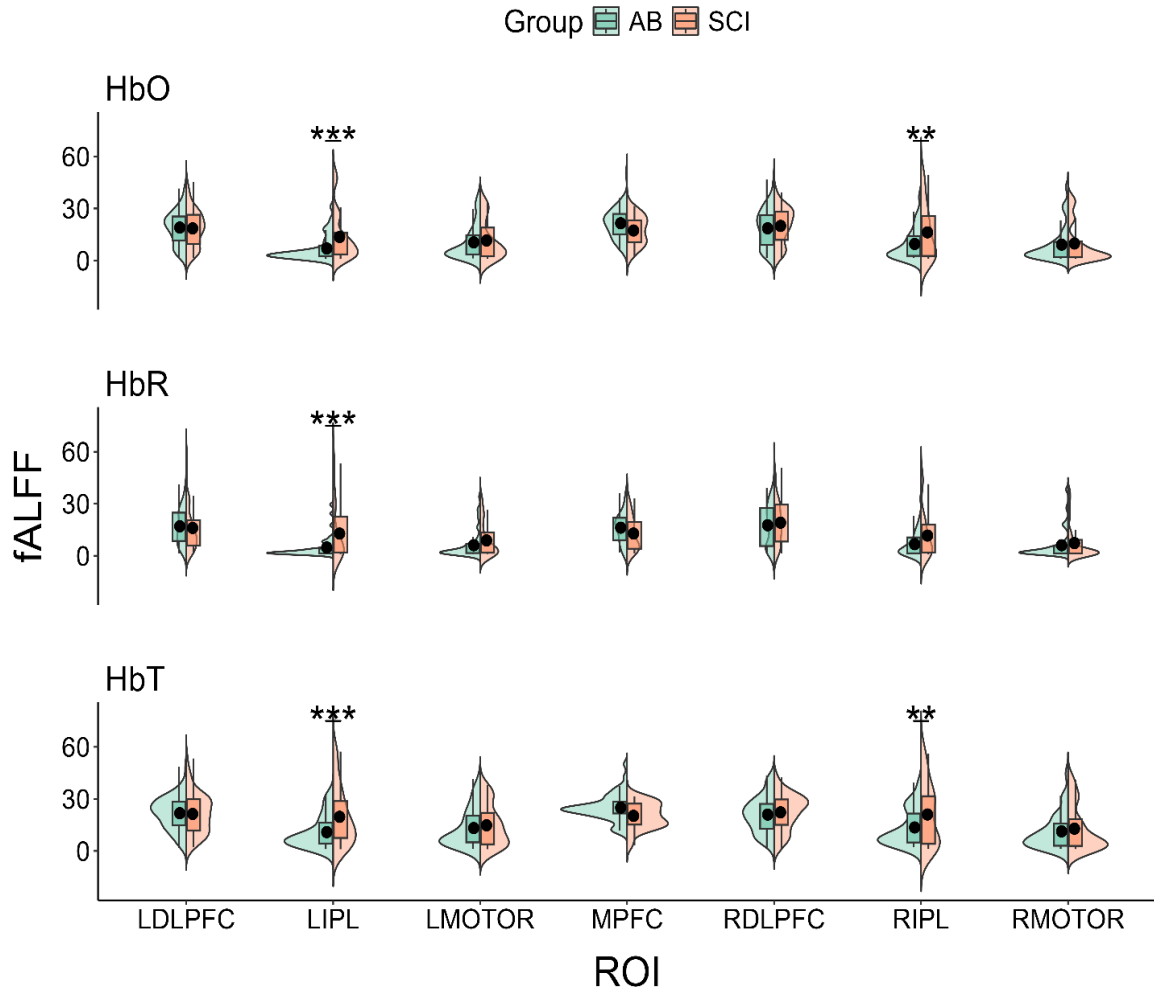


Figure 5.3 fALFF scores shown between the AB and SCI group for each ROI. Significantly higher fALFF scores are observed for the left inferior parietal lobe (LIPL) and the right inferior parietal lobe (RIPL) region.

Table 5.3 Mixed-effects Modeling Results for fALFF Scores Comparing Between the SCI and AB Groups across all ROI. The LDLPFC Region is not Shown Here for the Mixed-effects Modeling Results due to being Held Out as the Reference Level for Comparisons

ROI	Estimate			Standard Error			t-value			p-value		
	HbO	HbR	HbT	HbO	HbR	HbT	HbO	HbR	HbT	HbO	HbR	HbT
LIPL	7.991	9.535	9.188	2.190	2.260	2.322	3.650	4.219	3.957	0.000281 ***	2.75E-05 ***	8.29E-05 ***
LMOTOR	0.651	2.478	0.476	1.931	1.993	2.048	0.337	1.243	0.233	0.7362	0.2142	0.8161
MPFC	-3.647	-2.286	-4.518	2.044	2.109	2.167	-1.785	-1.084	-2.085	0.0747	0.2787	0.0374
RDLPFC	2.308	2.849	1.979	1.692	1.747	1.794	1.364	1.631	1.103	0.1729	0.1033	0.2704
RIPL	6.218	4.075	6.296	2.141	2.210	2.271	2.904	1.844	2.773	0.0037**	0.0656	0.0056**
RMOTOR	1.049	1.845	1.700	1.837	1.896	1.948	0.571	0.973	0.873	0.5681	0.3308	0.3831

5.3.2 fALFF in Slow-5, Slow-4, and Slow-3 frequency bands

In order to obtain more specific frequency information, the resting-state data were separated into the Slow-5 (0.01 to 0.027 Hz) and Slow-4 (0.027 to 0.073 Hz) frequencies, which reveal distinct characteristics of the resting-state signal. The Slow-5 and Slow-4 frequency bands showed region-specificity in fALFF scores. For all hemoglobin concentrations, we observed significant differences specifically in the LIPL region for the

Slow-5 frequency band (linear mixed effects modeling, fixed-effects estimate = HbO: 17.285, HbR: 21.369, HbT: 19.563, t = HbO: 3.307, HbR: 3.665, HbT: 3.385, p = HbO: 0.000988, HbR: 0.000264, HbT: 0.000749) (Table 5.4). In the LIPL region, the SCI group showed significantly higher Slow-5 fALFF scores than the AB group, which was consistent across HbO, HbR, and HbT (Figure 5.4). On the other hand, for the Slow-4 frequency band, both the LIPL and RIPL regions showed significant differences between the AB and SCI groups, in which the SCI group had higher fALFF-Slow-4 scores overall than the AB group (linear mixed effects modeling; LIPL: p = 0.00115 (HbO), p = 6.90E-05 (HbR), and p = 0.000458 (HbT); RIPL: p = 0.0027 (HbO), p = 0.0195 (HbR), and p = 0.0037 (HbT) (Figure 5.5) (Table 5.5). This is more similar to the results observed with the full-band fALFF scores, compared to that of the Slow-5 frequency band.

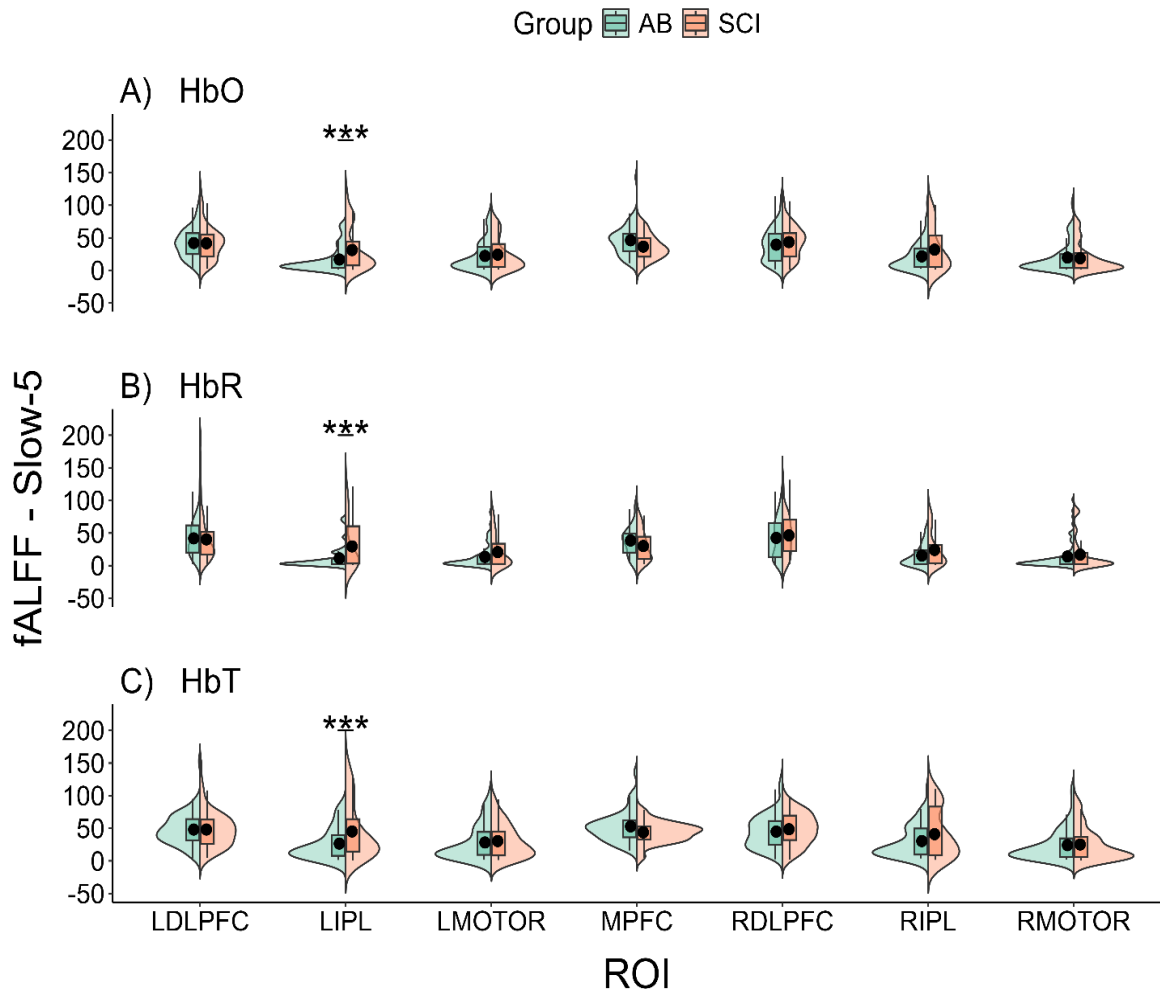


Figure 5.4 fALFF-Slow-5 scores between the AB and SCI group for each ROI. Significant differences found between the AB and SCI groups in the LIPL region.

Table 5.4 Mixed-effects Modeling Results for fALFF-Slow-5 Scores Comparing Between the SCI and AB Groups across all ROI. The LDLPFC Region is not Shown Here for the Mixed-effects Modeling Results due to being Held Out as the Reference Level for Comparisons

ROI	Estimate			Standard Error			t-value			p-value		
	HbO	HbR	HbT	HbO	HbR	HbT	HbO	HbR	HbT	HbO	HbR	HbT
LIPL	17.285	21.369	19.563	5.227	5.830	5.780	3.307	3.665	3.385	0.000988 ***	0.000264 ***	0.000749 ***
LMOTOR	0.0427	5.343	-1.495	4.610	5.142	5.097	0.0093	1.039	-0.293	0.992	0.299	0.769
MPFC	-9.666	-6.872	-10.44	4.878	5.441	5.394	-1.982	-1.263	-1.936	0.047	0.206	0.0532
RDLPFC	5.003	6.293	3.598	4.039	4.506	4.467	1.239	1.397	0.805	0.215	0.162	0.420
RIPL	8.874	5.509	7.752	5.111	5.701	5.652	1.736	0.966	1.372	0.082	0.334	0.170
RMOTOR	-0.896	3.611	0.581	4.386	4.892	4.850	-0.204	0.738	0.120	0.838	0.460	0.904

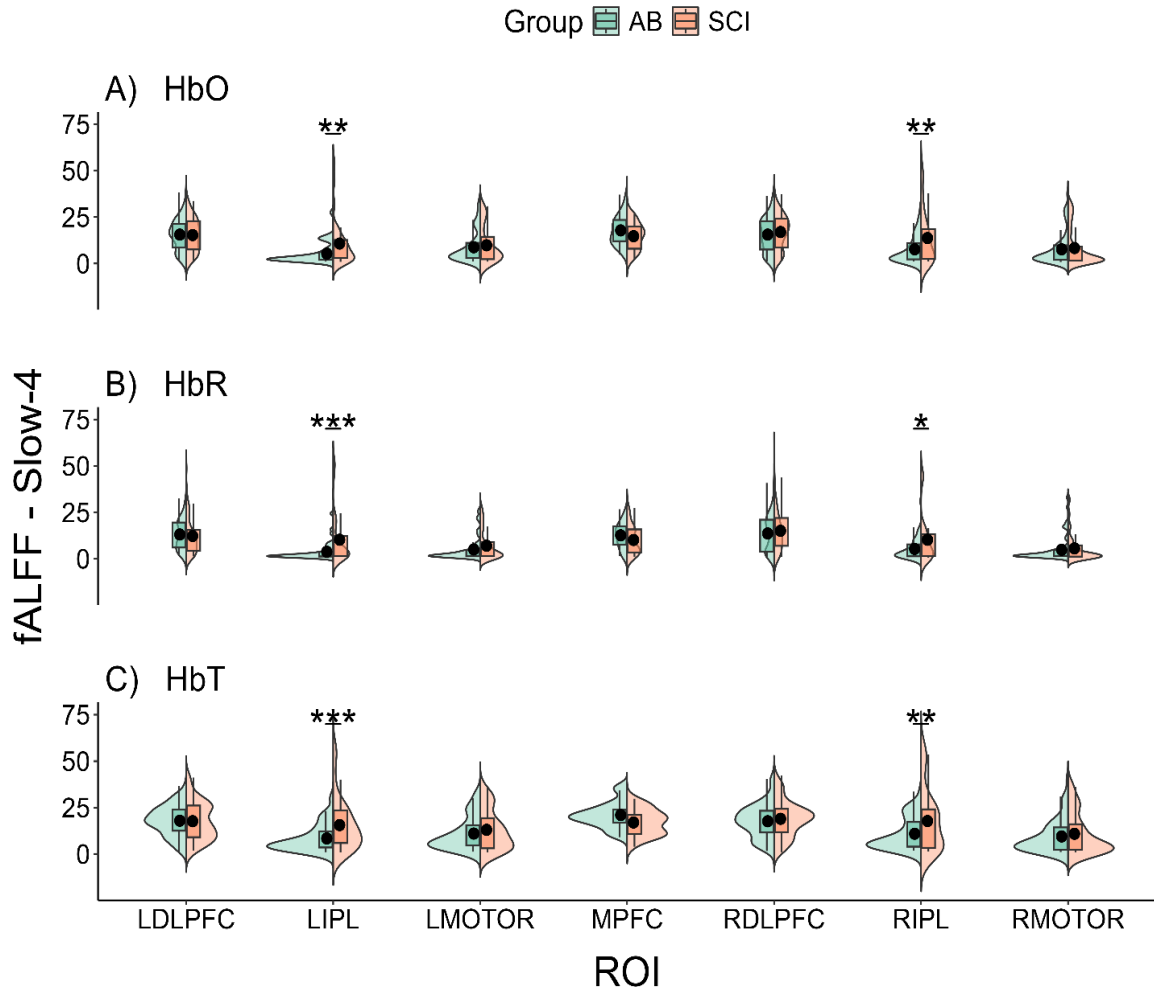


Figure 5.5 fALFF-Slow-4 scores between the AB and SCI group for each ROI. Significant differences found between the AB and SCI groups in the LIPL and RIPL regions.

Table 5.5 Mixed-effects Modeling Results for fALFF-Slow-4 Scores Comparing Between the SCI and AB Groups across all ROI. The LDLPFC Region is not Shown Here for the Mixed-effects Modeling Results due to being Held Out as the Reference Level for Comparisons

ROI	Estimate			Standard Error			t-value			p-value		
	HbO	HbR	HbT	HbO	HbR	HbT	HbO	HbR	HbT	HbO	HbR	HbT
LIPL	6.118	7.517	6.991	1.875	1.878	1.986	3.263	4.002	3.520	0.00115 **	6.90E-05 ***	0.000458 ***
LMOTOR	0.662	1.978	1.017	1.654	1.657	1.752	0.400	1.194	0.581	0.689	0.232	0.561
MPFC	-2.709	-1.528	-3.665	1.750	1.753	1.854	-1.548	-0.872	-1.977	0.122	0.383	0.0484
RDLPFC	2.137	2.583	1.954	1.449	1.452	1.535	1.475	1.779	1.273	0.140	0.075	0.203
RIPL	5.500	4.300	5.650	1.833	1.837	1.943	3.000	2.341	2.909	0.0027 **	0.0195 *	0.0037 **
RMOTOR	0.871	1.287	1.342	1.573	1.576	1.667	0.553	0.816	0.805	0.580	0.414	0.421

The Slow-3 fALFF scores showed similar patterns of differences between the AB and SCI groups in the RIPL and LIPL regions, similar to that of the Slow-4 fALFF scores (Figure 5.6). The fALFF scores in the Slow-3 band are of lower magnitude than that of the Slow-4 and Slow-5 bands. In contrast to the fALFF scores in the full resting-state band (0.01 to 0.1 Hz), Slow-5, and Slow-4 bands, the Slow-3 band also showed significant differences between the AB and SCI groups in the right motor (RMOTOR) region for HbT

concentration, although the effect is weak (Slow-3: fixed-effects estimate = 1.504, $t = 2.302$, $p = 0.021$) (Table 5.6).

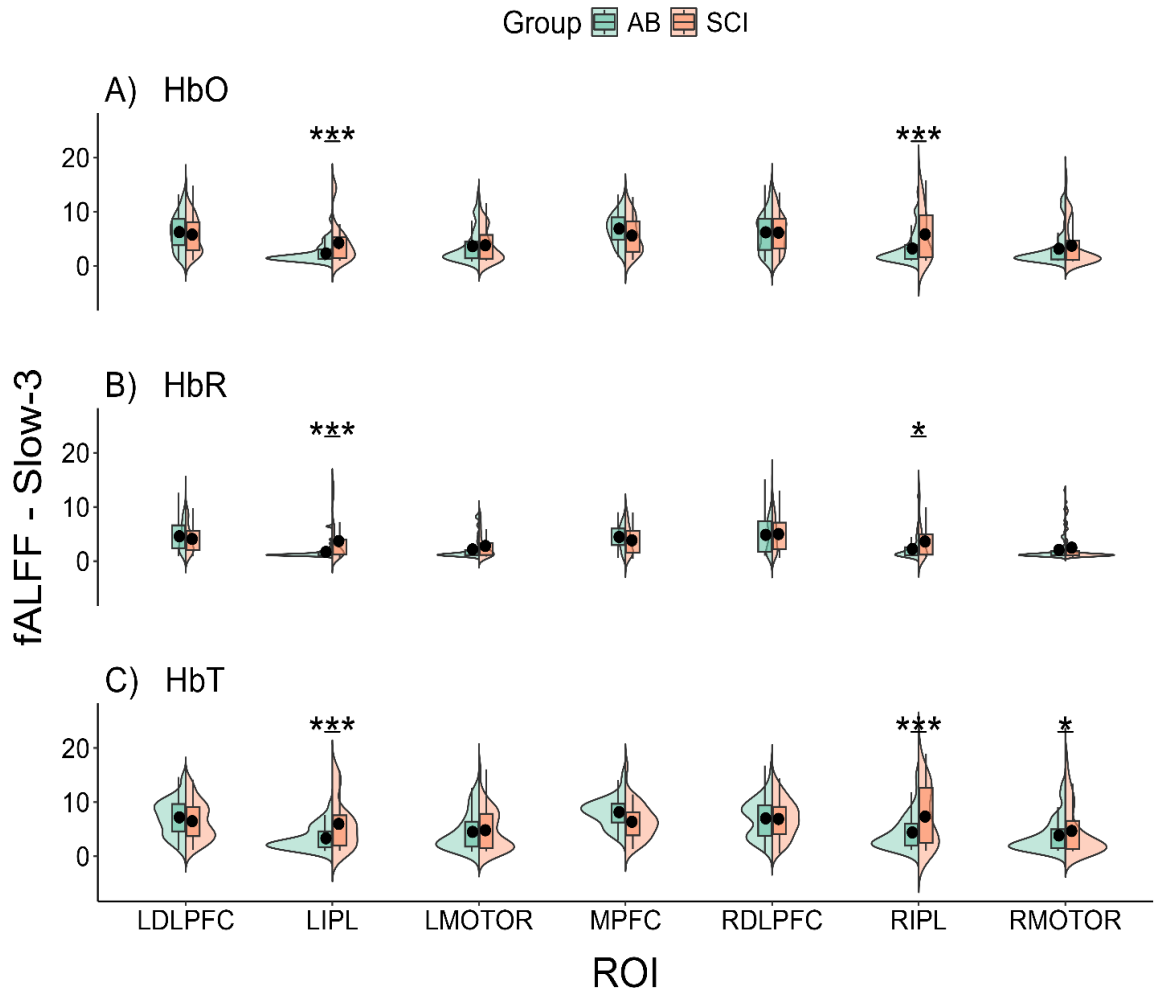


Figure 5.6 fALFF-Slow-3 scores between the AB and SCI group for each ROI. Significant differences found between the AB and SCI groups in the LIPL and RIPL regions.

Table 5.6 Mixed-effects Modeling Results for fALFF-Slow-3 Scores Comparing Between the SCI and AB Groups across all ROI. The LDLPFC Region is not Shown Here for the Mixed-effects Modeling Results due to being Held Out as the Reference Level for Comparisons

ROI	Estimate			Standard Error			t-value			p-value		
	HbO	HbR	HbT	HbO	HbR	HbT	HbO	HbR	HbT	HbO	HbR	HbT
LIPL	2.760	2.725	3.505	0.733	0.601	0.778	3.764	4.536	4.502	0.00018 ***	6.66E-06 ***	7.80E-06 ***
LMOTOR	0.548	0.928	0.775	0.647	0.530	0.687	0.847	1.752	1.129	0.397	0.080093	0.25923
MPFC	-0.751	-0.065	-1.055	0.684	0.561	0.726	-1.098	-0.116	-1.452	0.272	0.907	0.146
RDLPFC	0.546	0.760	0.696	0.567	0.464	0.602	0.963	1.636	1.157	0.335	0.102	0.247
RIPL	2.813	1.445	3.156	0.717	0.587	0.761	3.923	2.459	4.146	9.53E-05 ***	0.014 *	3.76E-05 ***
RMOTOR	1.046	0.826	1.504	0.615	0.504	0.653	1.699	1.638	2.302	0.0896	0.101	0.021 *

5.3.3 RSFC comparison between SCI and AB groups

The mean RSFC maps were obtained for both the SCI and AB groups for HbO, HbR, and HbT concentrations, from the resting-state band of 0.01 to 0.1 Hz. We observed no significant differences between the SCI and AB groups (two-sample t-tests with multiple comparison correction using the BH-FDR method, $\alpha = 0.05$, p-values > 0.05) (Figure 5.7). Distinct RSFC patterns were observed between the HbO, HbR, and HbT concentrations for both the AB and SCI groups; however, between the AB and SCI groups, the RSFC patterns were similar.

RSFC

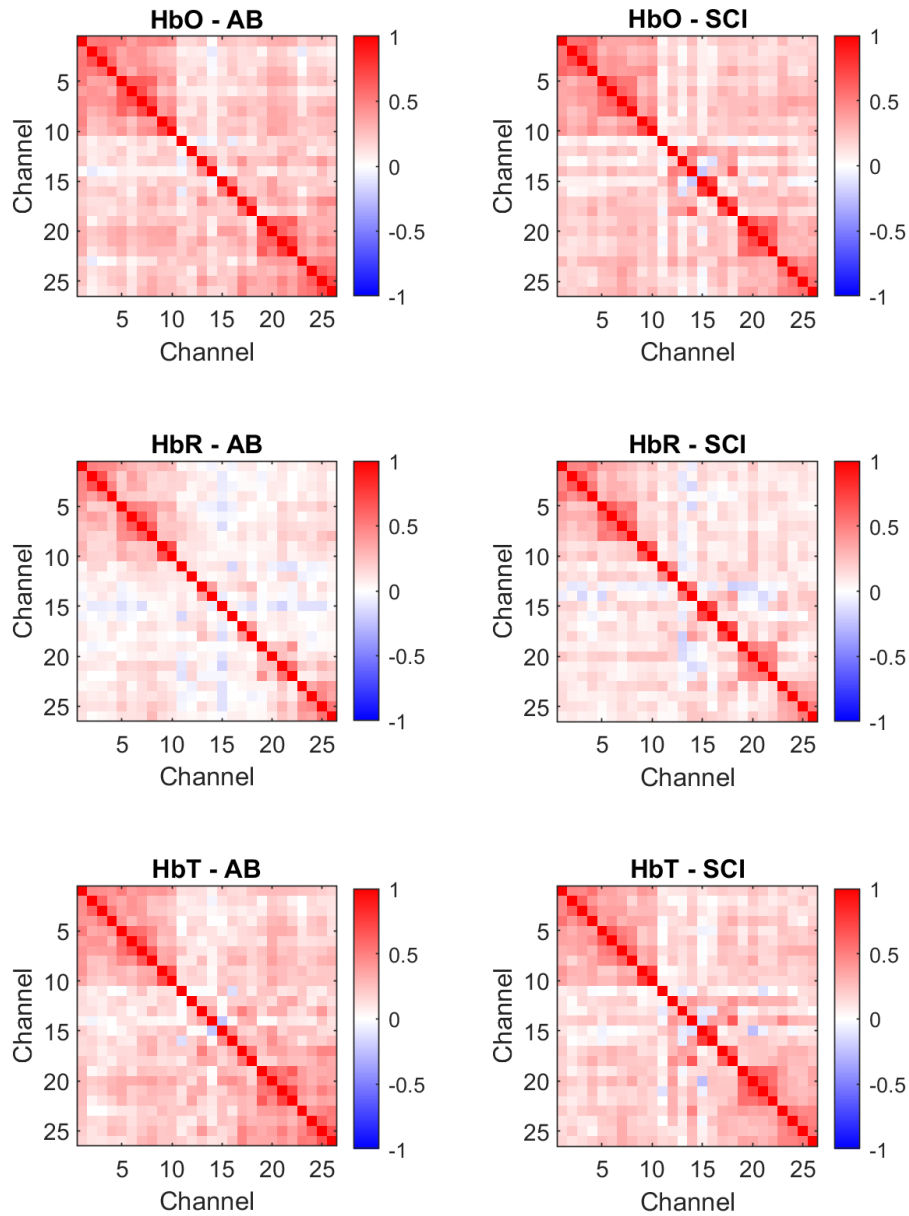


Figure 5.7 Resting-state functional connectivity (RSFC) maps for SCI and AB groups (right and left columns, respectively). The RSFC maps are generated for HbO, HbR, and HbT concentrations using Pearson's correlation. A total of 26 channels were utilized for the calculation of RSFC.

5.4 Discussion

Using fALFF in different frequency bands, regional resting-state activity was compared between individuals with SCI and AB controls using fNIRS with an optode layout placed across cognitive and motor regions of the cortical area. This study reports increased fALFF scores in individuals with SCI as compared to age and sex-matched AB controls, particularly in the right and left inferior parietal lobes. The fALFF scores calculated using the Slow-5 frequency range showed region-specificity to the LIPL region, whereas the Slow-4 and Slow-3 frequency ranges showed significant differences in both the LIPL and RIPL regions. This shows that regional resting-state fALFF activity differs between the SCI and AB groups and frequency-specific bands such as Slow-5, Slow-4, and Slow-3 can further distinguish regional differences.

5.4.1 fALFF is increased in individuals with SCI in the inferior parietal lobes

We observed increased fALFF scores in the inferior parietal lobes (RIPL & LIPL) in the SCI group compared to the AB group. The inferior parietal lobes are responsible for a range of functions including sensory processing, sensorimotor integration, social cognition, and attention (Clower et al., 2001; Mattingley et al., 1998; Numssen et al., 2021). In particular, the inferior parietal lobe has distinct functions pertaining to each hemisphere, in which the RIPL region is involved in visuospatial attention while the LIPL region is involved more dominantly in language function and semantic processing (Corbetta & Shulman, 2002; Numssen et al., 2021). Our findings of increased fALFF scores in individuals with SCI are consistent with that of Vallesi and colleagues', in which they found increased ALFF scores in individuals with SCI, although their primary focus was on the cerebellum and vermis regions, using resting-state fMRI (Vallesi et al., 2022). Additionally, Zheng and colleagues

found increased ALFF scores in individuals with complete thoracolumbar SCI in the right middle frontal gyrus, which is involved in expressive language processes and semantics (Zheng et al., 2021). Conversely, they found decreased ALFF scores in the lingual gyrus, which is part of the visual association cortex. These studies revealed altered ALFF scores in regions other than the sensorimotor regions, which is in line with our findings.

5.4.2 Distinct fALFF patterns in Slow-5, Slow-4, and Slow-3 frequency bands

Further separating the resting-state low-frequency fluctuations into Slow-5, Slow-4, and Slow-3 frequencies bands revealed region-specific differences between the SCI and AB groups. In particular, differences in the Slow-5 fALFF scores were specifically restricted to the LIPL regions, in contrast to the Slow-4 and Slow-3 fALFF scores, which showed significant differences in both the LIPL and RIPL regions. This suggests that differences between the SCI and AB groups in the Slow-5 frequency range, from 0.01 to 0.027 Hz, may be restricted to the LIPL region, whereas activity in the Slow-4 and Slow-3 frequency ranges is represented bilaterally in both the LIPL and RIPL regions. The different regional patterns of fALFF scores in different frequency bands have been reported by others (Ding et al., 2023; Han et al., 2011; Tang et al., 2023; Wang et al., 2014; Yue et al., 2015), and suggests the use of frequency-specific biomarkers when investigating resting-state differences in patient populations. Here we show that the differences in fALFF scores between the SCI and AB groups are frequency-dependent; therefore future studies may want to decompose the full resting-state signal into distinct frequency bins, revealing different modes of neuronal cortical oscillations (Buzsáki & Draguhn, 2004; Penttonen & Buzsáki, 2003).

5.4.3 Limitations

It is important to note limitations of the present study, such as the heterogeneous nature of the SCI population. Across different individuals, individuals with SCI may present injury characteristics distinctively, which would influence the resting-state results. Future studies may want to further investigate resting-state fALFF changes in different regions of the brain in particular sub-groups of the SCI population and perform comparisons within the SCI group, such as comparing individuals with and without neuropathic pain, or individuals with complete vs. incomplete injury. Another limitation of the current study is the lack of anatomical information that was able to be obtained from subjects, since there may be structural alterations in addition to the functional alterations in individuals with SCI as compared to AB individuals. Furthermore, the present study lacked external recording devices such as a pneumatic belt or heart-rate monitor, which could be helpful in regressing sources of physiological noise from the fNIRS data. This would allow for a more comprehensive and accurate study of the Slow-2 (0.198 to 0.5 Hz) and Slow-1 (0.5 to 1.5 Hz) bands, which overlap with respiratory and cardiac frequencies, respectively.

5.5 Conclusion

The present study used resting-state fNIRS to quantify changes in fALFF scores between individuals with SCI and AB controls. We found significantly higher fALFF scores in individuals with SCI in the right and left inferior parietal lobes. Further separation of the resting-state signal into Slow-5, Slow-4, and Slow-3 frequencies revealed brain region-specific oscillation differences between the two groups, in which Slow-5 activity differences were predominant the LIPL region. This study reveals differences in resting-

state regional and frequency-dependent metrics between individuals with SCI and AB controls, using fNIRS.

CHAPTER 6

DELAYED CEREBROVASCULAR REACTIVITY IN INDIVIDUALS WITH SPINAL CORD INJURY IN THE RIGHT INFERIOR PARIETAL LOBE: A BREATH-HOLD FNIRS STUDY (AIM 3)

6.1 Introduction

Spinal cord injury (SCI) is caused by damage to the spinal cord that can be either traumatic or non-traumatic, and affects over 15 million individuals world-wide (World Health Organization, 2024). Traumatic cases of SCI are caused by external physical forces that damage the spinal cord whereas non-traumatic cases of SCI are typically caused by chronic disease processes such as degenerative disc disease (Ahuja et al., 2017). In both cases, SCI leads to socioeconomic burdens on the individuals and increased difficulties with daily tasks, causing psychological distress in many individuals (Craig et al., 2009). Following a primary spinal cord injury event, secondary injury mechanisms occur, such as the increase in neuroinflammation (David & Kroner, 2011; Donnelly & Popovich, 2008; Faulkner et al., 2004; Hellenbrand et al., 2021), increased oxidative stress (Anwar et al., 2016; Carlson et al., 1998), vascular disruption (Siddiqui et al., 2015; Sinescu et al., 2010), cell death (Couillard-Despres et al., 2017), and autonomic dysfunction (Alizadeh et al., 2019). These secondary injury mechanisms often cause further neurological damage and health complications (Silva et al., 2014). Therefore, it is critical to investigate chronic injury mechanisms and monitor potential secondary health conditions to improve the quality of life for individuals with SCI.

A particular secondary health concern for individuals with SCI is the risk of autonomic dysfunction, which could lead to ischemic stroke and autonomic dysreflexia (Banerjea et al., 2008; Cragg et al., 2013; LaVela et al., 2012; J.-C. Wu et al., 2012). After

injury to the spinal cord, afferent and efferent nerve fibers of the autonomic nervous system may be severed, resulting in altered autonomic nervous system function due to disrupted supraspinal pathways (Henke et al., 2022). This in turn causes impairments in cardiovascular function, which contributes to reduced function in brain perfusion, as well as cerebral autoregulation, cerebrovascular reactivity, and neurovascular coupling (Kim & Tan, 2018). In particular, cerebrovascular reactivity (CVR) has been widely used as a tool to investigate the state of vascular health in the brain (Sleight et al., 2021). CVR reflects how well blood vessels can constrict or dilate in response to a vasoactive stimulus, and can be measured using different tools, such as using functional magnetic resonance imaging (fMRI) coupled with hypercapnic or hypocapnia stimuli (Bright & Murphy, 2013; Di, Kannurpatti, et al., 2013; Fierstra et al., 2013; Kastrup et al., 1999, 2001; Pinto et al., 2021). Reduced CVR has been associated with cognitive impairments, which has been commonly reported after SCI, with individuals with SCI having a 13 times greater risk for cognitive impairments than able-bodied individuals (Alcántar-Garibay et al., 2022; Craig et al., 2017; Davenport et al., 2012; Nightingale et al., 2020; Sachdeva et al., 2018). However, there is currently a lack of studies investigating how CVR is altered after SCI.

Weber and colleagues used fMRI to investigate CVR in individuals with SCI via administration of CO₂ gas and found increased CVR response time (delay) in individuals with SCI compared to that of able-bodied controls (Weber et al., 2022). However, they found no significant differences in the CVR metric on its own when it was not separated into its steady-state and active components. They also report significant associations between the time-since-injury and the neurological level of injury of the SCI participants and the steady-state CVR component; however, the authors note the limitations in sample

size of 7 SCI and 6 controls in their study (Weber et al., 2022). This shows that CVR changes with different injury characteristics and specific components of CVR are altered after one sustains an injury to the spinal cord. It is important to note that there are practical issues with getting individuals with SCI into an MRI scanner, such as the possibility of having metallic implants that are not MRI-compatible, difficulties with placing individuals from the wheelchair to the supine position in the MRI scanner, and potential discomfort in the rigid supine position in the MRI scanner, particularly for those who may feel claustrophobic (Blight et al., 2019; Weber et al., 2022).

The use of functional near-infrared spectroscopy (fNIRS) may resolve some of these issues in measuring brain hemodynamic activity in individuals with SCI. fNIRS is a relatively comfortable device placed on the scalp that uses near-infrared light to measure brain hemodynamic activity, similar to that of fMRI, based on the optical properties of deoxygenated and oxygenated hemoglobin in the cortical brain area (Jöbsis, 1977; Delpy et al., 1988; Villringer et al., 1993; Yücel et al., 2017). Despite its lower spatial resolution, it has a higher temporal resolution than fMRI (Ferrari & Quaresima, 2012), up to 100 Hz, which offers an advantage in better characterizing the delays in CVR (Amyot et al., 2020; MacIntosh et al., 2003). fNIRS has been previously used to quantify CVR in both breath-holding and gas inhalation settings (Amyot et al., 2020, 2022; Karunakaran et al., 2021; S. Miller & Mitra, 2021; Reddy et al., 2021; Smielewski et al., 1995; Vagné et al., 2020). Wilson and colleagues measured CVR in 6 individuals with tetraplegia using both transcranial doppler and fNIRS, and reported similar CVR in response to CO₂ in tetraplegia and able-bodied control groups, suggesting cerebrovascular adaptation with chronic tetraplegia (Wilson et al., 2010). It is not clear whether CVR as measured by fNIRS

is altered in individuals with chronic paraplegia, as the level of injury and completeness of injury can impact the degree of autonomic dysfunction (Henke et al., 2022; West et al., 2013).

In the present study, we investigated both the amplitude and delay of CVR in SCI and able-bodied (AB) groups, as measured by fNIRS during a hypercapnic breath-hold task. We used principal component analysis (PCA) and cross correlation analysis (CCA) to determine the amplitude and delays associated with the breath-hold CVR response, respectively. These CVR metrics were obtained for all subjects and then compared between the AB and SCI groups, across cognitive and motor brain regions, for all hemoglobin species. We then investigated the association between CVR characteristics and injury characteristics in the SCI group for particular brain regions which revealed differences between the AB and SCI groups. By studying CVR in individuals with SCI, we can better understand secondary injury mechanisms which occur after spinal cord injury and develop more effective rehabilitative treatments.

6.2 Materials and Methods

6.2.1 Participants

All participants were recruited from the New Jersey/New York metropolitan area. A total of 20 participants with SCI (14M, 6F, mean age = 46.3 ± 10.2 years) and 25 age- and sex-matched able-bodied (AB) controls (19M, 6F, mean age = 43.2 ± 12.28 years) participated in this study. Participants were excluded from the study if any of the following applied to them: (1) within one-year post-spinal cord injury or in the acute phase of injury, (2) presence of tetraplegia or inability to perform upper limb motor movements, (3) history of

or concurrent traumatic brain injury (TBI), (4) history of or concurrently has psychiatric disorders such as post-traumatic stress disorder, addiction, bipolar disorder, or schizophrenia, (5) presence of acute illness or infection, (6) history of chronic hypertension, diabetes mellitus, stroke, epilepsy or seizure disorders, multiple sclerosis, Parkinson’s disease, (7) illicit drug abuse within the past 6 months, (8) has Alzheimer’s disease or dementia, (9) not able to speak English, and (10) younger than 18 years of age or older than 65 years of age (D. Y. Chen, Di, Amaya, et al., 2024). The level of spinal injury, completeness of injury, and the duration since injury were collected from participants with SCI (Table 6.1).

Table 6.1 Demographic Information and Clinical Characteristics from Participants with SCI Enrolled in the Current Study

ID	Age (years)	Sex	Spinal Level of Injury	# Spinal Segments Affected	Complete (C) /Incomplete (I)	Duration since Injury (years)	Handedness
SCI-01	46	M	T11	11	C	12	Right
SCI-02	46	M	T2	20	C	16	Left
SCI-03	57	M	T10/11	12	C	6	Right
SCI-04	34	M	T12	10	C	9	Right
SCI-05	35	M	T11	11	C	14	Right
SCI-06	60	M	T4	18	C	10	Right
SCI-07	29	F	T4	18	I	8	Right
SCI-08	37	F	L1	9	I	12	Left
SCI-09	49	M	T6	16	C	24	Right
SCI-10	43	F	T11	11	C	26	Left
SCI-11	46	M	T11/T12	11	C	26	Right
SCI-12	54	M	T1	21	I	27	Right
SCI-13	60	M	C5	24	I	30	Right
SCI-14	28	M	T6	16	I	2	Right
SCI-15	48	F	L1	9	I	30	Right
SCI-16	45	M	T7	15	I	30	Right
SCI-17	47	M	T7	15	C	10	Right
SCI-18	61	F	C4/C5	25	I	10	Left
SCI-19	55	M	T4	18	C	16	Right
SCI-20	35	F	C5/C6	24	I	11	Left

6.2.2 Breath-hold task paradigm

All participants performed a breath-hold task paradigm consisting of 6 blocks of alternating periods of 15 s breath-hold and 30 s resting periods (Figure 6.1A). The task started off with 30 s of rest initially, during which the participants were instructed to breathe at their own comfortable pace in a relaxed manner. All instructions were displayed via a computer screen using E-Prime 2.0 software (Psychology Software Tools, Pittsburgh, PA), instructing the participants when to hold their breath and when to breathe normally. The words “rest” and “hold” were displayed in white font at the center of the screen on a black background. The participants also performed a resting-state task and N-back working memory task as part of a larger study; however, due to the focus of this study being cerebrovascular reactivity, only the breath-hold task results are analyzed and discussed here.

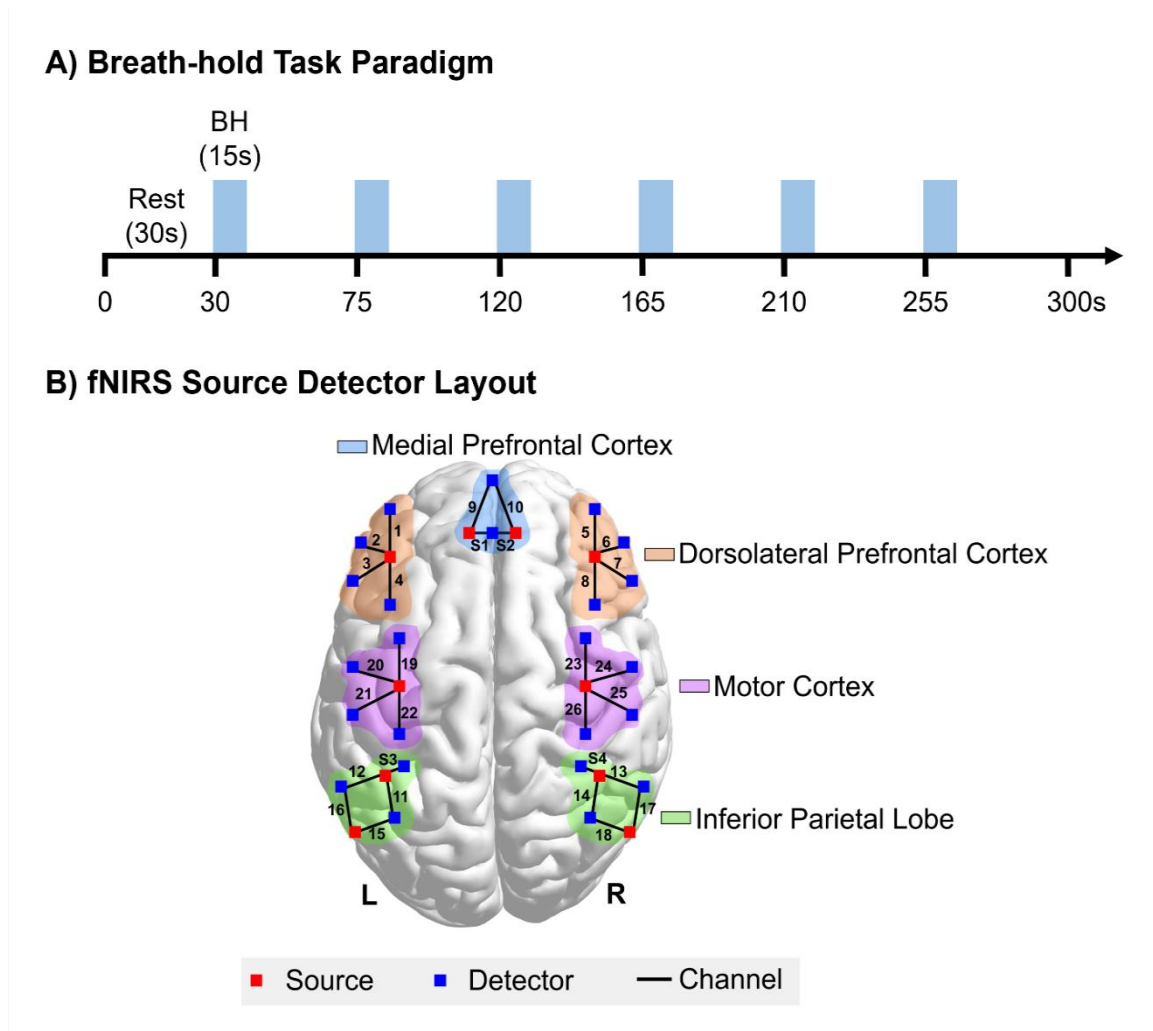


Figure 6.1 **A)** fNIRS Breath-hold (BH) task paradigm consisting of 6 breath-hold sessions, 15s each, interleaved with 30s of rest. **B)** fNIRS Optode layout with 10 optode sources and 24 detectors configured across the medial prefrontal cortex, dorsolateral prefrontal cortex, motor cortex, and inferior parietal lobe. A total of 26 channels are used with a source-detector distance of 30mm and 4 short separation channels are used with a source-detector distance of 8.4mm, as denoted by S1, S2, S3, and S4.

6.2.3 fNIRS data acquisition

A continuous wave fNIRS system was used for all fNIRS data acquisition at a sampling frequency of 25 Hz, using both 690 nm and 830 nm of light (CW6 System, TechEn Inc., Milford, MA). A total of 10 optode sources and 24 detectors were arranged across the head

to construct 26 long source-detector separation channels and 4 short channels (Figure 6.1B). The long channels were placed at a source to detector distance of 30 mm while the short channels were placed at a source to detector distance of 8.4 mm (Brigadoi & Cooper, 2015). These short channels were placed bilaterally on the left and right inferior parietal lobes and in the medial prefrontal cortex to reduce the impact of physiological noise from extracerebral regions on the data of interest. The 26 long channels covered the following regions of interest (ROI): the left and right dorsolateral prefrontal cortex (LDLPFC, RDLPFC, channels 1-4 and channels 5-8, respectively), medial prefrontal cortex (MPFC, channels 9&10), left and right motor cortex (LMOTOR, RMOTOR, channels 19-22 and channels 23-26, respectively), and left and right inferior parietal lobes (LIPL, RIPL, channels 11, 12, 15, & 16, and channels 13, 14, 17, & 18, respectively). The ROI were identified on each participant's head using a neural navigation system (Brain Sight Neural Navigator, Rogue Research Inc., Canada) with the Montreal Neurological Institute's (MNI-152) average structural brain template as a reference.

6.2.4 fNIRS data preprocessing

The fNIRS data were preprocessed in the following order: (1) raw light intensity values were converted to optical density values, (2) wavelet-based head-motion correction was performed using a threshold of 1.5 times the interquartile range (Molavi & Dumont, 2012), (3) band-pass filtering was applied using a pass-band from 0.01 to 0.15 Hz, (4) data were then converted to oxygenated hemoglobin (HbO), deoxygenated hemoglobin (HbR), and total hemoglobin (HbT) using the modified Beer-Lambert law (Delpy et al., 1988), (5) short channel regression was applied, and (6) channels were excluded based on the relative power in the task frequency range (Figure 6.2). Short channel regression was

implemented using the proximal channel method, in which a short channel regressor was chosen for each long channel based on its proximity to the long channel (Gagnon et al., 2012). In this case, channel S1 was used to regress out noise from channels 1-4, & 9, channel S2 was used to regress out noise from channels 5-8, & 11, channel S3 was used to regress out noise from channels 11, 12, 15, 16, & 19-22, and channel S4 was used to regress out noise from channels 13, 14, 17, 18, & 23-26 (Figure 6.2). The short channel regression models were solved using the ordinary least squares method and were formatted as

$$Y_{long\ channel} = X_{short\ channel} \times \beta_{short\ channel} + \varepsilon \quad (6.1)$$

where $Y_{long\ channel}$ represents the fNIRS data from one of the long channels, $X_{short\ channel}$ represents the fNIRS data from the proximal short channel, and ε represents the residuals. Short channel regression was performed on all subject data, across each channel separately and the residuals were kept for further analyses (Equation 6.1).

After short channel regression, fNIRS channels were excluded based on the relative power in the breath-hold frequency range. Since the breath-hold task period occurred every 45 s (15 s breath-hold and 30 s rest), the dominant breath-hold task frequency range was defined as 40 s to 65 s, or 0.0154 Hz to 0.025 Hz. Therefore, the relative power was computed as the average power in the breath-hold frequency range (0.0154 to 0.025 Hz) divided by the total average power in the frequency range from 0 to 12 Hz (up to the Nyquist frequency) (Equation 6.2).

$$Relative\ Power\ (\%) = \frac{Breath\ hold\ Avg.\ Power}{Total\ Avg.\ Power} \times 100 \quad (6.2)$$

The average power was computed using the *bandpower* function in MATLAB 2024a (The MathWorks Inc., Natick, Massachusetts). Channels with less than 50% relative power in the breath-hold frequency range were considered “insufficient” and were excluded from subsequent analyses (Zvolanek et al., 2023). This method of channel exclusion not only allows us to remove noisy data, but also offers a measure of task compliance, since those who did not comply with the task would likely not show high power in the breath-hold frequency range. Short channel regression and channel exclusion were applied to HbO, HbR, and HbT separately, and sufficient data from each hemoglobin species were analyzed in the subsequent steps. Data from the start of the breath-hold task (beginning of the first 15s breath-hold period) to the end of the entire task (including the last 30s rest period) were analyzed. The first 30s of rest were discarded since it was included for the participants to relax and serve as a buffer period before the breath-hold stimuli began. All data preprocessing scripts were written and executed in MATLAB 2024a (The MathWorks Inc., Natick, Massachusetts) and used HOMER3 functions (Huppert et al., 2009).

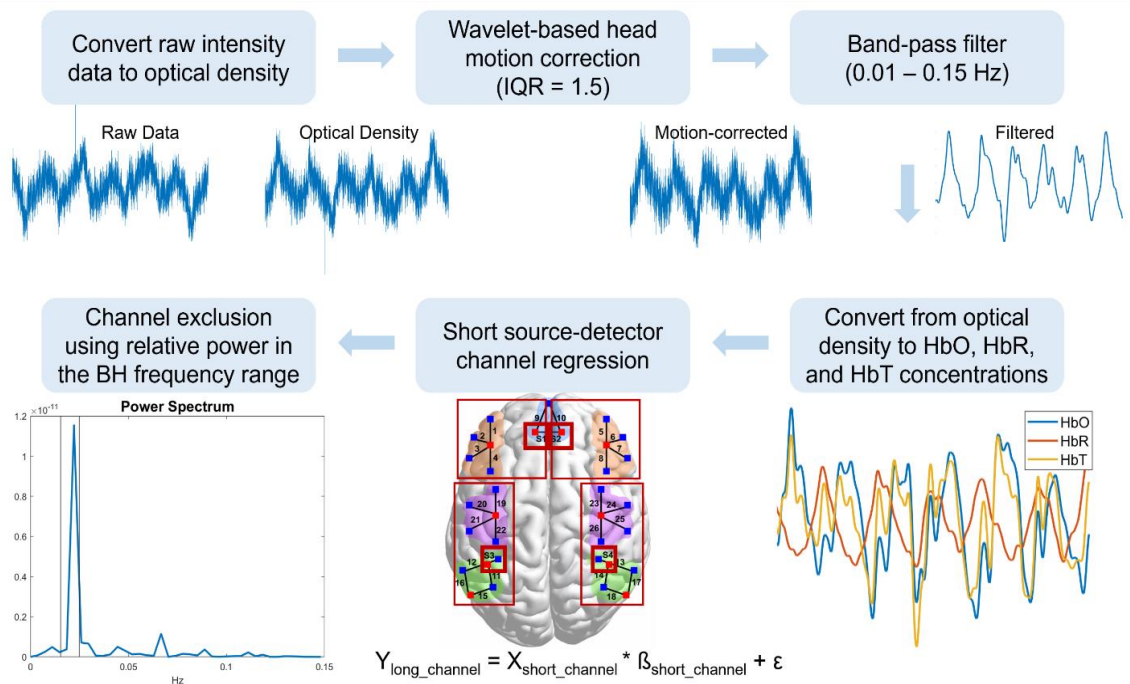


Figure 6.2 fNIRS preprocessing pipeline applied to both SCI and AB groups. The preprocessing steps were carried out in the following order: 1) convert raw intensity data to optical density data, 2) perform wavelet-based head motion correction with 1.5 times the interquartile range threshold, 3) band-pass filter from 0.01 to 0.15 Hz, 4) convert the filtered optical density data to oxy-hemoglobin (HbO), deoxy-hemoglobin (HbR), and total-hemoglobin (HbT) data, 5) regress the short source-detector channel from the long channels, and 6) perform channel exclusion using the relative power in the breath-hold frequency range. The short source-detector channel regression and channel exclusion steps were applied to all hemoglobin species.

6.2.5 Principal component analysis

After the fNIRS data were preprocessed, all data were standardized to z-scores by subtracting each timepoint by the mean of the entire time-series and then dividing by the standard deviation. Z-score standardization was performed for all channels and all subjects, for each hemoglobin species concentration separately. Principal component analysis (PCA) using a singular value decomposition algorithm was then applied to the z-scored data for each channel, in which the data from subjects in both AB and SCI groups were aggregated together in a [timepoint x subject] matrix. The square root of the eigenvalues of the

covariance matrix was taken and multiplied by the eigenvector to obtain the principal component loadings. Since the first principal component explained the most variance, the coefficients of the first principal component (PC1 loading) were analyzed further. The PC1 loading value was inferred to represent the breath-hold response and serves as a measure of CVR amplitude, in which a higher PC1 loading represents a greater CVR amplitude response. PCA is a model-free method that allows us to forgo *a priori* assumptions on the shape and delay of the hemodynamic response function (HRF) (Di & Biswal, 2022; Hejnar et al., 2007), thus offering a more unbiased measure of the breath-hold CVR amplitude response. The PC1 loading values were compared between the AB and SCI groups for each brain region and each hemoglobin species.

6.2.6 Breath-hold CVR response delays

In addition to obtaining a measure of CVR amplitude, we investigated differences in the delays of the breath-hold CVR response by performing cross-correlation analysis. Cross-correlation analysis was applied between the preprocessed fNIRS data and the task design convolved with the canonical HRF model (Friston et al., 1998). The fNIRS time-series data were shifted by a delay range of 0 s to 20 s in increments of 0.04 s (sampling frequency of 25 Hz) with respect to the convolved task design data. This delay range was chosen based on the physiological range of breath-hold delays that has been reported in the literature (K. Chen et al., 2021; Gong et al., 2023; Moia et al., 2020; Stickland et al., 2022; Tong et al., 2011). The “optimal” delay was chosen based on the delay or lag value that yielded the highest correlation value when shifting the time-series data. The optimal delay was calculated for each subject, each channel, and each hemoglobin species. These delay values were then compared between the AB and SCI groups across all brain regions.

6.2.7 CVR and injury characteristics

After comparing the CVR amplitude and delay values between the AB and SCI groups, we further investigated whether injury characteristics in the SCI group were associated with CVR characteristics. To reduce the number of comparisons, injury characteristics were correlated with PC1 loading and delay values for any regions that showed significant differences between the AB and SCI group. For the SCI group, we investigated the duration since injury (in years) and the level of spinal injury score, calculated as the number of spinal segments affected that are below the level of injury (Table 6.1). The mean of the CVR amplitude and delay values were taken across all channels within the particular ROI to obtain a single ROI-specific CVR metric for each subject. The mean value was taken since not all subjects had data from all channels within a particular ROI, due to the channel pruning procedure implemented.

6.2.8 Statistical analysis

We compared CVR amplitude and delays between the SCI and AB groups using mixed-effects modeling. The linear mixed-effects models were implemented in R using the *lme4* package (Bates et al., 2015) and were formatted as follows:

$$\text{CVR amplitude} \sim \text{Group} * \text{ROI} + (1|\text{Subject})$$

$$\text{CVR delay} \sim \text{Group} * \text{ROI} + (1|\text{Subject})$$

Linear mixed effects models were applied to all HbO, HbR, and HbT concentration data separately. The “Group” variable consisted of either the SCI or AB category and the “ROI” variable consisted of the 7 ROI across the fNIRS cap: the LDLPFC, RDLPFC, MPFC, LMOTOR, RMOTOR, LIPL, and RIPL regions. The “Group” and “ROI” variables were treated as fixed effects while the “Subject” variable was treated as a random effect. Not all

subjects had data for all channels within a particular ROI due to the channel pruning procedure. Therefore, by implementing a mixed-effects modeling approach, we were able to account for the differences in the number of channels with sufficient data quality from each subject. All linear mixed effects models were fit by using the restricted maximum likelihood algorithm and t-tests were performed using Satterthwaite's method (Kuznetsova et al., 2017). For analysis of associations between CVR amplitude and delays with the injury characteristics in the SCI group, Pearson's r correlation was used for each hemoglobin species concentration.

6.3. Results

For our quality control analyses, after preprocessing all fNIRS data, the relative power in the breath-hold frequency range was calculated for all HbO, HbR, and HbT concentrations, across all subjects and channels. High relative power values were observed across Channels 1-10, while lower relative power values were observed in Channels 11-26, across all hemoglobin concentrations (Figure 6.3 A-C). The data included in subsequent analyses and determined as "sufficient" were consistent across hemoglobin concentrations and consistent between the AB and SCI groups (Figure 6.3 D-F).

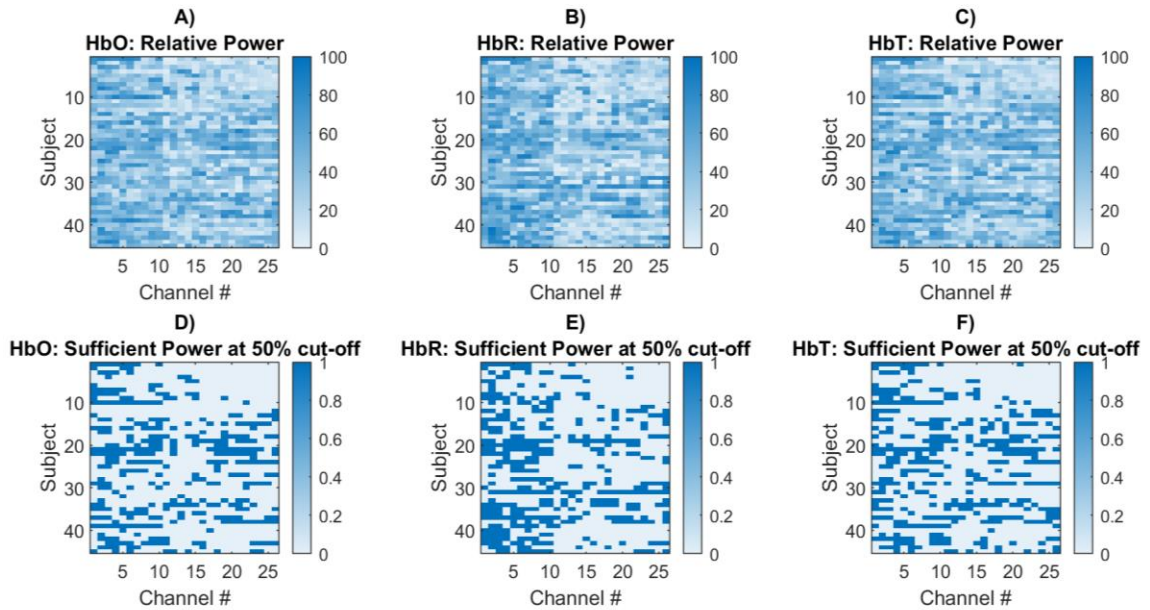


Figure 6.3 Relative power in the breath-hold frequency range shown for each subject across all channels, shown for **A)** oxygenated hemoglobin (HbO), **B)** deoxygenated hemoglobin (HbR), and **C)** total hemoglobin (HbT). Subjects 1-25 are individuals in the AB group whereas subjects 26-45 are individuals in the SCI group. After applying a threshold of 50% relative power, channels that were included are indicated by 1's and channels that were excluded are indicated by 0's, for **D)** HbO, **E)** HbR, and **F)** HbT.

6.3.1 CVR amplitude in SCI vs. AB

Across all brain regions, there were no significant differences in CVR amplitude, as measured by PC1 Loading scores, between the SCI and AB groups (Figure 6.4 A-C). Separate linear mixed effects models were generated for each hemoglobin concentration species and no significant differences in CVR amplitude were observed between SCI and AB groups across HbO, HbR, and HbT (Table 6.2). For HbT, although the AB group showed higher CVR amplitude in the right motor region, the effect was weak (fixed-effect estimate = -0.187, $t = -2.214$, $p = 0.028$). Overall, the PC1 Loading values hovered around 0.1 for both SCI and AB groups and showed similar values across hemoglobin concentration species (Figure 6.4).

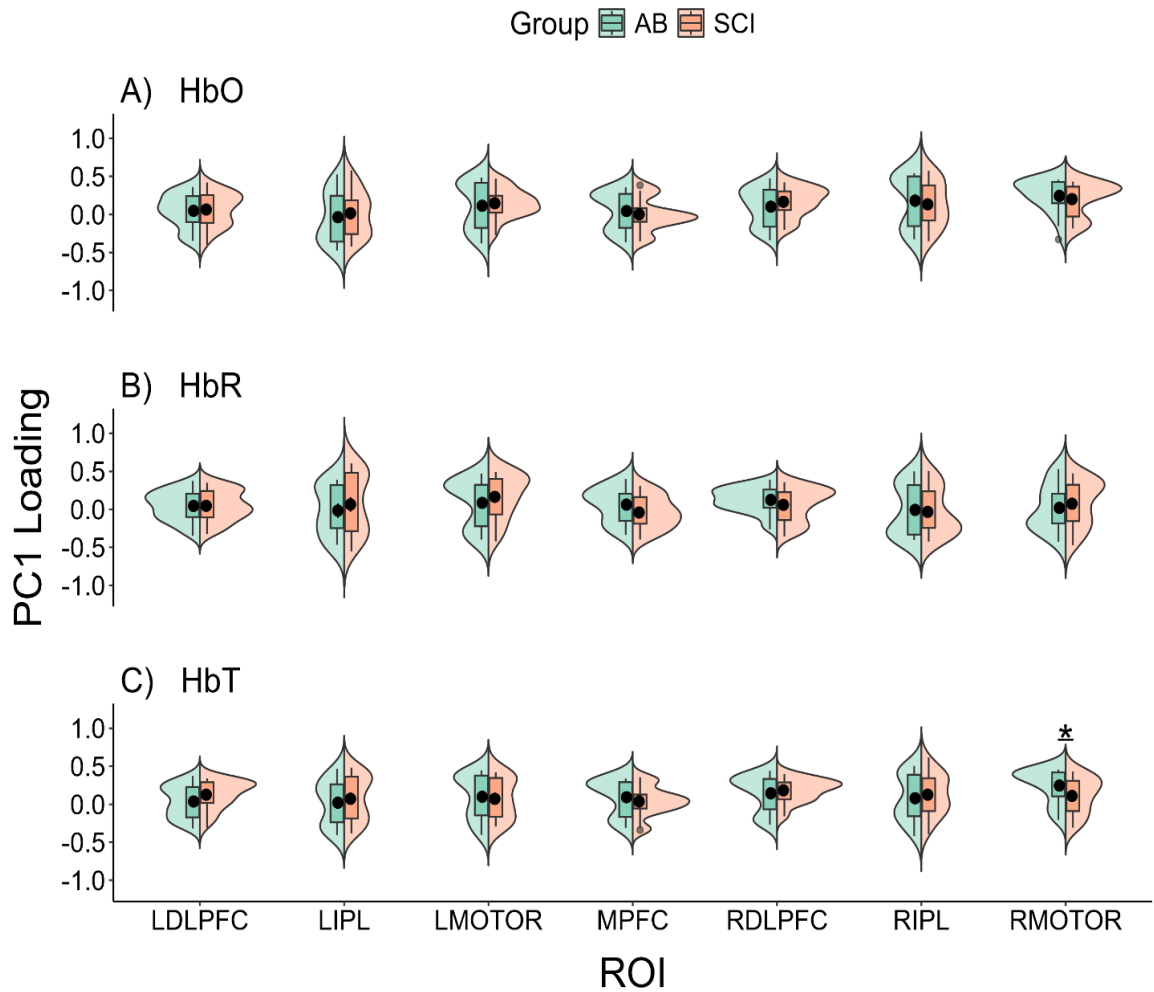


Figure 6.4 PC1 Loadings shown for both AB and SCI groups, for all hemoglobin species: **A)** oxy-hemoglobin (HbO), **B)** deoxy-hemoglobin (HbR), and **C)** total hemoglobin (HbT), across all brain regions of interest: left dorsolateral prefrontal cortex (LDLPFC), left inferior parietal lobe (LIPL), left motor cortex (LMOTOR), medial prefrontal cortex (MPFC), right dorsolateral prefrontal cortex (RDLPFC), right inferior parietal lobe (RIPL), and right motor cortex (RMOTOR). The means of the PC1 Loadings are indicated by black circles and the distribution of the AB and SCI groups are shown, denoted by green and orange, respectively.

Table 6.2 Mixed Effects Model Results for CVR Amplitude Comparisons between SCI and AB groups, across each ROI. One ROI is left out in the Reports (the LDLPFC region) due to being the Reference Level for all Comparisons

ROI	Estimate			Standard Error			t-value			p-value		
	HbO	HbR	HbT	HbO	HbR	HbT	HbO	HbR	HbT	HbO	HbR	HbT
LIPL	-0.007	0.086	-0.044	0.096	0.108	0.083	-0.070	0.792	-0.531	0.944	0.429	0.596
LMOTOR	0.044	0.061	-0.099	0.095	0.098	0.085	0.468	0.616	-1.176	0.640	0.538	0.241
MPFC	-0.081	-0.113	-0.102	0.102	0.096	0.090	-0.793	-1.187	-1.135	0.429	0.236	0.257
RDLPFC	0.072	-0.048	0.004	0.085	0.076	0.077	0.839	-0.630	0.057	0.402	0.529	0.955
RIPL	-0.029	-0.034	-0.014	0.105	0.096	0.086	-0.275	-0.350	-0.164	0.783	0.726	0.870
RMOTOR	-0.041	0.037	-0.187	0.097	0.096	0.085	-0.420	0.387	-2.214	0.675	0.699	0.028 *

6.3.2 CVR delays in SCI vs. AB

We observed significantly longer CVR delays in the SCI group compared to the AB group in the right inferior parietal lobe, for HbR concentration (linear mixed-effects model, fixed-effects estimate = 6.565, Satterthwaite's t-test, $t = 2.663$, $p = 0.008$) (Table 6.3). The average HbR CVR delay in the SCI group in the right inferior parietal lobe was 14.21 s (sd: 6.60 s), and for the AB group, the average delay in the right inferior parietal lobe was 7.08 s (sd: 7.39 s) (Figure 6.5). For HbO concentration, we observed slightly higher CVR delay values in the left inferior parietal lobe for the AB group compared to the SCI group (linear mixed-effects model, fixed-effects estimate = -6.027, Satterthwaite's t-test, $t = -2.518$, $p = 0.012$) (Table 6.3), with the mean delay values in the AB group being 9.53 s (sd = 7.42 s) and the mean delay in the SCI group being 8.20 s (sd = 8.80 s). Similarly, for HbO concentration in the right inferior parietal lobe, we observed slightly higher CVR

delay values in the AB group compared to that of the SCI group (linear mixed-effects model, fixed-effects estimate = -6.136, Satterthwaite's t-test, $t = -2.332$, $p = 0.020$) (Table 6.3). No significant differences in delays were observed between the SCI and AB groups for HbT concentration across all ROIs (Satterthwaite's t-tests, $p > 0.05$). The CVR delays varied across the different ROI investigated; however, since we were primarily interested in differences in CVR delays between the AB and SCI groups, statistical results from the linear mixed-effects models were only reported for group differences in each region (Table 6.3).

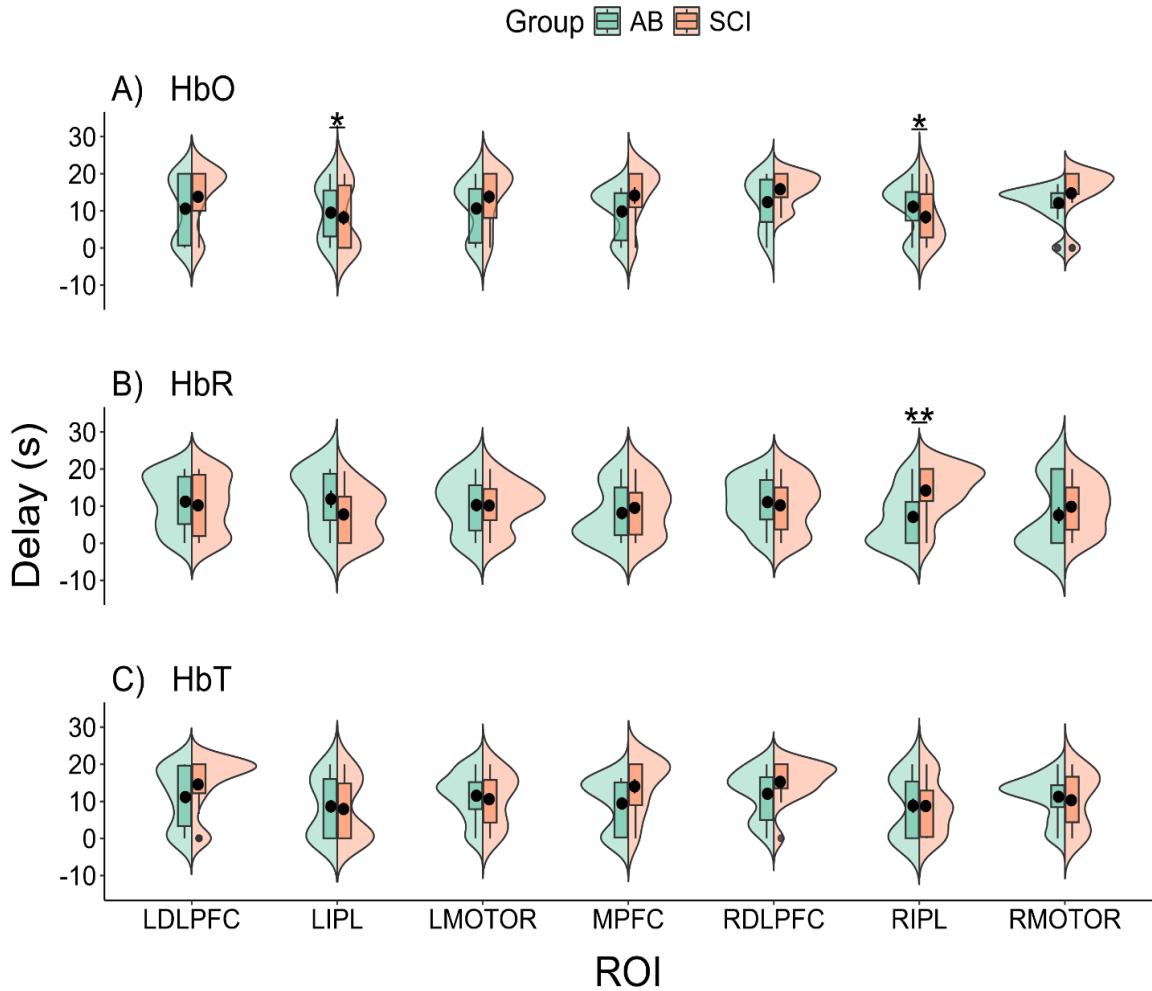


Figure 6.5 Breath-hold CVR delay values between AB and SCI groups for **A)** oxy-hemoglobin (HbO), **B)** deoxy-hemoglobin (HbR), and **C)** total hemoglobin (HbT), across the left dorsolateral prefrontal cortex (LDLPFC), left inferior parietal lobe (LIPL), left motor cortex (LMOTOR), medial prefrontal cortex (MPFC), right dorsolateral prefrontal cortex (RDLPFC), right inferior parietal lobe (RIPL), and right motor cortex (RMOTOR). The black circles indicate the mean of the CVR delays and the distributions of the delays are shown for the AB and SCI groups, denoted by green and orange, respectively.

Table 6.3 Mixed Effects Model Results for CVR Delay Comparisons between SCI and AB groups, across each ROI. One ROI is left out in the Reports (the LDLPFC region) due to being the Reference Level for all Comparisons

ROI	Estimate			Standard Error			t-value			p-value		
	HbO	HbR	HbT	HbO	HbR	HbT	HbO	HbR	HbT	HbO	HbR	HbT
LIPL	-6.027	-2.547	-3.919	2.394	2.768	2.254	-2.518	-0.920	-1.739	0.012 *	0.358	0.083
LMOTOR	-0.218	-1.318	-3.885	2.390	2.509	2.299	-0.091	-0.525	-1.690	0.927	0.600	0.092
MPFC	2.313	1.838	3.723	2.539	2.433	2.449	0.911	0.756	1.520	0.363	0.450	0.129
RDLPFC	0.653	-0.276	0.483	2.145	1.930	2.107	0.304	-0.143	0.229	0.761	0.887	0.819
RIPL	-6.136	6.565	-3.254	2.631	2.465	2.338	-2.332	2.663	-1.392	0.020 *	0.008 **	0.165
RMOTOR	-0.425	2.681	-2.803	2.444	2.504	2.303	-0.174	1.071	-1.217	0.862	0.285	0.224

6.3.3 CVR association with duration since injury and injury level

Upon further investigation of the right inferior parietal region's CVR delays, we found a significant association between the CVR delay and duration since injury for HbT concentration values in the right inferior parietal lobe. As the duration since injury increased, the CVR delay values decreased (Pearson's r correlation, $r = -0.59$, $p = 0.04$) (Figure 6.6 A). For HbO and HbR concentration values, no significant associations were found between the mean CVR delays in the right inferior parietal lobe and the duration since injury (Pearson's r correlation, HbO: $r = -0.09$, $p = 0.82$, HbR: $r = 0.28$, $p = 0.41$). Similarly, no significant associations were found between the CVR delays in the right inferior parietal lobe and the injury level score for either HbO, HbR, or HbT (Pearson's r correlation, $p > 0.05$) (Figure 6.6 B). For subjects without sufficient data in any of the

channels in the right inferior parietal lobe (channels 13, 14, 17, and 18), the data were not included in the correlational analyses.

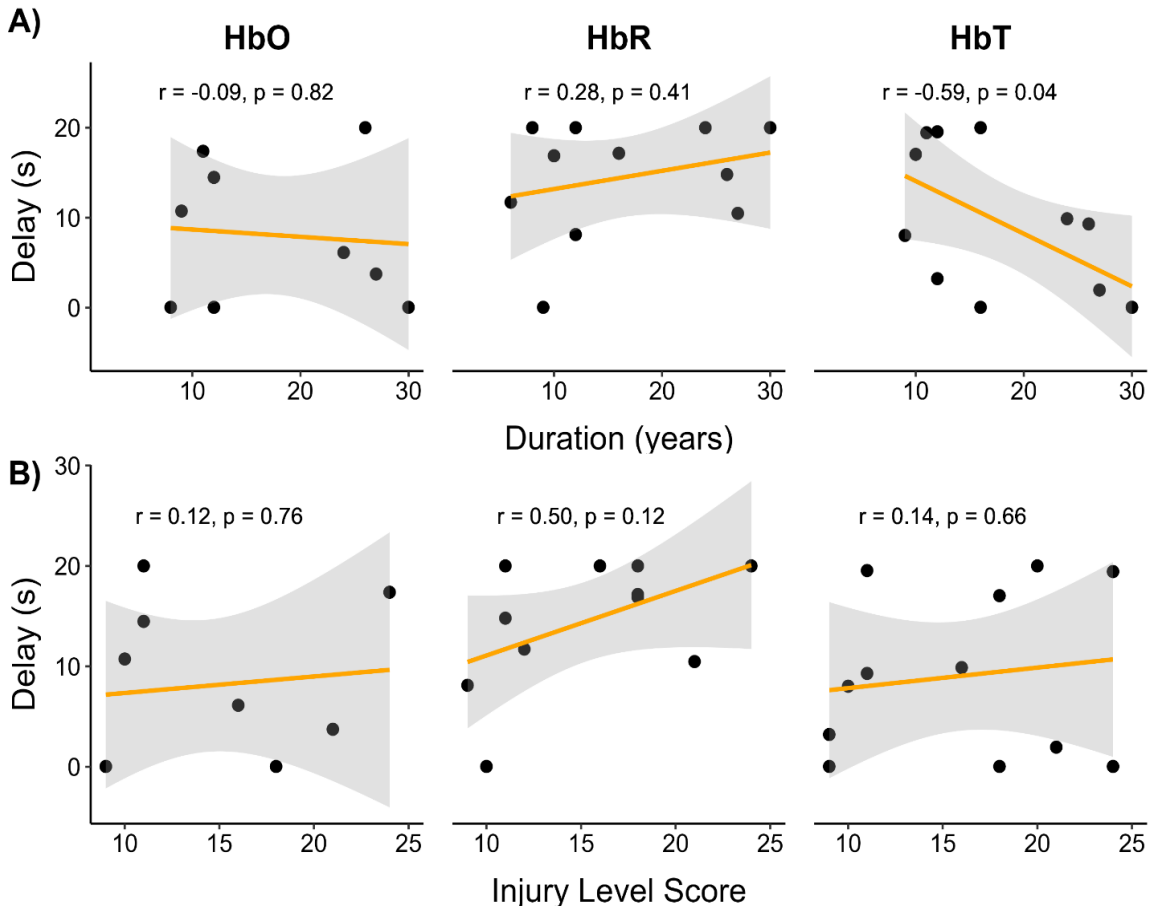


Figure 6.6 Association between the mean CVR delays in the right inferior parietal lobe and the **A)** duration since injury (years) and **B)** spinal injury level score in the SCI group, for oxygenated hemoglobin (HbO), deoxygenated hemoglobin (HbR), and total hemoglobin (HbT) concentrations. Pearson’s correlation was performed and a least-squares line is shown in orange with the standard error of the mean in gray.

6.3.4 Variability in CVR across the brain

The SCI group showed significantly higher variability of CVR delays for HbO concentration compared to the AB group, as calculated by the standard deviation of CVR values across the brain (across all channels) (two-sample independent t-test, $p = 0.0168$)

(Figure 6.7 B). For CVR amplitude, there were no significant differences in variability across the brain between the AB and SCI groups across HbO, HbR, and HbT concentrations (independent-samples t-test, $p > 0.05$) (Figure 6.7 A). For CVR amplitude, the whole-brain variability ranged from 0.15 to 0.25 for both AB and SCI groups, showing minimal differences in variability.

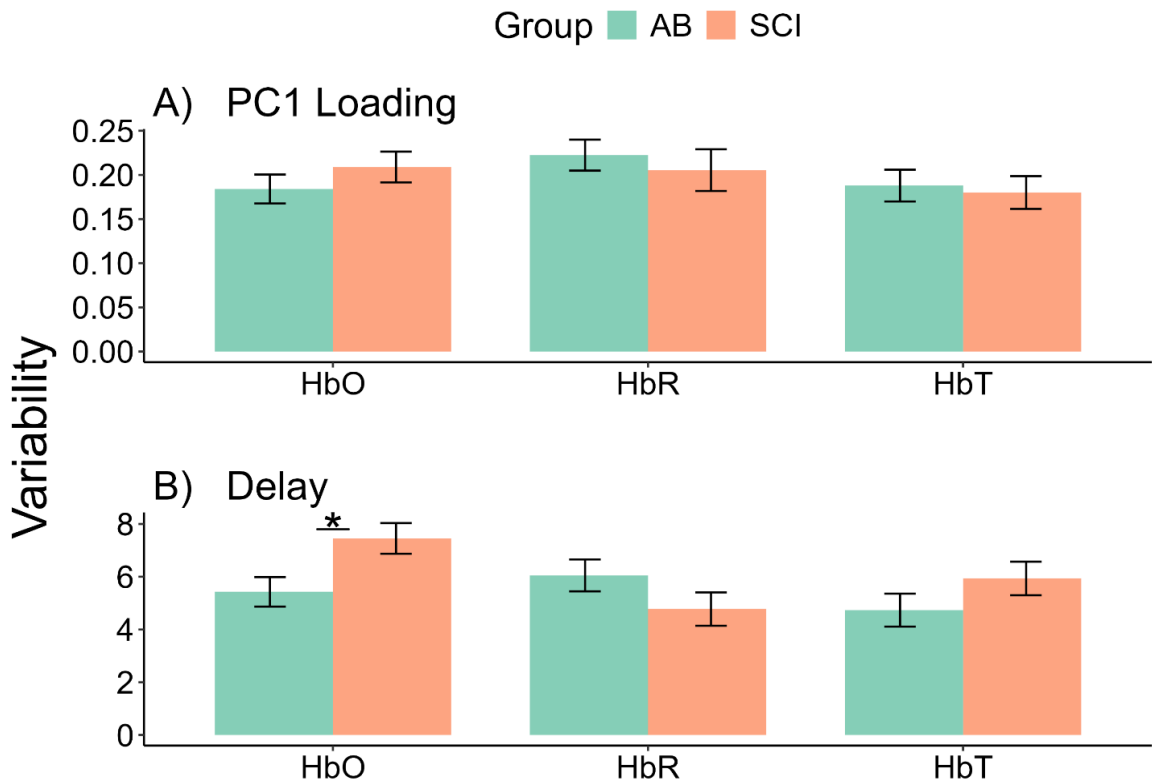


Figure 6.7 Variability in breath-hold CVR **A)** amplitude (PC1 Loading) and **B)** delays across the brain between the AB and SCI groups, shown in green and orange, respectively. For HbO data, we found significant differences between the AB and SCI groups in the variability of delays across the brain (across channels) (two-sample t-test, $p = 0.0168$). Error bars indicate ± 1 standard error of the mean.

6.4 Discussion

In this study, we examined differences in the CVR amplitude and delays between SCI and AB individuals using fNIRS during a hypercapnic breath-holding task. We also investigated the association between CVR components and injury characteristics in individuals with SCI. We report significantly delayed CVR in the right inferior parietal lobe in individuals with SCI compared to AB individuals, while the amplitude of CVR was unchanged. CVR also showed different characteristics between HbO, HbR, and HbT concentrations. As the duration since injury increased for individuals with SCI, CVR delay in the right inferior parietal lobe was found to decrease. To the best of our knowledge, this is the first study to report differences in CVR delays between SCI and AB individuals quantified by breath-hold fNIRS and cross-correlation analysis.

6.4.1 No differences in CVR amplitude between the SCI and AB groups

When comparing CVR amplitude between SCI and AB groups, we observed no significant differences between the two groups. This is consistent with Weber and colleagues' results that used fMRI to quantify CVR, in which no significant differences were observed in the standalone and steady-state CVR results between SCI and AB groups (Weber et al., 2022). They argue that unchanged full CVR may be masked by increased CVR in individuals with thoracic injuries and decreased CVR in those with cervical injuries. Furthermore, Wilson and colleagues reported that CVR is maintained in individuals with tetraplegia, whereas dynamic cerebral autoregulation may be altered, suggesting adaptive mechanisms in those with chronic tetraplegia (Wilson et al., 2010). Although our CVR metric was quantified using a hypercapnic breath-hold stimulus, the previous studies investigating CVR in individuals with SCI used CO₂ gas inhalation and may be limited by the small sample sizes

(7 and 6 SCI participants, respectively) (Weber et al., 2022; Wilson et al., 2010). Despite these differences, our results on the time-independent CVR metric are consistent with their conclusions. An advantage of our method to quantify CVR amplitude by using PCA is that there is no biased assumption on the specific HRF shape associated with the breath-hold CVR response, thus providing a time-independent and HRF-shape independent metric of CVR.

6.4.2 Individuals with SCI have significantly longer CVR delays than AB individuals

We found significantly longer CVR delays in the SCI group compared to the AB group in the right inferior parietal lobe. Longer delays in CVR is associated with poorer vascular health (K. B. Miller et al., 2019; Sobczyk et al., 2021; Stringer et al., 2021), suggesting reduced vascular health in the right inferior parietal lobe in individuals with SCI. The right inferior parietal lobe is involved in visuospatial attention and sensorimotor integration, in addition to executive function (Corbetta & Shulman, 2002; Numssen et al., 2021). Delays in this region may be due to loss of sensorimotor function in individuals with SCI after injury, particularly for the paraplegic cohort recruited in the present study. However, it is important to note that we did not find significant differences in the CVR amplitude despite finding differences in the CVR delays. This may suggest a compensatory mechanism in which a longer CVR delay in individuals with SCI is required for comparable CVR amplitudes to that of the AB group. Furthermore, a significant delay in CVR in the SCI group was observed for HbR only, which may reflect more sensitive changes to a breath-hold task in HbR rather than to HbO concentrations in the blood. CVR quantified using blood-oxygen-level-dependent (BOLD) fMRI techniques cannot fully capture differences in CVR dynamics between the different hemoglobin species. This is due to HbR being

paramagnetic, causing dephasing and shortening of the transverse relaxation time (T_2^*) weight, which decreases the fMRI BOLD signal; therefore, a decrease in HbR subsequently increases the strength of the signal (Mcintyre et al., 2003). HbO on the other hand, is not paramagnetic and has very little contribution to relaxation rates. Therefore, using fNIRS, we can better distinguish between CVR measured by dynamic changes not only in HbR, but also in that of HbO and HbT. This shows a unique characteristic of quantifying CVR using fNIRS as compared to that of fMRI, which relies primarily on HbR changes. Future studies may want to further investigate the different sensitivities of HbO, HbR, and HbT in quantifying CVR using fNIRS.

6.4.3 CVR delays in the right inferior parietal lobe is associated with the duration since injury

We further investigated the CVR delays in the right inferior parietal lobe in individuals with SCI and found a significant association between CVR delays with the duration since injury, for HbT concentration. As the duration since injury increased for the SCI group, the CVR delays decreased. This suggests that over time, the cerebrovascular health of individuals with SCI may improve, as the cerebrovasculature remodels and motor region connections reorganize after injury (Kokotilo et al., 2009). These improvements in CVR delays in the right inferior parietal lobe may also be related to the frequency of rehabilitation or exercise programs that individuals may be enrolled in. Although it is not clear the extent to which individuals with SCI in this cohort actively participate in physical rehabilitation training, generally, exercise improves cerebrovascular health, as blood perfusion is increased in the brain (Bliss et al., 2021; Davenport et al., 2012).

6.4.4 Variability in CVR across the brain

We found significantly higher variability in the delay of CVR across the brain in individuals with SCI compared to AB individuals, for HbO concentration. This may be explained by the differences in injury characteristics in the SCI group, whereas those in the AB group were more likely to be more homogeneous. As injury characteristics such as the completeness of injury, level of injury, duration since injury, and cause of injury differ across individuals in the SCI group, it is consistent that the CVR characteristics across the brain would also differ more in the SCI group. In healthy aging subjects, CVR has been shown to differ across brain regions, with CVR in particular regions such as the hippocampus being associated with memory scores (Catchlove et al., 2018). The heterogeneous nature of CVR has been reported in previous studies (D. Y. Chen, Di, & Biswal, 2024; D. Y. Chen, Di, Yu, et al., 2024; Kastrup et al., 1999; Moia et al., 2020; van Niftrik et al., 2023); however, it is unclear whether a measure of the heterogeneity of CVR may reveal vascular pathologies in the brain, particularly in patient populations.

6.4.5 Limitations

The present study contains a lack of physiological measures such as end-tidal CO₂ measures and respiratory belt data. However, it is important to note that the use of a respiratory belt on patient populations such as those with SCI may be too constricting and may not be comfortable to wear while performing a breath-holding task. It is important that participants were as comfortable as possible when performing the breath-holding tasks, thus although extra physiological sensors would be helpful, it may cause other unwanted side effects from the patients. Future studies may also want to look at the differences in CVR in individuals with thoracic vs. cervical injuries and those who have tetraplegia vs.

paraplegia, since autonomic dysfunction can vary greatly based on the severity of injury. Furthermore, future studies may also want to look into using breath-hold CVR as a regressor in fNIRS studies to account for possible differences between patient populations and controls that may be due primarily to vascular differences rather than neuronal differences.

6.5 Conclusion

Using fNIRS and a breath-holding hypercapnic task, the present study investigated differences in CVR between individuals with SCI and AB controls. We found significantly delayed CVR in the right inferior parietal lobe in individuals with SCI compared to AB controls, and no significant differences in the amplitude of CVR between the SCI and AB groups. The delays in CVR in the SCI group were also associated with the duration since injury, in which a longer duration since injury resulted in a shortened delay in CVR. This suggests adaptive CVR mechanisms with time as individuals with SCI recover and undergo functional brain reorganization.

CHAPTER 7

SUMMARY AND FUTURE WORK

7.1 Summary

This dissertation used fNIRS to evaluate the neurovascular correlates of cognitive function in individuals with SCI as compared to AB controls. The study focused on three main aspects of brain activity as quantified by fNIRS – task-based fNIRS neurovascular activation, resting-state functional connectivity, and cerebrovascular reactivity. To evaluate these three aspects of brain function respectively, the following tasks were employed: a working-memory N-back task with 3 different difficulty levels, a 10-minute resting-state scan, and a breath-holding task. A total of 20 individuals with SCI (14M, 6F, mean age = 46.3 ± 10.2 years) and 25 AB individuals (19M, 6F, mean age = 43.2 ± 12.28 years) were recruited for this study. In addition to the fNIRS metrics evaluated, all subjects undertook neurocognitive testing via the Neuropsychiatric Unit Cognitive Assessment Tool (NUCOG) (Walterfang et al., 2006). This assessment was performed prior to fNIRS data collection and evaluated between the SCI and AB groups to observe any differences in cognitive function between the two groups.

This dissertation is the first to comprehensively examine cognitive function in individuals with SCI using fNIRS. In Aim 1, an N-back working memory task was utilized in conjunction with fNIRS. From that study, we found increased neurovascular activity in the right inferior parietal lobe in individuals with SCI during the 2-back task as compared to the AB group. Differences were also observed in the executive function domain of the NUCOG test, in which the SCI group scored significantly lower than the AB group. In Aim

2, resting-state fNIRS was implemented to quantify changes in the resting-state functional connectivity and regional resting-state activity, as measured by fALFF scores, between individuals with SCI and AB controls. We observed significantly higher fALFF scores in individuals with SCI in both the left and right inferior parietal lobes, with further separation of the resting-state signal into Slow-5, Slow-4, and Slow-3 frequencies revealing brain-region specific oscillation differences. This shows both regional resting-state differences and frequency-dependent metrics between the SCI and AB groups. Lastly, in Aim 3, a breath-holding hypercapnic task was utilized in conjunction with fNIRS, to investigate the differences in CVR between individuals with SCI and AB controls. Significantly delayed CVR was found in the right inferior parietal lobe in individuals with SCI compared to AB controls, while no significant differences in the amplitude of CVR was observed. This shows specificity in the CVR response, in which the amplitude and delay components reveal distinct characteristics of CVR and one may possibly compensate for the other. The CVR delays were also associated with the duration since injury for the SCI group, in which a longer duration since injury resulted in a shortened delay, suggesting potential adaptive mechanisms as individuals with SCI undergo functional brain reorganization. Altogether, these three aims reveal distinct regional and frequency-dependent differences in neurovascular activity between individuals with SCI and AB controls, which can be quantified using fNIRS. This supports the use of fNIRS to study cognitive function in individuals with SCI and the techniques utilized in this study can be applied to other patient populations such as traumatic brain injury (TBI), Alzheimer's disease, Parkinson's disease, etc.

7.2 Future Work

Future studies may want to extend this work by incorporating a longitudinal design, such that changes in neurovascular activity can be monitored over time, particularly in individuals receiving physical therapy or rehabilitation services. One avenue of motor rehabilitation that can be explored is exoskeleton-assisted walking for individuals with SCI, in which fNIRS metrics are recorded and functional mobility is evaluated across time. This would allow clinicians to not only evaluate progress in motor function, but also observe direct supraspinal changes that reorganize over time. In addition to motor-focused rehabilitation training, it is possible to focus more on the impacts of cognitive rehabilitation or dual motor-cognitive rehabilitation, to evaluate the effects of different training paradigms and whether individuals with SCI benefit more from one over the other, as assessed by functional connectivity and neurovascular activation biomarkers. Furthermore, as fNIRS equipment and methodology advance, it is possible to increase the number of channels surrounding the scalp and evaluate the changes in neurovascular activity at a higher spatial resolution to better understand the distinct regional differences between individuals with SCI and AB controls. It is important to note that the recruitment of individuals with SCI pose inherent challenges; however, future studies may want to further investigate different heterogeneities within the SCI population, such as the functional level of recovery, the effects of different pain medications, the type of injury, the severity of injury, the degree of motor mobility loss, and the effects of comorbidities, which are all factors that can be better evaluated with a larger sample size.

REFERENCES

- Ahuja, C. S., Wilson, J. R., Nori, S., Kotter, M. R. N., Druschel, C., Curt, A., & Fehlings, M. G. (2017). Traumatic spinal cord injury. *Nature Reviews Disease Primers*, 3(1), 1–21. <https://doi.org/10.1038/nrdp.2017.18>
- Alcántar-Garibay, O. V., Incontri-Abraham, D., & Ibarra, A. (2022). Spinal cord injury-induced cognitive impairment: A narrative review. *Neural Regeneration Research*, 17(12), 2649–2654. <https://doi.org/10.4103/1673-5374.339475>
- Alizadeh, A., Dyck, S. M., & Karimi-Abdolrezaee, S. (2019). Traumatic Spinal Cord Injury: An Overview of Pathophysiology, Models and Acute Injury Mechanisms. *Frontiers in Neurology*, 10. <https://doi.org/10.3389/fneur.2019.00282>
- Amyot, F., Davis, C., Sangobowale, M., Moore, C., Silverman, E., Gandjbakhche, A., Diaz-Arrastia, R., & Kenney, K. (2022). Cerebrovascular Reactivity Measurement with Functional Near Infrared Spectroscopy. *JoVE (Journal of Visualized Experiments)*, 184, e61284. <https://doi.org/10.3791/61284>
- Amyot, F., Kenney, K., Spessert, E., Moore, C., Haber, M., Silverman, E., Gandjbakhche, A., & Diaz-Arrastia, R. (2020). Assessment of cerebrovascular dysfunction after traumatic brain injury with fMRI and fNIRS. *NeuroImage Clinical*, 25, 102086. <https://doi.org/10.1016/j.nicl.2019.102086>
- Anwar, M. A., Al Shehabi, T. S., & Eid, A. H. (2016). Inflammogenesis of secondary spinal cord injury. *Frontiers in Cellular Neuroscience*, 10(APR). Scopus. <https://doi.org/10.3389/fncel.2016.00098>
- Ashburner, J., Barnes, G., Chen, C.-C., Daunizeau, J., Flandin, G., Friston, K., Kiebel, S., Kilner, J., Litvak, V., & Moran, R. (2014). SPM12 manual. *Wellcome Trust Centre for Neuroimaging, London, UK*, 2464(4).
- Athanasίου, A., Klados, M. A., Pandria, N., Foroglou, N., Kavazidi, K. R., Polyzoidis, K., & Bamidis, P. D. (2017). A Systematic Review of Investigations into Functional Brain Connectivity Following Spinal Cord Injury. *Frontiers in Human Neuroscience*, 11, 517. <https://doi.org/10.3389/fnhum.2017.00517>
- Attwell, D., & Iadecola, C. (2002). The neural basis of functional brain imaging signals. *Trends in Neurosciences*, 25(12), 621–625. [https://doi.org/10.1016/s0166-2236\(02\)02264-6](https://doi.org/10.1016/s0166-2236(02)02264-6)
- Banerjea, R., Sambamoorthi, U., Weaver, F., Maney, M., Pogach, L. M., & Findley, T. (2008). Risk of Stroke, Heart Attack, and Diabetes Complications Among Veterans With Spinal Cord Injury. *Archives of Physical Medicine and Rehabilitation*, 89(8), 1448–1453. <https://doi.org/10.1016/j.apmr.2007.12.047>

- Bates, D., Mächler, M., Bolker, B., & Walker, S. (2015). Fitting Linear Mixed-Effects Models Using lme4. *Journal of Statistical Software*, *67*, 1–48. <https://doi.org/10.18637/jss.v067.i01>
- Benjamini, Y., & Hochberg, Y. (1995). Controlling the False Discovery Rate: A Practical and Powerful Approach to Multiple Testing. *Journal of the Royal Statistical Society: Series B (Methodological)*, *57*(1), 289–300. <https://doi.org/10.1111/j.2517-6161.1995.tb02031.x>
- Blight, A. R., Hsieh, J., Curt, A., Fawcett, J. W., Guest, J. D., Kleitman, N., Kurpad, S. N., Kwon, B. K., Lammertse, D. P., Weidner, N., & Steeves, J. D. (2019). The challenge of recruitment for neurotherapeutic clinical trials in spinal cord injury. *Spinal Cord*, *57*(5), 348–359. <https://doi.org/10.1038/s41393-019-0276-2>
- Bliss, E. S., Wong, R. H., Howe, P. R., & Mills, D. E. (2021). Benefits of exercise training on cerebrovascular and cognitive function in ageing. *Journal of Cerebral Blood Flow and Metabolism*, *41*(3), 447–470. <https://doi.org/10.1177/0271678X20957807>
- Bradbury, C. L., Wodchis, W. P., Mikulis, D. J., Pano, E. G., Hitzig, S. L., McGillivray, C. F., Ahmad, F. N., Craven, B. C., & Green, R. E. (2008). Traumatic brain injury in patients with traumatic spinal cord injury: Clinical and economic consequences. *Archives of Physical Medicine and Rehabilitation*, *89*(12 Suppl), S77–84. <https://doi.org/10.1016/j.apmr.2008.07.008>
- Braver, T. S., Cohen, J. D., Nystrom, L. E., Jonides, J., Smith, E. E., & Noll, D. C. (1997). A Parametric Study of Prefrontal Cortex Involvement in Human Working Memory. *NeuroImage*, *5*(1), 49–62. <https://doi.org/10.1006/nimg.1996.0247>
- Brier, M. R., Thomas, J. B., Snyder, A. Z., Benzinger, T. L., Zhang, D., Raichle, M. E., Holtzman, D. M., Morris, J. C., & Ances, B. M. (2012). Loss of intranetwork and internetwork resting state functional connections with Alzheimer’s disease progression. *The Journal of Neuroscience: The Official Journal of the Society for Neuroscience*, *32*(26), 8890–8899. <https://doi.org/10.1523/JNEUROSCI.5698-11.2012>
- Brigadoi, S., & Cooper, R. J. (2015). How short is short? Optimum source-detector distance for short-separation channels in functional near-infrared spectroscopy. *Neurophotonics*, *2*(2), 025005. <https://doi.org/10.1117/1.NPh.2.2.025005>
- Bright, M. G., & Murphy, K. (2013). Reliable quantification of BOLD fMRI cerebrovascular reactivity despite poor breath-hold performance. *Neuroimage*, *83*, 559–568. <https://doi.org/10.1016/j.neuroimage.2013.07.007>

- Buxton, R. B. (2010). Interpreting Oxygenation-Based Neuroimaging Signals: The Importance and the Challenge of Understanding Brain Oxygen Metabolism. *Frontiers in Neuroenergetics*, 2, 8. <https://doi.org/10.3389/fnene.2010.00008>
- Buxton, R. B. (2012). Dynamic models of BOLD contrast. *NeuroImage*, 62(2), 953–961. <https://doi.org/10.1016/j.neuroimage.2012.01.012>
- Buzsáki, G., Buhl, D. L., Harris, K. D., Csicsvari, J., Czéh, B., & Morozov, A. (2003). Hippocampal network patterns of activity in the mouse. *Neuroscience*, 116(1), 201–211. [https://doi.org/10.1016/S0306-4522\(02\)00669-3](https://doi.org/10.1016/S0306-4522(02)00669-3)
- Buzsáki, G., & Draguhn, A. (2004). Neuronal Oscillations in Cortical Networks. *Science*, 304(5679), 1926–1929. <https://doi.org/10.1126/science.1099745>
- Carlozzi, N. E., Troost, J. P., Molton, I. R., Ehde, D. M., Freedman, J., Cao, J., Miner, J. A., Najarian, K., & Kratz, A. L. (2022). The association between sleep and cognitive function in people with spinal cord injury (SCI). *Rehabilitation Psychology*, 67(3), 325–336. <https://doi.org/10.1037/rep0000418>
- Carlson, S. L., Parrish, M. E., Springer, J. E., Doty, K., & Dossett, L. (1998). Acute inflammatory response in spinal cord following impact injury. *Experimental Neurology*, 151(1), 77–88. Scopus. <https://doi.org/10.1006/exnr.1998.6785>
- Caspers, S., Schleicher, A., Bacha-Trams, M., Palomero-Gallagher, N., Amunts, K., & Zilles, K. (2013). Organization of the Human Inferior Parietal Lobule Based on Receptor Architectonics. *Cerebral Cortex*, 23(3), 615–628. <https://doi.org/10.1093/cercor/bhs048>
- Catchlove, S. J., Parrish, T. B., Chen, Y., Macpherson, H., Hughes, M. E., & Pipingas, A. (2018). Regional Cerebrovascular Reactivity and Cognitive Performance in Healthy Aging. *Journal of Experimental Neuroscience*, 12, 1179069518785151. <https://doi.org/10.1177/1179069518785151>
- Chen, D. Y., Di, X., Amaya, N., Sun, H., Pal, S., & Biswal, B. B. (2024). *Brain activation during the N-back working memory task in individuals with spinal cord injury: A functional near-infrared spectroscopy study* (p. 2024.02.09.579655). bioRxiv. <https://doi.org/10.1101/2024.02.09.579655>
- Chen, D. Y., Di, X., & Biswal, B. (2024). Cerebrovascular reactivity increases across development in multiple networks as revealed by a breath-holding task: A longitudinal fMRI study. *Human Brain Mapping*, 45(1), e26515. <https://doi.org/10.1002/hbm.26515>
- Chen, D. Y., Di, X., Yu, X., & Biswal, B. B. (2024). The significance and limited influence of cerebrovascular reactivity on age and sex effects in task- and resting-state brain activity. *Cerebral Cortex (New York, N.Y.: 1991)*, 34(2), bhad448. <https://doi.org/10.1093/cercor/bhad448>

- Chen, K., Yang, H., Zhang, H., Meng, C., Becker, B., & Biswal, B. (2021). Altered cerebrovascular reactivity due to respiratory rate and breath holding: A BOLD-fMRI study on healthy adults. *Brain Structure and Function*, 226(4), 1229–1239. <https://doi.org/10.1007/s00429-021-02236-5>
- Chiaravalloti, N. D., Weber, E., Wylie, G., Dyson-Hudson, T., & Wecht, J. M. (2018). Patterns of cognitive deficits in persons with spinal cord injury as compared with both age-matched and older individuals without spinal cord injury. *The Journal of Spinal Cord Medicine*, 43(1), 88–97. <https://doi.org/10.1080/10790268.2018.1543103>
- Choe, A. S., Belegu, V., Yoshida, S., Joel, S., Sadowsky, C. L., Smith, S. A., van Zijl, P. C., Pekar, J. J., & McDonald, J. W. (2013). Extensive neurological recovery from a complete spinal cord injury: A case report and hypothesis on the role of cortical plasticity. *Frontiers in Human Neuroscience*, 7. <https://doi.org/10.3389/fnhum.2013.00290>
- Clower, D. M., West, R. A., Lynch, J. C., & Strick, P. L. (2001). The Inferior Parietal Lobule Is the Target of Output from the Superior Colliculus, Hippocampus, and Cerebellum. *The Journal of Neuroscience*, 21(16), 6283–6291. <https://doi.org/10.1523/JNEUROSCI.21-16-06283.2001>
- Cohen, M. L., Tulskey, D. S., Holdnack, J. A., Carlozzi, N. E., Wong, A., Magasi, S., Heaton, R. K., & Heinemann, A. W. (2017). Cognition among Community-Dwelling Individuals with Spinal Cord Injury. *Rehabilitation Psychology*, 62(4), 425–434. <https://doi.org/10.1037/rep0000140>
- Corbetta, M., & Shulman, G. L. (2002). Control of goal-directed and stimulus-driven attention in the brain. *Nature Reviews Neuroscience*, 3(3), 201–215. <https://doi.org/10.1038/nrn755>
- Couillard-Despres, S., Bieler, L., & Vogl, M. (2017). Pathophysiology of traumatic spinal cord injury. In *Neurological Aspects of Spinal Cord Injury* (pp. 503–528). Scopus. https://doi.org/10.1007/978-3-319-46293-6_19
- Cragg, J. J., Noonan, V. K., Krassioukov, A., & Borisoff, J. (2013). Cardiovascular disease and spinal cord injury. *Neurology*, 81(8), 723–728. <https://doi.org/10.1212/WNL.0b013e3182a1aa68>
- Craig, A., Guest, R., & Middleton, J. (2016). Screening for cognitive impairment in adults with spinal cord injury with the Neuropsychiatry Unit Cognitive Assessment Tool (NUCOG). *JWCRR: Sydney*.
- Craig, A., Guest, R., Tran, Y., & Middleton, J. (2017). Cognitive Impairment and Mood States after Spinal Cord Injury. *Journal of Neurotrauma*, 34(6), 1156–1163. <https://doi.org/10.1089/neu.2016.4632>

- Craig, A., Nicholson Perry, K., Guest, R., Tran, Y., Dezarnaulds, A., Hales, A., Ephraums, C., & Middleton, J. (2015). Prospective study of the occurrence of psychological disorders and comorbidities after spinal cord injury. *Archives of Physical Medicine and Rehabilitation*, *96*(8), 1426–1434. <https://doi.org/10.1016/j.apmr.2015.02.027>
- Craig, A., Tran, Y., & Middleton, J. (2009). Psychological morbidity and spinal cord injury: A systematic review. *Spinal Cord*, *47*(2), 108–114. <https://doi.org/10.1038/sc.2008.115>
- Davenport, M. H., Hogan, D. B., Eskes, G. A., Longman, R. S., & Poulin, M. J. (2012). Cerebrovascular Reserve: The Link Between Fitness and Cognitive Function? *Exercise and Sport Sciences Reviews*, *40*(3), 153. <https://doi.org/10.1097/JES.0b013e3182553430>
- David, S., & Kroner, A. (2011). Repertoire of microglial and macrophage responses after spinal cord injury. *Nature Reviews Neuroscience*, *12*(7), 388–399. <https://doi.org/10.1038/nrn3053>
- Davidoff, G. N., Roth, E. J., & Richards, J. S. (1992). Cognitive deficits in spinal cord injury: Epidemiology and outcome. *Archives of Physical Medicine and Rehabilitation*, *73*(3), 275–284. <https://doi.org/10.5555/uri:pii:000399939290078B>
- Delpy, D. T., Cope, M., van der Zee, P., Arridge, S., Wray, S., & Wyatt, J. (1988). Estimation of optical pathlength through tissue from direct time of flight measurement. *Physics in Medicine and Biology*, *33*(12), 1433–1442. <https://doi.org/10.1088/0031-9155/33/12/008>
- Di, X., & Biswal, B. B. (2022). Principal component analysis reveals multiple consistent responses to naturalistic stimuli in children and adults. *Human Brain Mapping*, *43*(11), 3332–3345. <https://doi.org/10.1002/hbm.25568>
- Di, X., Kannurpatti, S. S., Rypma, B., & Biswal, B. B. (2013). Calibrating BOLD fMRI Activations with Neurovascular and Anatomical Constraints. *Cerebral Cortex*, *23*(2), 255–263. <https://doi.org/10.1093/cercor/bhs001>
- Di, X., Kim, E. H., Huang, C.-C., Lin, C.-P., & Biswal, B. B. (2013). The Influence of the Amplitude of Low-Frequency Fluctuations on Resting-State Functional Connectivity. *Frontiers in Human Neuroscience*, *7*. <https://doi.org/10.3389/fnhum.2013.00118>

- Ding, J., Zhang, H., Hua, B., Feng, C., Yang, M., Ding, X., & Yang, C. (2023). Frequency specificity in the amplitude of low frequency oscillations in patients with white matter lesions. *Journal of Clinical Neuroscience*, *113*, 86–92. <https://doi.org/10.1016/j.jocn.2023.05.011>
- Donnelly, D. J., & Popovich, P. G. (2008). Inflammation and its role in neuroprotection, axonal regeneration and functional recovery after spinal cord injury. *Experimental Neurology*, *209*(2), 378–388. Scopus. <https://doi.org/10.1016/j.expneurol.2007.06.009>
- Dowler, R. N., Harrington, D. L., Haaland, K. Y., Swanda, R. M., Fee, F., & Fiedler, K. (1997). Profiles of cognitive functioning in chronic spinal cord injury and the role of moderating variables. *Journal of the International Neuropsychological Society: JINS*, *3*(5), 464–472.
- Ellermann, J. M., Siegal, J. D., Strupp, J. P., Ebner, T. J., & Ugurbil, K. (1998). Activation of Visuomotor Systems during Visually Guided Movements: A Functional MRI Study. *Journal of Magnetic Resonance*, *131*(2), 272–285. <https://doi.org/10.1006/jmre.1998.1379>
- Faden, A. I., Wu, J., Stoica, B. A., & Loane, D. J. (2016). Progressive inflammation-mediated neurodegeneration after traumatic brain or spinal cord injury. *British Journal of Pharmacology*, *173*(4), 681–691. <https://doi.org/10.1111/bph.13179>
- Faulkner, J. R., Herrmann, J. E., Woo, M. J., Tansey, K. E., Doan, N. B., & Sofroniew, M. V. (2004). Reactive Astrocytes Protect Tissue and Preserve Function after Spinal Cord Injury. *Journal of Neuroscience*, *24*(9), 2143–2155. Scopus. <https://doi.org/10.1523/JNEUROSCI.3547-03.2004>
- Ferrari, M., & Quaresima, V. (2012). A brief review on the history of human functional near-infrared spectroscopy (fNIRS) development and fields of application. *NeuroImage*, *63*(2), 921–935. <https://doi.org/10.1016/j.neuroimage.2012.03.049>
- Fierstra, J., Sobczyk, O., Battisti-Charbonney, A., Mandell, D. M., Poublanc, J., Crawley, A. P., Mikulis, D. J., Duffin, J., & Fisher, J. A. (2013). Measuring cerebrovascular reactivity: What stimulus to use? *The Journal of Physiology*, *591*(Pt 23), 5809–5821. <https://doi.org/10.1113/jphysiol.2013.259150>
- Fox, M. D., Zhang, D., Snyder, A. Z., & Raichle, M. E. (2009). The global signal and observed anticorrelated resting state brain networks. *Journal of Neurophysiology*, *101*(6), 3270–3283. <https://doi.org/10.1152/jn.90777.2008>
- Friston, K. J. (1994). Functional and effective connectivity in neuroimaging: A synthesis. *Human Brain Mapping*, *2*(1–2), 56–78. <https://doi.org/10.1002/hbm.460020107>

- Friston, K. J., Fletcher, P., Josephs, O., Holmes, A., Rugg, M. D., & Turner, R. (1998). Event-related fMRI: Characterizing differential responses. *NeuroImage*, 7(1), 30–40. <https://doi.org/10.1006/nimg.1997.0306>
- Fuchs, E., & Flügge, G. (2014). Adult Neuroplasticity: More Than 40 Years of Research. *Neural Plasticity*, 2014(1), 541870. <https://doi.org/10.1155/2014/541870>
- Gagnon, L., Cooper, R. J., Yücel, M. A., Perdue, K. L., Greve, D. N., & Boas, D. A. (2012). Short separation channel location impacts the performance of short channel regression in NIRS. *NeuroImage*, 59(3), 2518–2528. <https://doi.org/10.1016/j.neuroimage.2011.08.095>
- Girouard, H., & Iadecola, C. (2006). Neurovascular coupling in the normal brain and in hypertension, stroke, and Alzheimer disease. *Journal of Applied Physiology (Bethesda, Md.: 1985)*, 100(1), 328–335. <https://doi.org/10.1152/jappphysiol.00966.2005>
- Gohel, S. R., & Biswal, B. B. (2015). Functional integration between brain regions at rest occurs in multiple-frequency bands. *Brain Connectivity*, 5(1), 23–34. <https://doi.org/10.1089/brain.2013.0210>
- Gong, J., Stickland, R. C., & Bright, M. G. (2023). Hemodynamic timing in resting-state and breathing-task BOLD fMRI. *NeuroImage*, 274, 120120. <https://doi.org/10.1016/j.neuroimage.2023.120120>
- Greicius, M. D., Srivastava, G., Reiss, A. L., & Menon, V. (2004). Default-mode network activity distinguishes Alzheimer’s disease from healthy aging: Evidence from functional MRI. *Proceedings of the National Academy of Sciences of the United States of America*, 101(13), 4637–4642. <https://doi.org/10.1073/pnas.0308627101>
- Gu, Y., Miao, S., Han, J., Zeng, K., Ouyang, G., Yang, J., & Li, X. (2017). Complexity analysis of fNIRS signals in ADHD children during working memory task. *Scientific Reports*, 7(1), 829. <https://doi.org/10.1038/s41598-017-00965-4>
- Hall, K. M., Cohen, M. E., Wright, J., Call, M., & Werner, P. (1999). Characteristics of the functional independence measure in traumatic spinal cord injury. *Archives of Physical Medicine and Rehabilitation*, 80(11), 1471–1476. [https://doi.org/10.1016/S0003-9993\(99\)90260-5](https://doi.org/10.1016/S0003-9993(99)90260-5)
- Han, Y., Wang, J., Zhao, Z., Min, B., Lu, J., Li, K., He, Y., & Jia, J. (2011). Frequency-dependent changes in the amplitude of low-frequency fluctuations in amnesic mild cognitive impairment: A resting-state fMRI study. *NeuroImage*, 55(1), 287–295. <https://doi.org/10.1016/j.neuroimage.2010.11.059>

- Hawasli, A. H., Rutlin, J., Roland, J. L., Murphy, R. K. J., Song, S.-K., Leuthardt, E. C., Shimony, J. S., & Ray, W. Z. (2018). Spinal Cord Injury Disrupts Resting-State Networks in the Human Brain. *Journal of Neurotrauma*, *35*(6), 864–873. <https://doi.org/10.1089/neu.2017.5212>
- Hejnar, M. P., Kiehl, K. A., & Calhoun, V. D. (2007). Interparticipant correlations: A model free fMRI analysis technique. *Human Brain Mapping*, *28*(9), 860–867. <https://doi.org/10.1002/hbm.20321>
- Hellenbrand, D. J., Quinn, C. M., Piper, Z. J., Morehouse, C. N., Fixel, J. A., & Hanna, A. S. (2021). Inflammation after spinal cord injury: A review of the critical timeline of signaling cues and cellular infiltration. *Journal of Neuroinflammation*, *18*(1), 284. <https://doi.org/10.1186/s12974-021-02337-2>
- Henderson, L. A., Gustin, S. M., Macey, P. M., Wrigley, P. J., & Siddall, P. J. (2011). Functional Reorganization of the Brain in Humans Following Spinal Cord Injury: Evidence for Underlying Changes in Cortical Anatomy. *The Journal of Neuroscience*, *31*(7), 2630–2637. <https://doi.org/10.1523/JNEUROSCI.2717-10.2011>
- Henke, A. M., Billington, Z. J., & Gater, D. R. (2022). Autonomic Dysfunction and Management after Spinal Cord Injury: A Narrative Review. *Journal of Personalized Medicine*, *12*(7), 1110. <https://doi.org/10.3390/jpm12071110>
- Herff, C., Heger, D., Fortmann, O., Hennrich, J., Putze, F., & Schultz, T. (2014). Mental workload during n-back task—Quantified in the prefrontal cortex using fNIRS. *Frontiers in Human Neuroscience*, *7*. <https://www.frontiersin.org/articles/10.3389/fnhum.2013.00935>
- Hernandez-Gerez, E., Fleming, I. N., & Parson, S. H. (2019). A role for spinal cord hypoxia in neurodegeneration. *Cell Death and Disease*, *10*(11), Article 11. <https://doi.org/10.1038/s41419-019-2104-1>
- Hou, J., Xiang, Z., Yan, R., Zhao, M., Wu, Y., Zhong, J., Guo, L., Li, H., Wang, J., Wu, J., Sun, T., & Liu, H. (2016). Motor recovery at 6 months after admission is related to structural and functional reorganization of the spine and brain in patients with spinal cord injury. *Human Brain Mapping*, *37*(6), 2195–2209. <https://doi.org/10.1002/hbm.23163>
- Hou, J.-M., Sun, T.-S., Xiang, Z.-M., Zhang, J.-Z., Zhang, Z.-C., Zhao, M., Zhong, J.-F., Liu, J., Zhang, H., Liu, H.-L., Yan, R.-B., & Li, H.-T. (2014). Alterations of resting-state regional and network-level neural function after acute spinal cord injury. *Neuroscience*, *277*, 446–454. <https://doi.org/10.1016/j.neuroscience.2014.07.045>

- Huppert, T. J., Diamond, S. G., Franceschini, M. A., & Boas, D. A. (2009). HomER: A review of time-series analysis methods for near-infrared spectroscopy of the brain. *Applied Optics*, *48*(10), D280–D298.
- Jöbsis, F. F. (1977). Noninvasive, Infrared Monitoring of Cerebral and Myocardial Oxygen Sufficiency and Circulatory Parameters. *Science*, *198*(4323), 1264–1267. <https://doi.org/10.1126/science.929199>
- Jurkiewicz, M. T., Mikulis, D. J., McIlroy, W. E., Fehlings, M. G., & Verrier, M. C. (2007). Sensorimotor Cortical Plasticity During Recovery Following Spinal Cord Injury: A Longitudinal fMRI Study. *Neurorehabilitation and Neural Repair*, *21*(6), 527–538. <https://doi.org/10.1177/1545968307301872>
- Kane, M. J., Conway, A. R. A., Miura, T. K., & Colflesh, G. J. H. (2007). Working memory, attention control, and the N-back task: A question of construct validity. *Journal of Experimental Psychology. Learning, Memory, and Cognition*, *33*(3), 615–622. <https://doi.org/10.1037/0278-7393.33.3.615>
- Karunakaran, K. D., Chen, D. Y., Ji, K., Chiaravalotti, N., & Biswal, B. B. (2022). Task-based and Resting-state Cortical Functional Differences after Spinal Cord Injury: A Pilot Functional Near-Infrared Spectroscopy Study. *Journal of Neurotrauma*. <https://doi.org/10.1089/neu.2022.0131>
- Karunakaran, K. D., He, J., Zhao, J., Cui, J.-L., Zang, Y.-F., Zhang, Z., & Biswal, B. B. (2019). Differences in Cortical Gray Matter Atrophy of Paraplegia and Tetraplegia after Complete Spinal Cord Injury. *Journal of Neurotrauma*, *36*(12), 2045–2051. <https://doi.org/10.1089/neu.2018.6040>
- Karunakaran, K. D., Ji, K., Chen, D. Y., Chiaravalloti, N. D., Niu, H., Alvarez, T. L., & Biswal, B. B. (2021). Relationship Between Age and Cerebral Hemodynamic Response to Breath Holding: A Functional Near-Infrared Spectroscopy Study. *Brain Topography*, *34*(2), 154–166. <https://doi.org/10.1007/s10548-021-00818-4>
- Karunakaran, K. D., Yuan, R., He, J., Zhao, J., Cui, J.-L., Zang, Y.-F., Zhang, Z., Alvarez, T. L., & Biswal, B. B. (2020). Resting-State Functional Connectivity of the Thalamus in Complete Spinal Cord Injury. *Neurorehabilitation and Neural Repair*, *34*(2), 122–133. <https://doi.org/10.1177/1545968319893299>
- Kastrup, A., Krüger, G., Glover, G. H., Neumann-Haefelin, T., & Moseley, M. E. (1999). Regional variability of cerebral blood oxygenation response to hypercapnia. *NeuroImage*, *10*(6), 675–681. <https://doi.org/10.1006/nimg.1999.0505>
- Kastrup, A., Krüger, G., Neumann-Haefelin, T., & Moseley, M. E. (2001). Assessment of cerebrovascular reactivity with functional magnetic resonance imaging: Comparison of CO₂ and breath holding. *Magnetic Resonance Imaging*, *19*(1), 13–20. [https://doi.org/10.1016/S0730-725X\(01\)00227-2](https://doi.org/10.1016/S0730-725X(01)00227-2)

- Kim, D.-I., & Tan, C. O. (2018). Alterations in autonomic cerebrovascular control after spinal cord injury. *Autonomic Neuroscience : Basic and Clinical*, 209, 43–50. <https://doi.org/10.1016/j.autneu.2017.04.001>
- Kocsis, L., Herman, P., & Eke, A. (2006). The modified Beer–Lambert law revisited. *Physics in Medicine and Biology*, 51(5), N91. <https://doi.org/10.1088/0031-9155/51/5/N02>
- Kokotilo, K. J., Eng, J. J., & Curt, A. (2009). Reorganization and Preservation of Motor Control of the Brain in Spinal Cord Injury: A Systematic Review. *Journal of Neurotrauma*, 26(11), 2113–2126. <https://doi.org/10.1089/neu.2008.0688>
- Kuznetsova, A., Brockhoff, P. B., & Christensen, R. H. B. (2017). lmerTest Package: Tests in Linear Mixed Effects Models. *Journal of Statistical Software*, 82, 1–26. <https://doi.org/10.18637/jss.v082.i13>
- Lamichhane, B., Westbrook, A., Cole, M. W., & Braver, T. S. (2020). Exploring brain-behavior relationships in the N-back task. *NeuroImage*, 212, 116683. <https://doi.org/10.1016/j.neuroimage.2020.116683>
- LaVela, S. L., Evans, C. T., Prohaska, T. R., Miskevics, S., Ganesh, S. P., & Weaver, F. M. (2012). Males Aging With a Spinal Cord Injury: Prevalence of Cardiovascular and Metabolic Conditions. *Archives of Physical Medicine and Rehabilitation*, 93(1), 90–95. <https://doi.org/10.1016/j.apmr.2011.07.201>
- Lee, C. Y., Chooi, W. H., Ng, S., & Chew, S. Y. (2022). Modulating neuroinflammation through molecular, cellular and biomaterial-based approaches to treat spinal cord injury. *Bioengineering and Translational Medicine*, 8(2), e10389. <https://doi.org/10.1002/btm2.10389>
- Lim, S.-W., Shiue, Y.-L., Ho, C.-H., Yu, S.-C., Kao, P.-H., Wang, J.-J., & Kuo, J.-R. (2017). Anxiety and Depression in Patients with Traumatic Spinal Cord Injury: A Nationwide Population-Based Cohort Study. *PLoS ONE*, 12(1), e0169623. <https://doi.org/10.1371/journal.pone.0169623>
- Macciocchi, S. N., Seel, R. T., & Thompson, N. (2013). The impact of mild traumatic brain injury on cognitive functioning following co-occurring spinal cord injury. *Archives of Clinical Neuropsychology: The Official Journal of the National Academy of Neuropsychologists*, 28(7), 684–691. <https://doi.org/10.1093/arclin/act049>
- MacIntosh, B. J., Klassen, L. M., & Menon, R. S. (2003). Transient hemodynamics during a breath hold challenge in a two part functional imaging study with simultaneous near-infrared spectroscopy in adult humans. *NeuroImage*, 20(2), 1246–1252. [https://doi.org/10.1016/S1053-8119\(03\)00417-8](https://doi.org/10.1016/S1053-8119(03)00417-8)

- Macmillan, N. A., & Kaplan, H. L. (1985). Detection theory analysis of group data: Estimating sensitivity from average hit and false-alarm rates. *Psychological Bulletin*, 98(1), 185–199. <https://doi.org/10.1037/0033-2909.98.1.185>
- Masedo, A. I., Hanley, M., Jensen, M. P., Ehde, D., & Cardenas, D. D. (2005). Reliability and validity of a self-report FIM (FIM-SR) in persons with amputation or spinal cord injury and chronic pain. *American Journal of Physical Medicine and Rehabilitation*, 84(3), 167–176; quiz 177–179, 198. <https://doi.org/10.1097/01.phm.0000154898.25609.4a>
- Mattingley, J. B., Husain, M., Rorden, C., Kennard, C., & Driver, J. (1998). Motor role of human inferior parietal lobe revealed in unilateral neglect patients. *Nature*, 392(6672), 179–182. <https://doi.org/10.1038/32413>
- Mcintyre, M., Richter, W., Morden, D., Wennerberg, A., & Frankenstein, U. (2003). Blood oxygenation level dependent functional magnetic resonance imaging. *Concepts in Magnetic Resonance Part A*, 16A(1), 5–15. <https://doi.org/10.1002/cmr.a.10049>
- Meidenbauer, K. L., Choe, K. W., Cardenas-Iniguez, C., Huppert, T. J., & Berman, M. G. (2021). Load-dependent relationships between frontal fNIRS activity and performance: A data-driven PLS approach. *NeuroImage*, 230, 117795. <https://doi.org/10.1016/j.neuroimage.2021.117795>
- Miller, K. B., Howery, A. J., Rivera-Rivera, L. A., Johnson, S. C., Rowley, H. A., Wieben, O., & Barnes, J. N. (2019). Age-Related Reductions in Cerebrovascular Reactivity Using 4D Flow MRI. *Frontiers in Aging Neuroscience*, 11, 281. <https://doi.org/10.3389/fnagi.2019.00281>
- Miller, S., & Mitra, K. (2021). Near-infrared spectroscopy-based system for assessment of cerebrovascular activity during stress. *Biophotonics in Exercise Science, Sports Medicine, Health Monitoring Technologies, and Wearables II*, 11638, 16–28. <https://doi.org/10.1117/12.2590851>
- Miró-Padilla, A., Bueichekú, E., Ventura-Campos, N., Flores-Compañ, M.-J., Parcet, M. A., & Ávila, C. (2019). Long-term brain effects of N-back training: An fMRI study. *Brain Imaging and Behavior*, 13(4), 1115–1127. <https://doi.org/10.1007/s11682-018-9925-x>
- Moia, S., Stickland, R. C., Ayyagari, A., Termenon, M., Caballero-Gaudes, C., & Bright, M. G. (2020). Voxelwise optimization of hemodynamic lags to improve regional CVR estimates in breath-hold fMRI. *Annual International Conference of the IEEE Engineering in Medicine and Biology Society. IEEE Engineering in Medicine and Biology Society. Annual International Conference, 2020*, 1489–1492. <https://doi.org/10.1109/EMBC44109.2020.9176225>

- Molavi, B., & Dumont, G. A. (2012). Wavelet-based motion artifact removal for functional near-infrared spectroscopy. *Physiological Measurement*, *33*(2), 259. <https://doi.org/10.1088/0967-3334/33/2/259>
- Molina, B., Segura, A., Serrano, J. P., Alonso, F. J., Molina, L., Pérez-Borrego, Y. A., Ugarte, M. I., & Oliviero, A. (2018). Cognitive performance of people with traumatic spinal cord injury: A cross-sectional study comparing people with subacute and chronic injuries. *Spinal Cord*, *56*(8), Article 8. <https://doi.org/10.1038/s41393-018-0076-0>
- National Spinal Cord Injury Statistical Center, Birmingham, AL. (2022). *Traumatic Spinal Cord Injury Facts and Figures at a Glance*. chrome-extension://efaidnbmnnnibpcajpcgiclfefndmkaj/<https://www.nscisc.uab.edu/public/Facts%20and%20Figures%202022%20-%20English%20Final.pdf>
- Nguyen, T., Kim, M., Gwak, J., Lee, J. J., Choi, K. Y., Lee, K. H., & Kim, J. G. (2019). Investigation of brain functional connectivity in patients with mild cognitive impairment: A functional near-infrared spectroscopy (fNIRS) study. *Journal of Biophotonics*, *12*(9), e201800298. <https://doi.org/10.1002/jbio.201800298>
- Nightingale, T. E., Zheng, M. M. Z., Sachdeva, R., Phillips, A. A., & Krassioukov, A. V. (2020). Diverse cognitive impairment after spinal cord injury is associated with orthostatic hypotension symptom burden. *Physiology and Behavior*, *213*, 112742. <https://doi.org/10.1016/j.physbeh.2019.112742>
- Nott, M., Baguley, I., Heriseanu, R., Weber, G., Middleton, J., Meares, S., Batchelor, J., Jones, A., Boyle, C., & Chilko, S. (2014). Effects of Concomitant Spinal Cord Injury and Brain Injury on Medical and Functional Outcomes and Community Participation. *Topics in Spinal Cord Injury Rehabilitation*, *20*(3), 225–235. <https://doi.org/10.1310/sci2003-225>
- Numssen, O., Bzdok, D., & Hartwigsen, G. (2021). Functional specialization within the inferior parietal lobes across cognitive domains. *eLife*, *10*, e63591. <https://doi.org/10.7554/eLife.63591>
- Oni-Orisan, A., Kaushal, M., Li, W., Leschke, J., Ward, B. D., Vedantam, A., Kalinosky, B., Budde, M. D., Schmit, B. D., Li, S.-J., Muqet, V., & Kurpad, S. N. (2016). Alterations in Cortical Sensorimotor Connectivity following Complete Cervical Spinal Cord Injury: A Prospective Resting-State fMRI Study. *PLoS ONE*, *11*(3), e0150351. <https://doi.org/10.1371/journal.pone.0150351>
- Oudega, M., & Perez, M. A. (2012). Corticospinal reorganization after spinal cord injury. *The Journal of Physiology*, *590*(16), 3647–3663. <https://doi.org/10.1113/jphysiol.2012.233189>

- Owen, A. M., McMillan, K. M., Laird, A. R., & Bullmore, E. (2005). N-back working memory paradigm: A meta-analysis of normative functional neuroimaging studies. *Human Brain Mapping, 25*(1), 46–59. <https://doi.org/10.1002/hbm.20131>
- Pasipanodya, E. C., Dirlikov, B., Castillo, K., & Shem, K. L. (2021). Cognitive Profiles Among Individuals With Spinal Cord Injuries: Predictors and Relations With Psychological Well-being. *Archives of Physical Medicine and Rehabilitation, 102*(3), 431–439. <https://doi.org/10.1016/j.apmr.2020.06.022>
- Paulson, O. B., Hasselbalch, S. G., Rostrup, E., Knudsen, G. M., & Pelligrino, D. (2010). Cerebral blood flow response to functional activation. *Journal of Cerebral Blood Flow and Metabolism: Official Journal of the International Society of Cerebral Blood Flow and Metabolism, 30*(1), 2–14. <https://doi.org/10.1038/jcbfm.2009.188>
- Penttonen, M., & Buzsáki, G. (2003). Natural logarithmic relationship between brain oscillators. *Thalamus and Related Systems, 2*(2), 145–152. [https://doi.org/10.1016/S1472-9288\(03\)00007-4](https://doi.org/10.1016/S1472-9288(03)00007-4)
- Phillips, A. A., Chan, F. H., Zheng, M. M. Z., Krassioukov, A. V., & Ainslie, P. N. (2016). Neurovascular coupling in humans: Physiology, methodological advances and clinical implications. *Journal of Cerebral Blood Flow and Metabolism, 36*(4), 647–664. <https://doi.org/10.1177/0271678X15617954>
- Pinto, J., Bright, M. G., Bulte, D. P., & Figueiredo, P. (2021). Cerebrovascular Reactivity Mapping Without Gas Challenges: A Methodological Guide. *Frontiers in Physiology, 11*, 608475. <https://doi.org/10.3389/fphys.2020.608475>
- Pozzato, I., Arora, M., McBain, C., Wijesuriya, N., Tran, Y., Middleton, J. W., & Craig, A. R. (2023). Cognitive Failure in Adults with Spinal Cord Injury: A Valuable Adjunct Measure for Enhancing Cognitive Assessment and Rehabilitation Outcomes. *Neurology International, 15*(4), Article 4. <https://doi.org/10.3390/neurolint15040087>
- Quaresima, V., Giosuè, P., Roncone, R., Casacchia, M., & Ferrari, M. (2009). Prefrontal cortex dysfunction during cognitive tests evidenced by functional near-infrared spectroscopy. *Psychiatry Research, 171*(3), 252–257. <https://doi.org/10.1016/j.psychresns.2008.02.002>
- R Core Team. (2023). *R: A language and environment for statistical computing*. [R Foundation for Statistical Computing.]. <https://www.R-project.org/>.
- Reddy, P., Izzetoglu, M., Shewokis, P. A., Sangobowale, M., Diaz-Arrastia, R., & Izzetoglu, K. (2021). Evaluation of fNIRS signal components elicited by cognitive and hypercapnic stimuli. *Scientific Reports, 11*(1), 23457. <https://doi.org/10.1038/s41598-021-02076-7>

- Rekand, T., Hagen, E. M., & Grønning, M. (2012). Chronic pain following spinal cord injury. *Tidsskrift for Den Norske Laegeforening: Tidsskrift for Praktisk Medicin, Ny Raekke*, 132(8), 974–979. <https://doi.org/10.4045/tidsskr.11.0794>
- Roth, E., Davidoff, G., Thomas, P., Doljanac, R., Dijkers, M., Berent, S., Morris, J., & Yarkony, G. (1989). A controlled study of neuropsychological deficits in acute spinal cord injury patients. *Paraplegia*, 27(6), 480–489. <https://doi.org/10.1038/sc.1989.75>
- Sachdeva, R., Gao, F., Chan, C. C. H., & Krassioukov, A. V. (2018). Cognitive function after spinal cord injury. *Neurology*, 91(13), 611–621. <https://doi.org/10.1212/WNL.0000000000006244>
- Sachdeva, R., Nightingale, T. E., & Krassioukov, A. V. (2019). The Blood Pressure Pendulum following Spinal Cord Injury: Implications for Vascular Cognitive Impairment. *International Journal of Molecular Sciences*, 20(10), 2464. <https://doi.org/10.3390/ijms20102464>
- Sandalic, D., Craig, A., Tran, Y., Arora, M., Pozzato, I., McBain, C., Tonkin, H., Simpson, G., Gopinath, B., Kaur, J., Shetty, S., Weber, G., & Middleton, J. (2022). Cognitive Impairment in Individuals With Spinal Cord Injury. *Neurology*, 99(16), e1779–e1790. <https://doi.org/10.1212/WNL.0000000000200957>
- Sandalic, D., Tran, Y., Craig, A., Arora, M., Pozzato, I., Simpson, G., Gopinath, B., Kaur, J., Shetty, S., Weber, G., Benad, L., & Middleton, J. W. (2022). The Need for a Specialized Neurocognitive Screen and Consistent Cognitive Impairment Criteria in Spinal Cord Injury: Analysis of the Suitability of the Neuropsychiatry Unit Cognitive Assessment Tool. *Journal of Clinical Medicine*, 11(12), Article 12. <https://doi.org/10.3390/jcm11123344>
- Schecklmann, M., Romanos, M., Bretscher, F., Plichta, M. M., Warnke, A., & Fallgatter, A. J. (2010). Prefrontal oxygenation during working memory in ADHD. *Journal of Psychiatric Research*, 44(10), 621–628. <https://doi.org/10.1016/j.jpsychires.2009.11.018>
- Sekhon, L. H. S., & Fehlings, M. G. (2001). Epidemiology, Demographics, and Pathophysiology of Acute Spinal Cord Injury. *Spine*, 26(24S), S2.
- Sestieri, C., Corbetta, M., Romani, G. L., & Shulman, G. L. (2011). Episodic memory retrieval, parietal cortex, and the default mode network: Functional and topographic analyses. *The Journal of Neuroscience: The Official Journal of the Society for Neuroscience*, 31(12), 4407–4420. <https://doi.org/10.1523/JNEUROSCI.3335-10.2011>

- Shafazand, S., Anderson, K. D., & Nash, M. S. (2019). Sleep Complaints and Sleep Quality in Spinal Cord Injury: A Web-Based Survey. *Journal of Clinical Sleep Medicine : JCSM : Official Publication of the American Academy of Sleep Medicine*, 15(5), 719–724. <https://doi.org/10.5664/jcsm.7760>
- Siddiqui, A. M., Khazaei, M., & Fehlings, M. G. (2015). Translating mechanisms of neuroprotection, regeneration, and repair to treatment of spinal cord injury. *Progress in Brain Research*, 218, 15–54. Scopus. <https://doi.org/10.1016/bs.pbr.2014.12.007>
- Silva, N. A., Sousa, N., Reis, R. L., & Salgado, A. J. (2014). From basics to clinical: A comprehensive review on spinal cord injury. *Progress in Neurobiology*, 114, 25–57. <https://doi.org/10.1016/j.pneurobio.2013.11.002>
- Simis, M., Santos, K., Sato, J., Fregni, F., & Battistella, L. (2018). T107. Using Functional near Infrared Spectroscopy (fNIRS) to assess brain activity of spinal cord injury patient, during robot-assisted gait. *Clinical Neurophysiology*, 129, e43–e44. <https://doi.org/10.1016/j.clinph.2018.04.108>
- Sinescu, C., Popa, F., Grigorean, V. T., Onose, G., Sandu, A. M., Popescu, M., Burnei, G., Strambu, V., & Popa, C. (2010). Molecular basis of vascular events following spinal cord injury. *Journal of Medicine and Life*, 3(3), 254–261. Scopus.
- Sleight, E., Stringer, M. S., Marshall, I., Wardlaw, J. M., & Thrippleton, M. J. (2021). Cerebrovascular Reactivity Measurement Using Magnetic Resonance Imaging: A Systematic Review. *Frontiers in Physiology*, 12. <https://www.frontiersin.org/articles/10.3389/fphys.2021.643468>
- Smielewski, P., Kirkpatrick, P., Minhas, P., Pickard, J. D., & Czosnyka, M. (1995). Can Cerebrovascular Reactivity Be Measured With Near-Infrared Spectroscopy? *Stroke*, 26(12), 2285–2292. <https://doi.org/10.1161/01.STR.26.12.2285>
- Sobczyk, O., Fierstra, J., Venkatraghavan, L., Poublanc, J., Duffin, J., Fisher, J. A., & Mikulis, D. J. (2021). Measuring Cerebrovascular Reactivity: Sixteen Avoidable Pitfalls. *Frontiers in Physiology*, 12. <https://doi.org/10.3389/fphys.2021.665049>
- Soveri, A., Antfolk, J., Karlsson, L., Salo, B., & Laine, M. (2017). Working memory training revisited: A multi-level meta-analysis of n-back training studies. *Psychonomic Bulletin and Review*, 24(4), 1077–1096. <https://doi.org/10.3758/s13423-016-1217-0>
- Stanislaw, H., & Todorov, N. (1999). Calculation of signal detection theory measures. *Behavior Research Methods, Instruments, and Computers*, 31(1), 137–149. <https://doi.org/10.3758/BF03207704>

- Stickland, R. C., Zvolanek, K. M., Moia, S., Caballero-Gaudes, C., & Bright, M. G. (2022). Lag-Optimized Blood Oxygenation Level Dependent Cerebrovascular Reactivity Estimates Derived From Breathing Task Data Have a Stronger Relationship With Baseline Cerebral Blood Flow. *Frontiers in Neuroscience, 16*, 910025. <https://doi.org/10.3389/fnins.2022.910025>
- Strangman, G. E., Li, Z., & Zhang, Q. (2013). Depth Sensitivity and Source-Detector Separations for Near Infrared Spectroscopy Based on the Colin27 Brain Template. *PLOS ONE, 8*(8), e66319. <https://doi.org/10.1371/journal.pone.0066319>
- Stringer, M. S., Blair, G. W., Shi, Y., Hamilton, I., Dickie, D. A., Doubal, F. N., Marshall, I. M., Thrippleton, M. J., & Wardlaw, J. M. (2021). A Comparison of CVR Magnitude and Delay Assessed at 1.5 and 3T in Patients With Cerebral Small Vessel Disease. *Frontiers in Physiology, 12*, 644837. <https://doi.org/10.3389/fphys.2021.644837>
- Sun, X., Long, H., Zhao, C., Duan, Q., Zhu, H., Chen, C., Sun, W., Ju, F., Sun, X., Zhao, Y., Xue, B., Tian, F., Mou, X., & Yuan, H. (2019). Analgesia-enhancing effects of repetitive transcranial magnetic stimulation on neuropathic pain after spinal cord injury: An fNIRS study. *Restorative Neurology and Neuroscience, 37*(5), 497–507. <https://doi.org/10.3233/RNN-190934>
- Tang, X., Li, B., Wang, M., Gao, L., He, Y., & Xia, G. (2023). Frequency-Dependent Alterations in the Amplitude of Low-Frequency Fluctuations in Patients with Acute Pericoronitis: A Resting-State fMRI Study. *Journal of Pain Research, 16*, 501–511. <https://doi.org/10.2147/JPR.S397523>
- Thompson, T. W., Waskom, M. L., Garel, K.-L. A., Cardenas-Iniguez, C., Reynolds, G. O., Winter, R., Chang, P., Pollard, K., Lala, N., Alvarez, G. A., & Gabrieli, J. D. E. (2013). Failure of Working Memory Training to Enhance Cognition or Intelligence. *PLoS ONE, 8*(5). Scopus. <https://doi.org/10.1371/journal.pone.0063614>
- Tong, Y., Bergethon, P. R., & Frederick, B. deB. (2011). An improved method for mapping cerebrovascular reserve using concurrent fMRI and near-infrared spectroscopy with Regressor Interpolation at Progressive Time Delays (RIPTiDe). *NeuroImage, 56*(4), 2047–2057. <https://doi.org/10.1016/j.neuroimage.2011.03.071>
- Vagné, V., Le Bars, E., Deverdun, J., Rossel, O., Perrey, S., Costalat, V., & Guiraud, D. (2020). Quantitative assessment of near-infrared spectroscopy time course under hypercapnia using an a priori model-based fitting. *Computers in Biology and Medicine, 118*, 103638. <https://doi.org/10.1016/j.combiomed.2020.103638>

- Vallesi, V., Richter, J. K., Hunkeler, N., Abramovic, M., Hashagen, C., Christiaanse, E., Shetty, G., Verma, R. K., Berger, M., Frotzler, A., Eisenlohr, H., Eriks-Hoogland, I., Scheel-Sailer, A., Michels, L., & Wyss, P. O. (2022). Functional connectivity and amplitude of low-frequency fluctuations changes in people with complete subacute and chronic spinal cord injury. *Scientific Reports*, *12*, 20874. <https://doi.org/10.1038/s41598-022-25345-5>
- van Niftrik, C. H. B., Hiller, A., Sebök, M., Halter, M., Duffin, J., Fisher, J. A., Mikulis, D. J., Regli, L., Piccirelli, M., & Fierstra, J. (2023). Heterogeneous motor BOLD-fMRI responses in brain areas exhibiting negative BOLD cerebrovascular reactivity indicate that steal phenomenon does not always result from exhausted cerebrovascular reserve capacity. *Magnetic Resonance Imaging*, *103*, 124–130. <https://doi.org/10.1016/j.mri.2023.07.010>
- Vassena, E., Gerrits, R., Demanet, J., Verguts, T., & Siugzdaite, R. (2019). Anticipation of a mentally effortful task recruits Dorsolateral Prefrontal Cortex: An fNIRS validation study. *Neuropsychologia*, *123*, 106–115. <https://doi.org/10.1016/j.neuropsychologia.2018.04.033>
- Vermeij, A., Kessels, R. P. C., Heskamp, L., Simons, E. M. F., Dautzenberg, P. L. J., & Claassen, J. A. H. R. (2017). Prefrontal activation may predict working-memory training gain in normal aging and mild cognitive impairment. *Brain Imaging and Behavior*, *11*(1), 141–154. <https://doi.org/10.1007/s11682-016-9508-7>
- Villringer, A., Planck, J., Hock, C., Schleinkofer, L., & Dirnagl, U. (1993). Near infrared spectroscopy (NIRS): A new tool to study hemodynamic changes during activation of brain function in human adults. *Neuroscience Letters*, *154*(1), 101–104. [https://doi.org/10.1016/0304-3940\(93\)90181-J](https://doi.org/10.1016/0304-3940(93)90181-J)
- Walterfang, M., Siu, R., & Velakoulis, D. (2006). The NUCOG: Validity and Reliability of a Brief Cognitive Screening Tool in Neuropsychiatric Patients. *Australian & New Zealand Journal of Psychiatry*, *40*(11–12), 995–1002. <https://doi.org/10.1080/j.1440-1614.2006.01923.x>
- Wang, Z., Zhang, Z., Liao, W., Xu, Q., Zhang, J., Lu, W., Jiao, Q., Chen, G., Feng, J., & Lu, G. (2014). Frequency-dependent amplitude alterations of resting-state spontaneous fluctuations in idiopathic generalized epilepsy. *Epilepsy Research*, *108*(5), 853–860. <https://doi.org/10.1016/j.eplepsyres.2014.03.003>
- Watanabe, T., Hirose, S., Wada, H., Imai, Y., Machida, T., Shirouzu, I., Konishi, S., Miyashita, Y., & Masuda, N. (2013). A pairwise maximum entropy model accurately describes resting-state human brain networks. *Nature Communications*, *4*, 1370. <https://doi.org/10.1038/ncomms2388>

- Weber, A. M., Nightingale, T. E., Jarrett, M., Lee, A. H. X., Campbell, O., Walter, M., Lucas, S. J. E., Phillips, A., Rauscher, A., & Krassioukov, A. (2022). *Cerebrovascular Reactivity Following Spinal Cord Injury* (p. 2022.06.28.22276567). medRxiv. <https://doi.org/10.1101/2022.06.28.22276567>
- Wecht, J. M., & Bauman, W. A. (2013). Decentralized cardiovascular autonomic control and cognitive deficits in persons with spinal cord injury. *The Journal of Spinal Cord Medicine*, 36(2), 74–81. <https://doi.org/10.1179/2045772312Y.0000000056>
- Wecht, J. M., La Fountaine, M. F., Handrakis, J. P., West, C. R., Phillips, A., Ditor, D. S., Sharif, H., Bauman, W. A., & Krassioukov, A. V. (2015). Autonomic Nervous System Dysfunction Following Spinal Cord Injury: Cardiovascular, Cerebrovascular, and Thermoregulatory Effects. *Current Physical Medicine and Rehabilitation Reports*, 3(3), 197–205. <https://doi.org/10.1007/s40141-015-0093-2>
- West, C. R., Bellantoni, A., & Krassioukov, A. V. (2013). Cardiovascular Function in Individuals with Incomplete Spinal Cord Injury: A Systematic Review. *Topics in Spinal Cord Injury Rehabilitation*, 19(4), 267–278. <https://doi.org/10.1310/sci1904-267>
- Wilmot, C. B., Cope, D. N., Hall, K. M., & Acker, M. (1985). Occult head injury: Its incidence in spinal cord injury. *Archives of Physical Medicine and Rehabilitation*, 66(4), 227–231. [https://doi.org/10.1016/0003-9993\(85\)90148-0](https://doi.org/10.1016/0003-9993(85)90148-0)
- Wilson, L. C., Cotter, J. D., Fan, J.-L., Lucas, R. A. I., Thomas, K. N., & Ainslie, P. N. (2010). Cerebrovascular reactivity and dynamic autoregulation in tetraplegia. *American Journal of Physiology-Regulatory, Integrative and Comparative Physiology*, 298(4), R1035–R1042. <https://doi.org/10.1152/ajpregu.00815.2009>
- World Health Organization. (2024, April 16). *Spinal cord injury*. <https://www.who.int/news-room/fact-sheets/detail/spinal-cord-injury>
- Wrigley, P. J., Gustin, S. M., Macey, P. M., Nash, P. G., Gandevia, S. C., Macefield, V. G., Siddall, P. J., & Henderson, L. A. (2009). Anatomical changes in human motor cortex and motor pathways following complete thoracic spinal cord injury. *Cerebral Cortex (New York, N.Y.: 1991)*, 19(1), 224–232. <https://doi.org/10.1093/cercor/bhn072>
- Wu, J., Zhao, Z., Sabirzhanov, B., Stoica, B. A., Kumar, A., Luo, T., Skovira, J., & Faden, A. I. (2014). Spinal Cord Injury Causes Brain Inflammation Associated with Cognitive and Affective Changes: Role of Cell Cycle Pathways. *The Journal of Neuroscience*, 34(33), 10989–11006. <https://doi.org/10.1523/JNEUROSCI.5110-13.2014>

- Wu, J.-C., Chen, Y.-C., Liu, L., Chen, T.-J., Huang, W.-C., Cheng, H., & Tung-Ping, S. (2012). Increased risk of stroke after spinal cord injury. *Neurology*, *78*(14), 1051–1057. <https://doi.org/10.1212/WNL.0b013e31824e8eaa>
- Yang, B., Zhang, F., Cheng, F., Ying, L., Wang, C., Shi, K., Wang, J., Xia, K., Gong, Z., Huang, X., Yu, C., Li, F., Liang, C., & Chen, Q. (2020). Strategies and prospects of effective neural circuits reconstruction after spinal cord injury. *Cell Death & Disease*, *11*(6), Article 6. <https://doi.org/10.1038/s41419-020-2620-z>
- Yeung, M. K., & Han, Y. M. Y. (2023). Changes in task performance and frontal cortex activation within and over sessions during the n-back task. *Scientific Reports*, *13*(1), Article 1. <https://doi.org/10.1038/s41598-023-30552-9>
- Yücel, M. A., Lüthmann, A. v, Scholkmann, F., Gervain, J., Dan, I., Ayaz, H., Boas, D., Cooper, R. J., Culver, J., Elwell, C. E., Eggebrecht, A., Franceschini, M. A., Grova, C., Homae, F., Lesage, F., Obrig, H., Tachtsidis, I., Tak, S., Tong, Y., ... Wolf, M. (2021). Best practices for fNIRS publications. *Neurophotonics*, *8*(1), 012101. <https://doi.org/10.1117/1.NPh.8.1.012101>
- Yücel, M. A., Selb, J. J., Huppert, T. J., Franceschini, M. A., & Boas, D. A. (2017). Functional Near Infrared Spectroscopy: Enabling Routine Functional Brain Imaging. *Current Opinion in Biomedical Engineering*, *4*, 78–86. <https://doi.org/10.1016/j.cobme.2017.09.011>
- Yue, Y., Jia, X., Hou, Z., Zang, Y., & Yuan, Y. (2015). Frequency-dependent amplitude alterations of resting-state spontaneous fluctuations in late-onset depression. *BioMed Research International*, *2015*, 505479. <https://doi.org/10.1155/2015/505479>
- Zang, Y.-F., He, Y., Zhu, C.-Z., Cao, Q.-J., Sui, M.-Q., Liang, M., Tian, L.-X., Jiang, T.-Z., & Wang, Y.-F. (2007). Altered baseline brain activity in children with ADHD revealed by resting-state functional MRI. *Brain and Development*, *29*(2), 83–91. <https://doi.org/10.1016/j.braindev.2006.07.002>
- Zheng, W., Wang, L., Chen, Q., Li, X., Chen, X., Qin, W., Li, K., Lu, J., & Chen, N. (2021). Functional Reorganizations Outside the Sensorimotor Regions Following Complete Thoracolumbar Spinal Cord Injury. *Journal of Magnetic Resonance Imaging*, *54*(5), 1551–1559. <https://doi.org/10.1002/jmri.27764>
- Zou, Q.-H., Zhu, C.-Z., Yang, Y., Zuo, X.-N., Long, X.-Y., Cao, Q.-J., Wang, Y.-F., & Zang, Y.-F. (2008). An improved approach to detection of amplitude of low-frequency fluctuation (ALFF) for resting-state fMRI: Fractional ALFF. *Journal of Neuroscience Methods*, *172*(1), 137–141. <https://doi.org/10.1016/j.jneumeth.2008.04.012>

Zvolanek, K. M., Moia, S., Dean, J. N., Stickland, R. C., Caballero-Gaudes, C., & Bright, M. G. (2023). Comparing end-tidal CO₂, respiration volume per time (RVT), and average gray matter signal for mapping cerebrovascular reactivity amplitude and delay with breath-hold task BOLD fMRI. *NeuroImage*, 272, 120038. <https://doi.org/10.1016/j.neuroimage.2023.120038>